# MICROWAVE POWER DIVIDER

**EUGENE YONG WAI ZI**

**A project report submitted in partial fulfilment of the requirements for the award of Bachelor of Engineering (Hons.) Electronic and Communications Engineering**

**Faculty of Engineering and Science**
**Universiti Tunku Abdul Rahman**

**January 2012**

# DECLARATION

I hereby declare that this project report is based on my original work except for citations and quotations which have been duly acknowledged. I also declare that it has not been previously and concurrently submitted for any other degree or award at UTAR or other institutions.

Signature : _____

Name : EUGENE YONG WAI ZI___

ID No. : 08UEB04697_____

Date : 16th May 2012_____

## APPROVAL FOR SUBMISSION

I certify that this project report entitled **"MICROWAVE POWER DIVIDERS"** was prepared by **EUGENE YONG WAI ZI** has met the required standard for submission in partial fulfilment of the requirements for the award of Bachelor of Engineering (Hons.) Electronic and Communications Engineering at Universiti Tunku Abdul Rahman.

Approved by,

Signature : _____

Supervisor : Prof. Dr. Lim Eng Hok

Date : 16th May 2012

The copyright of this report belongs to the author under the terms of the copyright Act 1987 as qualified by Intellectual Property Policy of University Tunku Abdul Rahman. Due acknowledgement shall always be made of the use of any material contained in, or derived from, this report.

© 2012, Eugene Yong Wai Zi. All right reserved.

## ACKNOWLEDGEMENTS

I would like to thank everyone who had contributed to the successful completion of this project. I would like to express my gratitude to my research supervisor, Dr. Lim Eng Hock for his invaluable advice, guidance and his enormous patience throughout the development of the research.

In addition, I would also like to express my gratitude to my loving parent and friends who had helped and given me encouragement to overcome the problems that I had faced during the course of the research. Furthermore, I would like to express my sincere appreciation to UTAR for providing excellent facilities to perform experiments in order to validate my research results.

# MICROWAVE POWER DIVIDERS

## ABSTRACT

Power dividers are used to combine or split powers signals. They are widely used in various microwave devices and systems, such as microwave power amplifiers, linearization of power amplifiers, test setups and measurement circuits. Due to its commonality in microwave applications, it is vital to design power dividers that are able to perform well under low cost along with simple fabrication process. This thesis solely focuses on designing power dividers based upon microwave engineering principles using microstrip technology. All design configuration of the power dividers presented in this project implements rectangular patch resonators. A 2-way in-phase power divider, a 2-way out-of-phase power divider, and a 3-way power divider, with capabilities of equal power division ratio will be presented. Investigation on the design configurations were performed using a High Frequency Simulation Software (HFSS) to obtain the optimum performance. Fabricated dividers were measured and compared with the simulation ones. Overall, the comparison displays good agreement and it can be concluded that rectangular patch resonators can be used to design 2-way and multi-way power dividers.

# TABLE OF CONTENTS

**DECLARATION** **ii**
**APPROVAL FOR SUBMISSION** **iii**
**ACKNOWLEDGEMENTS** **v**
**ABSTRACT** **vi**
**TABLE OF CONTENTS** **vii**
**LIST OF TABLES** **x**
**LIST OF FIGURES** **xi**
**LIST OF SYMBOLS / ABBREVIATIONS** **xii**

**1 INTRODUCTION** **1**
1.1 Background 1
1.2 Microwave Devices & Components 2
1.2.1 Filters 2
1.2.2 Amplifiers 3
1.2.3 Directional Couplers 4
1.3 Project Aims & Objectives 5
1.4 Project Motivation 6
1.5 Thesis Overview 6

**2 LITERATURE REVIEW** **8**
2.1 Background 8
2.2 Power Divider 8
2.2.1 Theory 8
2.2.2 Design considerations (Performance parameters) 10
2.3 Recent Developments 11
2.3.1 Power Divider with Non-Uniform Transmission Lines 11

2.3.2 Power Divider with Generalize Negative Refractive Index Transmission Lines 14
2.3.3 Power Divider with Multilayer Slot line 18
2.4 Introduction of Simulation Tools 20
2.4.1 High Frequency Simulation Structure 21
2.4.2 Microwave Office 21

**3 PATCH POWER DIVDER 22**
3.1 Background 22
3.2 In-Phase Patch Power Divider 22
3.2.1 Configuration 22
3.2.2 Transmission Line Model 25
3.2.3 Results 28
3.2.4 Parametric Analysis 31
3.3 Out-of-Phase Power Divider 47
3.3.1 Configuration 47
3.3.2 Transmission Line Model 50
3.3.3 Results 51
3.3.4 Parametric Analysis 54
3.4 Discussion 75

**4 MULTI-WAY PATCH POWER DIVIDER 77**
4.1 Background 77
4.2 Three-Way Patch Power Divider 78
4.2.1 Configuration 78
4.2.2 Transmission Line Model 80
4.2.3 Results 83
4.2.4 Parametric Analysis 86
4.2.5 Discussion 104

**5 CONCLUSION AND RECOMMENDATIONS 106**
5.1 Achievements 106
5.2 Future Work 106

5.3 Conclusion 107

**REFERENCES 108**

# LIST OF TABLES


| TABLE | TITLE | PAGE |
|---|---|---|
| 3-1 | Element Parameters for In-Phase Power Dividers | 25 |
| 3-2 | Element Parameters for Out-Phase Divider | 50 |
| 4-1 | Types of three-way power divider | 77 |
| 4-2 | Element Parameters for Multi-Way Power Divider | 81 |

# LIST OF FIGURES


| FIGURE | TITLE | PAGE |
|---|---|---|
| 1-1 | Filter Frequency Response Characteristics | 3 |
| 2-1 | Three port microwave network | 9 |
| 2-2 | Configuration of the Non-Uniform Transmission Line Power Divider | 11 |
| 2-3 | Even-mode circuit | 12 |
| 2-4 | Odd-mode circuit | 12 |
| 2-5 | Photograph of the NTL Power Divider | 12 |
| 2-6 | Measured and Simulation results for S11 and S21 | 13 |
| 2-7 | Measured and Simulation results for S22 and S23 | 14 |
| 2-8 | Unit cell of generalized NRI-TL medium | 15 |
| 2-9 | Generalized NRI-TL Wilkinson divider topology in microstrip | 15 |
| 2-10 | Photograph of Generalized NRI-TL Wilkinson divider in microstrip | 16 |
| 2-11 | Simulated and Measured S21 Amplitude Response | 16 |
| 2-12 | Simulated and Measured S11 Amplitude Response | 17 |
| 2-13 | Simulated and Measured S22 Output Return Loss | 17 |
| 2-14 | Simulated and Measured S23 Output Port Isolation | 17 |
| 2-15 | 3D view of UWB multilayer slot line power divider | 18 |

| | | |
|---|---|---|
| 2-16 | Top view of UWB multilayer slot line power divider | 19 |
| 2-17 | Even-mode circuit mode | 19 |
| 2-18 | Odd-mode circuit model | 19 |
| 2-19 | Top and Bottom view of fabricated UWB multilayer slot line power divider | 20 |
| 2-20 | Amplitude Response of UWB multilayer slot line power divider | 20 |
| 3-1 | Configuration of In-Phase Power Divider | 23 |
| 3-2 | In-Phase Power Divider (Top View) | 24 |
| 3-3 | In-Phase Power Divider (3D view) | 24 |
| 3-4 | Photograph of In-Phase Power Divider | 24 |
| 3-5 | Transmission Line Model of In-Phase Power Divider | 25 |
| 3-6 | Feed lines representation | 26 |
| 3-7 | Rectangular patches representation | 27 |
| 3-8 | Coupled Microstrip Lines Representation | 27 |
| 3-9 | Centre Rectangular Patch Representation | 28 |
| 3-10 | Amplitude Response of In-Phase Power Divider (Simulation VS Experiment | 29 |
| 3-11 | Phase Response of In-Phase Power Divider (Simulation VS Experiment) | 30 |
| 3-12 | Amplitude Response of In-Phase Power Divider (Simulation VS Modelling) | 30 |
| 3-13 | Phase Response of In-Phase Power Divider (Simulation VS Modelling) | 31 |
| 3-14 | Dimensions of proposed In-Phase Power Divider | 32 |
| 3-15 | Amplitude Response due to uniform variation of gaps | 32 |
| 3-16 | Amplitude Response due to variation in gap 1 | 33 |

| | | |
|---|---|---|
| 3-17 | Amplitude Response due to variation in gap 2 | 34 |
| 3-18 | Amplitude Response due to variation in gap 3 | 35 |
| 3-19 | Amplitude Response due to variation in gap 4 and 5 | 36 |
| 3-20 | Amplitude Response due to uniform patch length variation | 37 |
| 3-21 | Amplitude Response due to patch length 1 variation | 38 |
| F3-22 | Amplitude Response due to patch length L2 variation | 39 |
| 3-23 | Phase Response due to patch length L2 variation | 39 |
| 3-24 | Amplitude Response due to patch length L3 variation | 40 |
| 3-25 | Phase Response due to patch length L3 variation | 40 |
| 3-26 | Amplitude Response due to patch length L4 variation | 41 |
| 3-27 | Amplitude Response due to patch length L5 variation | 42 |
| 3-28 | Amplitude Response due to uniform variation of patch width | 43 |
| 3-29 | Amplitude Response due to variation of patch width W1 | 44 |
| 3-30 | Amplitude Response due to variation of patch width W2 | 45 |
| 3-31 | Amplitude Response due to variation of patch width W3 | 46 |
| 3-32 | Amplitude Response due to variation of patch width W4 | 47 |
| 3-33 | Configuration of out-of-phase power divider | 48 |
| 3-34 | Out-of-phase power divider (Top View) | 49 |
| 3-35 | Out-of-phase power divider (3D View) | 49 |

| | | |
|---|---|---|
| 3-36 | Photograph of fabricated Out-of-Phase Power Divider | 49 |
| 3-37 | Transmission Line Model for Out-of-Phase Power Divider | 50 |
| 3-38 | Amplitude Response of Out-of-Phase Power Divider Simulation VS Experiment) | 51 |
| 3-39 | Phase Response of Out-of-Phase Power Divider (Simulation VS Experiment) | 52 |
| 3-40 | Amplitude Response of Out-of-Phase Power Divider (Simulation VS Modeling) | 53 |
| 3-41 | Phase Response of Out-of-Phase Power Divider (Simulation VS Modelling) | 53 |
| 3-42 | Dimensions of proposed Out-of-Phase Power Divider | 54 |
| 3-43 | Amplitude Response due to uniform gap variation | 55 |
| 3-44 | Phase Response due to uniform gap variation | 55 |
| 3-45 | Amplitude Response due to variation of gap 1 | 56 |
| 3-46 | Phase response due to variation of gap 1 | 56 |
| 3-47 | Amplitude Response due to variation of gap 2 | 57 |
| 3-48 | Phase Response due to variation of gap 2 | 58 |
| 3-49 | Amplitude Response due to variation of gap 3 | 59 |
| 3-50 | Phase Response due to variation of gap 3 | 59 |
| 3-51 | Amplitude Response due to variation of gap 4 and gap 5 | 60 |
| 3-52 | Phase response due to variation of gap 4 and gap 5 | 60 |
| 3-53 | Amplitude Response due to uniform variation of patch length | 61 |
| 3-54 | Phase Response due to uniform variation of patch length | 62 |
| 3-55 | Amplitude Response due to variation of patch length L1 | 63 |

| | | |
|---|---|---|
| 3-56 | Phase Response due to variation of patch length L1 | 63 |
| 3-57 | Amplitude Response due to variation of patch length L2 | 64 |
| 3-58 | Phase Response due to variation of patch length L2 | 64 |
| 3-59 | Amplitude Response due to variation of patch length L3 | 65 |
| 3-60 | Phase Response due to variation of patch length | 66 |
| 3-61 | Amplitude Response due to variation of patch length L4 | 67 |
| 3-62 | Phase Response due to variation of patch length L4 | 67 |
| 3-63 | Amplitude Response due to variation of patch length L5 | 68 |
| 3-64 | Phase Response due to variation of patch length L5 | 68 |
| 3-65 | Amplitude Response due to uniform variation of patch width | 69 |
| 3-66 | Phase Response due to uniform variation of patch width | 70 |
| 3-67 | Amplitude Response due to variation of patch width W1 | 70 |
| 3-68 | Phase Response due to variation of patch width W1 | 71 |
| 3-69 | Amplitude Response due to variation of patch width W2 | 72 |
| 3-70 | Phase Response due to variation of patch width W2 | 72 |
| 3-71 | Amplitude Response due to variation of patch width W3 | 73 |
| 3-72 | Phase Response due to variation of patch width W3 | 73 |
| 3-73 | Amplitude Response due to variation of patch width W4 | 74 |

| | | |
|---|---|---|
| 3-74 | Phase Response due to variation of patch width W4 | 74 |
| 3-75 | E-Field at 5.0GHz (In-Phase Divider) | 75 |
| 3-76 | E-Field at 3.58GHz (Out-Phase Divider) | 76 |
| 3-77 | E-Field at 5.00GHz (Out-Phase Divider) | 76 |
| 4-1 | Configuration of the 3-way power divider | 78 |
| 4-2 | 3-way Power Divider (Top View) | 79 |
| 4-3 | 3-way Power Divider (3D View) | 79 |
| 4-4 | Photograph of fabricated 3-way Power Divider | 80 |
| 4-5 | Transmission Line Model of 3-way Power Divider | 80 |
| 4-6 | Representation of feed line and partial rectangular patch | 81 |
| 4-7 | Representation of extra part of rectangular patch | 82 |
| 4-8 | Representation of centre patch | 82 |
| 4-9 | Representation of coupled lines | 83 |
| 4-10 | Amplitude Response of 3-Way Power Divider (Simulated VS Measured) | 84 |
| 4-11 | Phase Response of 3-Way Power Divider | 85 |
| 4-12 | Amplitude Response of 3-Way Power Divider (Simulated VS Modelling) | 85 |
| 4-13 | Phase Response of 3-Way Power Divider (Simulated VS Modelling) | 86 |
| 4-14 | Dimensions of proposed Multi-way Power Divider | 87 |
| 4-15 | Amplitude Response due to variation of length L1 | 87 |
| 4-16 | Phase Response due to variation of length L1 | 88 |
| 4-17 | Amplitude Response due to variation of length L2 | 89 |
| 4-18 | Phase Response due to variation of length L2 | 89 |
| 4-19 | Amplitude Response due to variation of length L3 | 90 |

| | | |
|---|---|---|
| 4-20 | Phase Response due to variation of length L3 | 90 |
| 4-21 | Amplitude Response due to variation of length L4 | 91 |
| 4-22 | Phase Response due to variation of length L4 | 92 |
| 4-23 | Amplitude Response due to variation of length L5 | 93 |
| 4-24 | Phase Response due to variation of length L5 | 93 |
| 4-25 | Amplitude Response due to variation of length L6 | 94 |
| 4-26 | Phase Response due to variation of length L6 | 94 |
| 4-27 | Amplitude Response due to variation of width W1 | 95 |
| 4-28 | Phase Response due to variation of width W1 | 95 |
| 4-29 | Amplitude Response due to variation of width W2 | 96 |
| 4-30 | Phase Response due to variation of width W2 | 96 |
| 4-31 | Amplitude Response due to variation of width W3 | 97 |
| 4-32 | Phase Response due to variation of width W3 | 97 |
| 4-33 | Amplitude Response due to variation of width W4 | 98 |
| 4-34 | Phase Response due to variation of width W4 | 98 |
| 4-35 | Amplitude Response due to variation of width W5 | 99 |
| 4-36 | Phase Response due to variation of width W5 | 99 |
| 4-37 | Amplitude Response due to variation of gap G1 | 100 |
| 4-38 | Phase Response due to variation of gap G1 | 100 |
| 4-39 | Amplitude Response due to variation of gap G2 | 101 |
| 4-40 | Phase Response due to variation of gap G2 | 101 |
| 4-41 | Amplitude Response due to variation of gap G3 | 102 |
| 4-42 | Phase Response due to variation of gap G3 | 102 |
| 4-43 | Amplitude Response due to variation of gap G6 | 103 |
| 4-44 | Phase Response due to variation of gap G6 | 103 |

| | | |
|---|---|---|
| 4-45 | E-field at 3.58GHz | 104 |
| 4-46 | E-field at 4.06GHz | 105 |
| 4-47 | E-field at frequency beyond passband | 105 |

# LIST OF SYMBOLS / ABBREVIATIONS

| | |
|---|---|
| $c_p$ | specific heat capacity, J/(kg·K) |
| $h$ | height, m |
| $K_d$ | discharge coefficient |
| $M$ | mass flow rate, kg/s |
| $P$ | pressure, kPa |
| $P_b$ | back pressure, kPa |
| $R$ | mass flow rate ratio |
| $T$ | temperature, K |
| $v$ | specific volume, $m^3$ |
| | |
| $\alpha$ | homogeneous void fraction |
| $\eta$ | pressure ratio |
| $\rho$ | density, $kg/m^3$ |
| $\omega$ | compressible flow parameter |
| | |
| ID | inner diameter, m |
| MAP | maximum allowable pressure, kPa |
| MAWP | maximum allowable working pressure, kPa |
| OD | outer diameter, m |
| RV | relief valve |

# CHAPTER 1

# INTRODUCTION

## 1.1 Background

Microwave Engineering comprises study and implementation of electromagnetic (EM) waves that encompass frequency range between 1 GHz to 100 GHz in the wave spectrum. It corresponds to a wavelength spanning from 30.0cm to 3.0mm in free space (Annapurna Das, Sisir K. Das, 2000, V.S Bagad, 2009). Since microwave engineering deals with short wavelengths, standard circuit theory can no longer be directly applied to solve microwave network problems because lumped circuit elements approximations are no longer valid at microwave frequencies (David M. Pozar, 2005).

Microwave engineering became essentially important in the 40's especially during World War II as it had enabled the development of high-resolution radars, which were extensively used for detecting and locating small objects such as enemy planes and ships through a narrow beam of EM energy (Annapurna Das, Sisir K. Das, 2000). Since the conception of radar, communication systems that are built upon microwave theory have begun to develop. Today, this field is playing a significant role in various applications such as radar, heating, environment remote sensing, and communication systems (David M. Pozar, 2005).

The new paradigm shift has resulted in tremendous social, economic and cultural impact to our society due to its superiority demonstrated by its power and great commercial value (Joseph Z Bih, 2003). Due to its vast potential and immense

benefits, most developed and developing countries have laid extensive efforts to further develop in the field. For instance, it has been reported that the Taiwan government has been placing enormous effort in accelerating microwave research activities for the past decade through the incorporation of various programs (Tzyy-Sheng Horng, Ching-KuangC.Tzuang, 2011). Several recent programs that were initiated include Promoting Academic Excellence at Universities (PPAEU), National Science Technology Program for Telecommunication (1999), Five Year Fifty Billion Plan for university development (2000 & 2006), Communications Engineering Program, and the Mobile Taiwan Program (2005) (Tzyy-Sheng Horng, Ching-KuangC.Tzuang, 2011).

## 1.2 Microwave Devices & Components

Generally, microwave devices and components can be divided into two categories, namely passive and active circuits. They are the fundamental building blocks of various microwave circuits and systems (Ke Wu, Lei Zhu, RuedigerVahldieck, 2006). Ke Wu *etal.*have observed that almost 75% of most microwave circuit elements are usually passive. Also, they further stated that active components (transistors, tubers, amplifiers, oscillators, etc) are not able to work without incorporating any passive ones (resistors, isolators, circulators, matching circuit, filters, etc).

### 1.2.1 Filters

Microwave filters are frequency selective transmission devices that incorporate a certain unique property which enables them to transmit energy in all passbands while attenuating energy beyond it (Ian C. Hunter, Laurent Billonet, Bernard Jarry, Pierre Guillon, 2002). Hence, they are solely used to control the frequency response at a certain point in the microwave system. Filters are categorized uniquely depending on the frequency response characteristics, namely low-pass, high-pass, band-pass, and band-reject/band-stop. Figure 1.0 illustrates the mentioned frequency response characteristics.

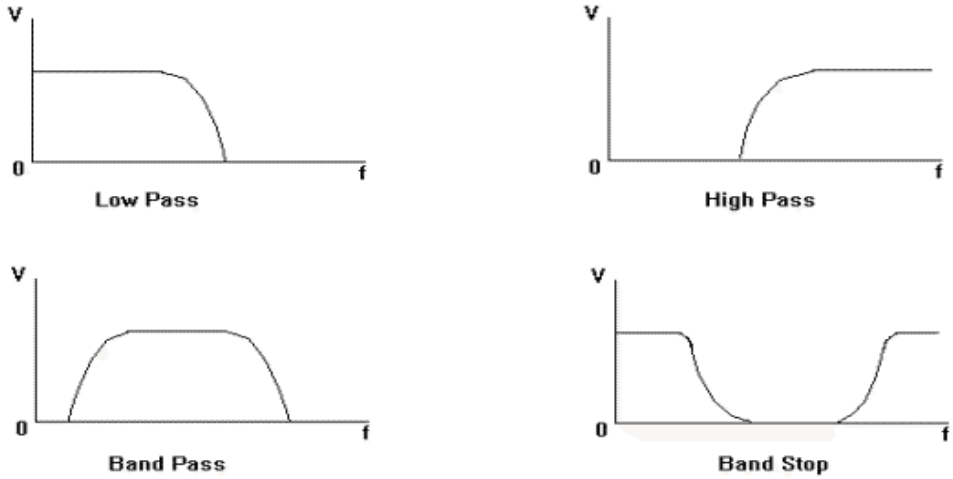


**Figure 1-1: Filter Frequency Response Characteristics**

Due to its importance, it is customary for microwave filters to exist virtually in any form of microwave systems, especially with the ever-increasing demand to conserve bandwidth given a congested microwave frequency spectrum (Albert E. Williams, Ali E. Atia, 1982). Microwave filter theory and practise began in the years preceding World War II, by pioneers like Mason, Sykes, Darlington, Fano, Lawson and Richards and was further developed by a group of researchers at Stanford Research Institute in the 50's (David M. Pozar, 1998).

Ian C. Hunter *etal.*, emphasised that designing microwave filters are normally achieved by using a low-pass prototype network as the point of origin, regardless of the eventual physical realization in transmission line, waveguide, or other media. They further added that a low-pass prototype networks are basically a two-port lumped-element networks that comprised an angular cut-off frequency of 1 rad/s and operates in a 1 ohm system. Today, most microwave filters design is done with sophisticated computer-aided-design (CAD) packages based on insertion loss method (David M. Pozar, 1998).

### 1.2.2 Amplifiers

A power amplifier is a circuit for converting dc-input power into a significant amount of microwave/RF output power (Frederick H. Raab et al, 2002) and is commonly found in most electronic systems (Carlos Fuentes, 2008), as amplification

is one of the most basic and prevalent microwave circuit functions (David M. Pozar, 1998). For instance, microwave amplifiers can be applied in testing passive elements, such as antennas, and active devices such as limiter diodes or MMIC based power amplifiers (Carlos Fuentes, 2008).

During the early days, microwave amplifiers were implemented using klystron or travelling-waves tubes or two-terminal solid-state devices such as tunnel or varactor diodes. However, with the drastic development in transistor processing technology over the years, most microwave amplifiers today use three-terminal solid-state devices such as gallium arsenide field effect transistors (FETs), silicon bipolar transistors, heterojunction bipolar transistors (HBTs), and high electron mobility transistors (HEMTs) (David M. Pozar, 1998).

### 1.2.3 Directional Couplers

Directional couplers are circuits that can be found in most optical communications systems (Carlos Sanchez Sierra, 2010). They are capable of extracting a part of a signal that travels over a transmission line or waveguide, leaving the rest of power not coupled direct route at the exit (Carlos Sanchez Sierra, 2010). According to Robert E. Collin book published in 2001, a directional coupler is basically a four-port microwave junction in which two transmission lines pass close enough to each other for energy propagating on one line to coupler to the other line. Unlike hybrid couplers which split an input signal into two equal amplitude outputs, a directional coupler produces outputs that are unequal in amplitude.

Robert E. Collin further added that for an ideal directional coupler, a wave incident at port 1 will be coupled to both port 2 and port 3 leaving port 4 as vacant. Similarly, a wave incident at port 4 will be coupled to both port 2 and port 3 leaving port 1 as vacant. Therefore, both port 1 and port 4 are basically uncoupled. The same concept is applied for wave incident at either port 2 or port 3.

In order to characterize a directional coupler, the following 3 quantities can be applied (David M. Pozar, 1998).

a. Coupling
b. Directivity
c. Isolation

The coupling factor indicates the fraction of the input power that is coupled to the output port. Directivity is a measure of the coupler's ability to isolate forward and backward waves, as is the isolation. An ideal coupler would have infinite directivity and isolation.

## 1.3 Project Aims & Objectives

The main aim of this project is to design a publishable novel power divider, which is a patch power divider that is able to operate within the microwave frequency spectrum using microstrip technology. Therefore, the operating frequency of the designed power divider should lie anywhere between 1GHz to 100GHz in the spectrum. However, the network spectrum analysers in the UTAR laboratory are only capable to measure performance between 0.5 GHz to 8 GHz. Due to the hardware limitation and constraint during measurement, the design should be limited to operate in the range of 0.5GHz to 8GHz. Moreover, it is important that the design of the patch power divider operating frequencies can be used in commercial products.

In addition to that, the patch power divider should be small in size and must be light-weight. This is to prevent the design from consuming a large amount of space during implementation. Meanwhile, this will also allow cost savings in terms of material and space.

Besides that, the patch power divider is aimed to produce the following outputs. All output powers should be equally divided. For an ideal case, the output power for a two output port will be -3 dB and a three output port will be -4.7 dB. The output signals should also either be in-phase, 180 degree out-phase, or both. Furthermore, the insertion loss should be less than -10 dB in the pass band of the power divider. Lastly, the power divider should operate with a reasonable bandwidth.

## 1.4 Project Motivation

The author main motivation of the project is to generate new design ideas that are still unknown in this research field. Generating novel ideas provides the author the opportunity to produce journals for publication. Publication allows the author to share new knowledge to others that are also involved in this research field. During the course of the research, the author will be able to learn proper research methodologies and analytical work which may be important in future researches.

## 1.5 Thesis Overview

In this section, the author will provide an overview of the thesis. Here, readers are able to anticipate the scope of discussion that will be incorporated by the author related to his work. Contents of each chapter will be briefly summarized.

To begin with, there are 5 major chapters which commence with the introduction, followed with literature review, patch power divider design, multi-way power divider design, and future work along with recommendations. References to journals are liberally included throughout the thesis to enable interested readers to delve into additional reading for additional learning.

Chapter 1 provide readers overview of the author entire project, his research aims and objectives, project motivation, and design methodologies applied to accomplish importance design tasks. In addition to that, this chapter also gives introduction to Microwave Engineering which touches on the background of microwave theory, its history and implementation in today systems, and efforts to further develop this field. Other common microwave elements are also briefly introduced to readers in this chapter.

In chapter 2, an extensive coverage based upon designing microwave power dividers will be presented. The author will begin this chapter by introducing power dividers to readers that are used in today microwave system incorporated with its theory, working principles, and some important design considerations. During the

course of this chapter, readers will also be exposed to recent development of power dividers along with tools used by author to perform simulations and demonstration of results.

Chapter 3 and 4 will emphasise on the author designs which comprises of an in-phase power divider, an out-phase power divider and a 3-way power divider. In this chapter, the author will provide detailed information on his design work. All design configurations, analysis work, final results and discussions will be exhibited here.

In the final chapter, the author will present work that can be performed in the future along with his achievement during the entire course of the projectt

# CHAPTER 2

# LITERATURE REVIEW

## 2.1 Background

Power dividers and combiners are widely used in microwave and millimetre-wave systems as basic circuit components (Y. Wu, Y. Liu, X. Liu, 2008). The components are passive devices and are used for power division or power combining (Jensen, Warnock, 2009). In power division process, an input signal is divided by a divider into two (or more) signals of lesser power (David M. Pozar, 2007).

The simplest power divider is generally a three port microwave network such as Tee power divider while more complex power dividers are four port microwave networks such as directional couplers or hybrids (Jensen, Warnock, 2009). In most cases, power dividers are of the equal-division (3dB) type, but unequal power division ratios are also possible (David M. Pozar, 2007).

## 2.2 Power Divider

### 2.2.1 Theory

An ideal power divider would be matched at all ports, lossless, and reciprocal (Jensen &Warnick, 2009). The simplest power divider is a three port network shown in figure 2.1.

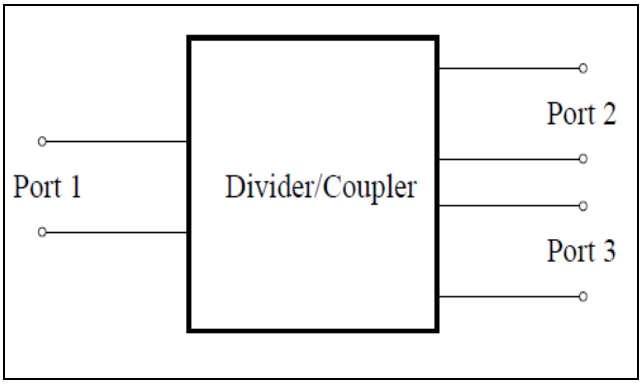


**Figure 2-1: Three port microwave network**

The S-parameters[1], can be used to illustrate the properties of the power divider network.

$$[S] = \begin{bmatrix} S_{11} & S_{12} & S_{13} \\ S_{21} & S_{22} & S_{23} \\ S_{31} & S_{32} & S_{33} \end{bmatrix}$$

[1]

Suppose all three ports are matched so that $S_{ii}= 0$, and that the network is reciprocal so that $S_{ij} = S_{ji}$. The most general possible S-matrix for a device with these properties is shown in [2]

$$[S] = \begin{bmatrix} 0 & S_{12} & S_{13} \\ S_{21} & 0 & S_{23} \\ S_{31} & S_{32} & 0 \end{bmatrix}$$

[2]

If the network is lossless, then this matrix must be unitary due to energy conservation (David M. Pozar, 2007), thus leading to [3].

$$|S_{12}|^2 + |S_{13}|^2 = 1 \; S_{13}S_{23} = 0$$
$$|S_{12}|^2 + |S_{23}|^2 = 1 \; S_{12}\, S_{13} = 0$$
$$|S_{13}|^2 + |S_{23}|^2 = 1 \; S_{12}\, S_{23} = 0$$

[3]

The second column in [3] shows that at least two of the three unique S-parameters must be zero. However, if two of the S-parameters were zero, then one of

the equations in the first column in [3] would not be valid. Therefore, it can strongly conclude that it is impossible to have lossless, matched, and reciprocal three port device. However, relaxing any one of these constraints makes it possible for the other two constraints to be satisfied, thus leading to possibilities for a network that is (Jensen & Warnock, 2009)

a. Lossless and reciprocal, but not matched;
b. Reciprocal and matched but lossy;
c. Matched and lossless using nonreciprocal material

### 2.2.2 Design considerations (Performance parameters)

There are various key parameters which are normally used in determining a power divider performance. The parameters are insertion loss, amplitude balance, phase balance, and isolation. These parameters are important to be considered during design.

Insertion loss is simply the difference in excess of the theoretical splitting loss (in dB) between the amplitude of any output signal and the amplitude of the input signal. Theoretically, the insertion loss for 2-way divider is 3dB, 6 dB for 4-way divider, 9-dB for 8-way divider and etc.

Amplitude balance is used to refer to the maximum amplitude difference between any two output signals. Normally for equal division power dividers, the maximum amplitude balance is kept below 1dB.

Phase Balance refers to the maximum phase deviation from theoretical, measured between any two output ports signals.

Isolation ( in dB) for a power divider is defined as the attenuation between a signal present at any output port and its level as measured at any other output port, with the input port terminated in 50 ohms. This is a critical parameter that allows design engineers to estimate “crosstalk” between various outputs.

## 2.3 Recent Developments

### 2.3.1 Power Divider with Non-Uniform Transmission Lines

A compact dual-band power divider using a non-uniform transmission line (NTL) is presented in this section. According to Y-F Bai *etal*., dual-band power dividers can be achieved by numerous design method, largely by using two cascaded sections of dual-band transmission lines or coupled resonator to achieve impedance transformation. As consequence, it is a challenge to reduce the power divider size effectively and the performance is too dependent on the fabrication techniques.

Here, Y-F Bai *etal.,* have discover a new method which is to directly synthesis pass-band impedance matching with a non-uniform transmission line. The concept behind it is to apply this direct synthesis method in a Wilkinson-type power divider. Using the theory of an even/odd mode equivalent circuit, a dual-band response can be illustrated. Y-F Bai *etal.,* further added that the size of power divider designed through this method is much more compact, since its length is approximately equivalent to one-quarter waveguide length of the lower design frequency of the two pass-band frequencies. Figures below illustrate the configuration of a non-uniform transmission line power divider by Y-F Bai *etal.,* ,both the even-mode and odd-mode circuit, and the photograph of the NTL power divider respectively.

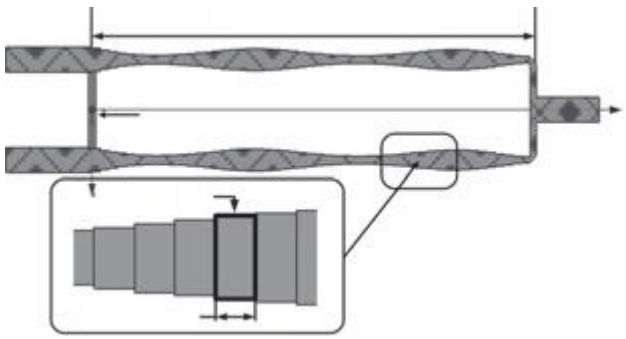

**Figure 2-2: Configuration of the Non-Uniform Transmission Line Power Divider**

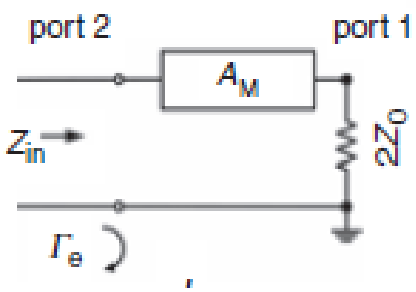


**Figure 2-3: Even-mode circuit**

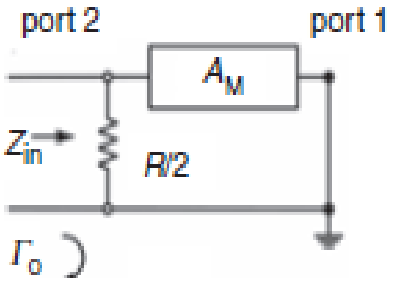


**Figure 2-4: Odd-mode circuit**

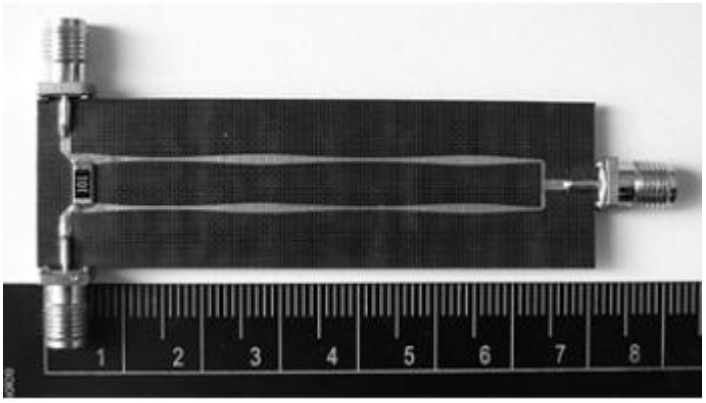


**Figure 2-5: Photograph of the NTL Power Divider**

According to Yao-Wen *etal.*, the characteristic impedance of the transmission line can represented by this function Z(x), where x is the coordinate in the direction of propagation, L is the total length of the transmission line that is equivalent to one-quarter waveguide length for the microstrip of the lower design frequency.

$$Z(x) = 50 \times \exp(x \ln 2/L - a_1 \sin(2\pi x/L)/(\pi x/L) - a_2 \sin(4\pi x/L)/(2\pi x/L)) \quad [1]$$

Based on the equation [1] shown above, $a_1$ and $a_2$ can be obtained from the equations [2] shown below.

$$\begin{pmatrix} C(1,1) & C(1,2) \\ C(2,1) & C(2,2) \end{pmatrix} \begin{pmatrix} a_1 \\ a_2 \end{pmatrix} = -(\ln 2/(2 \times L)) \begin{pmatrix} C(0,1) \\ C(0,2) \end{pmatrix} \quad [2]$$

C(m,n) is related to [3]

$$\iint_{-L/2}^{L/2} \int_{-L/2}^{L/2} Cos\left(\frac{2m\pi y}{L}\right) \cos\left(\frac{2n\pi y'}{L}\right) \left(sim\left(\frac{4\pi(y'-y)fa}{v}\right) - \sin\left(\frac{4\pi(y'-y)fb}{v}\right) + \sin\left(\frac{4\pi(y'-y)fc}{v}\right) - \sin\left(\frac{4\pi(y'-y)fd}{v}\right)\right)/2(y'-y)/v)dydy' \quad [3]$$

From the C(m,n) function [3], the two frequencies response bands can be obtained where $f_1$ =( $f_a$ + $f_b$) / 2 and $f_2$ =( $f_c$ + $f_d$) / 2.

Simulation and measurements of a 0.915 GHz/2.45 GHz power divider was carried out in order to validate the theory proposed. The results obtained from simulation and measurements are shown in figure below.

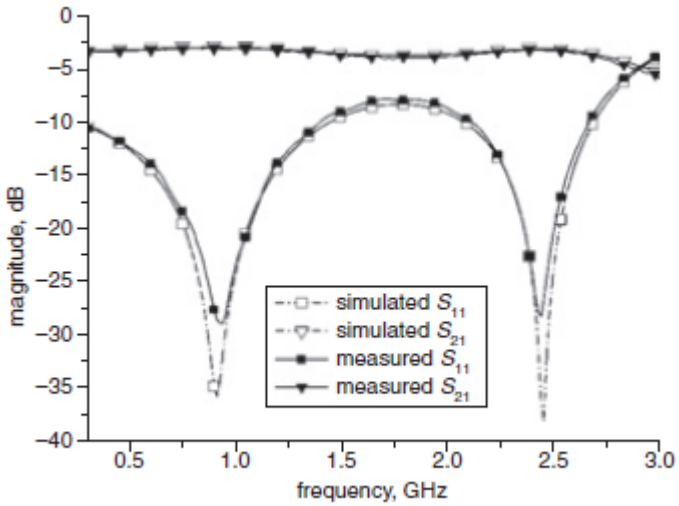


**Figure 2-6: Measured and Simulation results for S11 and S21**

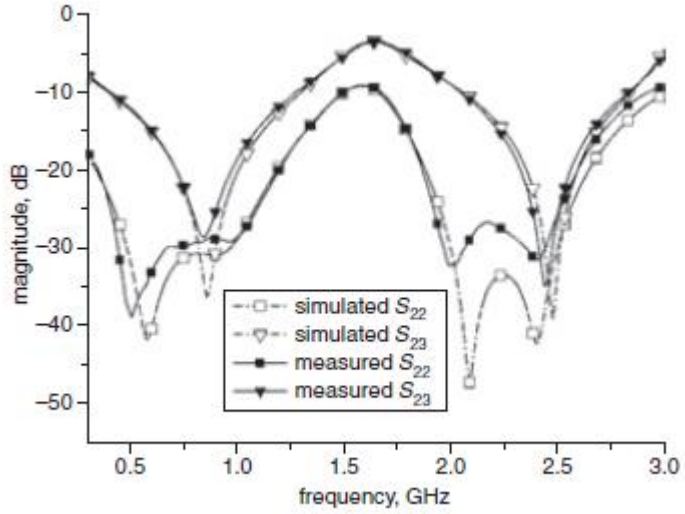


**Figure 2-7: Measured and Simulation results for S22 and S23**

From the graphs above, the measured data demonstrated good agreement with the anticipated results, thus concluding that a compact dual-bad power divider using a non-uniform transmission line can be develop from direct synthesis method.

### 2.3.2 Power Divider with Generalize Negative Refractive Index Transmission Lines

In the previous section, a dual-band power divider was reviewed. Here, the author will present the work of A. C. Papanastasiou, G. E. Georghiou and G. V. Eleftheriades which touches on a Quad-Band Wilkinson Power Divider that uses generalize negative-refractive-index transmission line unit cells.

According to A. C. Papanastasiou*etal.*,a band-controllable divider is essential in most quad-band applications. With the ability to control, four distinct pass bands of interest can be tailored. In addition to that, they also added that this divider also features a deep rejection band at its center frequency which can be applied for isolation and noise rejection.

Foremost, negative refractive index transmission line metamaterials holds unique dispersion properties (G. V. Eleftheriadesetal., 2002, C .Caloz and T. Itoh, 2003, M. Studniberg and G. V. Elefheriades, 2007) which is an important factor in

this power divider development. The concept of the design begins from the classical equal split Wilkinson divider. From there, A. C. Papanastasiou*etal.,*added two generalized NRI-TL unit cells in place of the γ/4 of the Wilkinson transmission line branches shown in figure 2-8. From the dispersion properties, four distinct frequencies for a transmission phase can be tabulated.

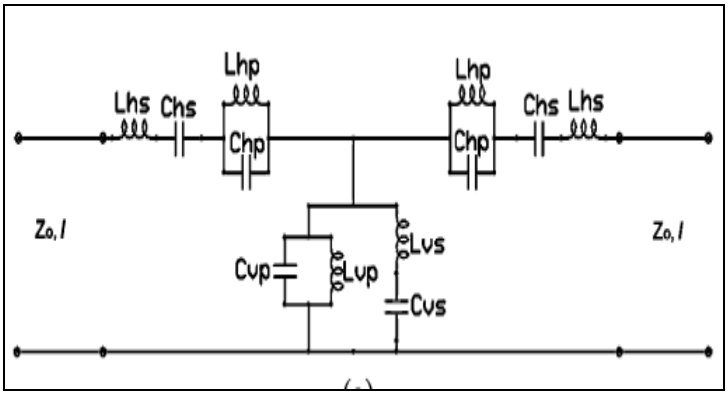


**Figure 2-8: Unit cell of generalized NRI-TL medium**

Figure 2-9 and figure 2-10 illustrate the generalized NRI-TL Wilkinson divider topology in microstrip and its actual fabrication.

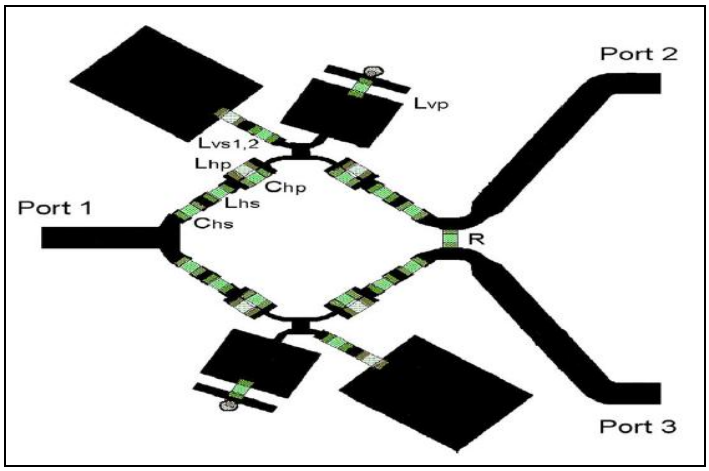


**Figure 2-9: Generalized NRI-TL Wilkinson divider topology in microstrip**

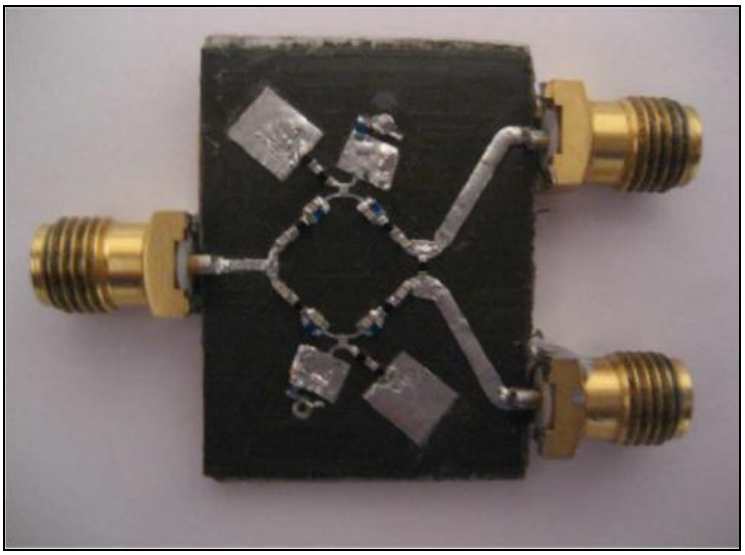

**Figure 2-10: Photograph of Generalized NRI-TL Wilkinson divider in microstrip**

The results that were obtained from the fabricated devices are shown in figures below.

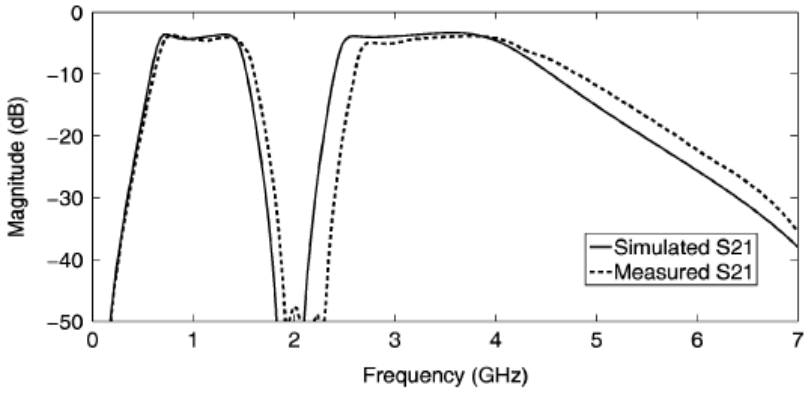


**Figure 2-11: Simulated and Measured S21 Amplitude Response**

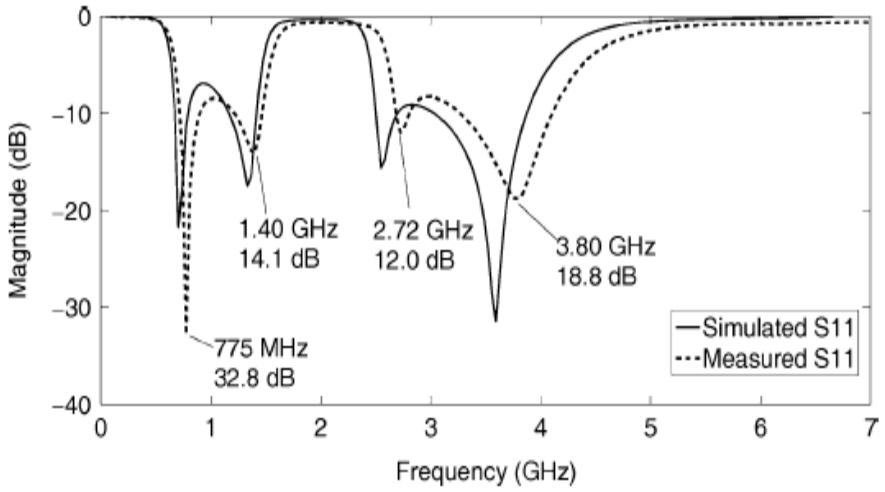


**Figure 2-12: Simulated and Measured S11 Amplitude Response**

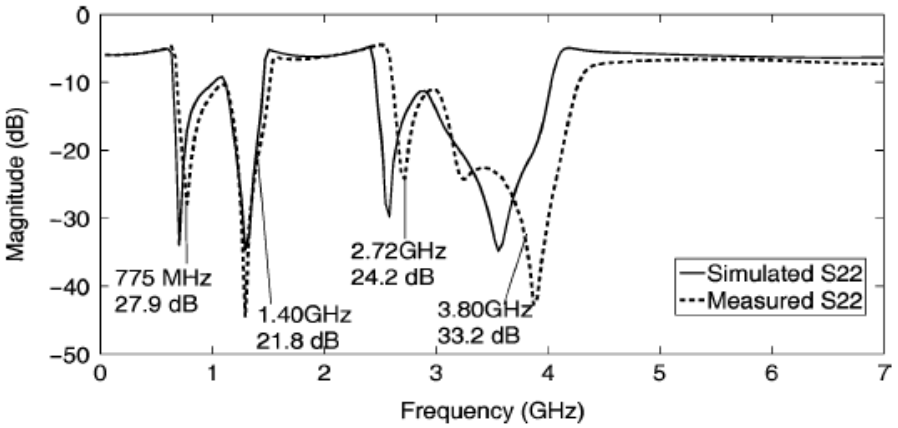


**Figure 2-13: Simulated and Measured S22 Output Return Loss**

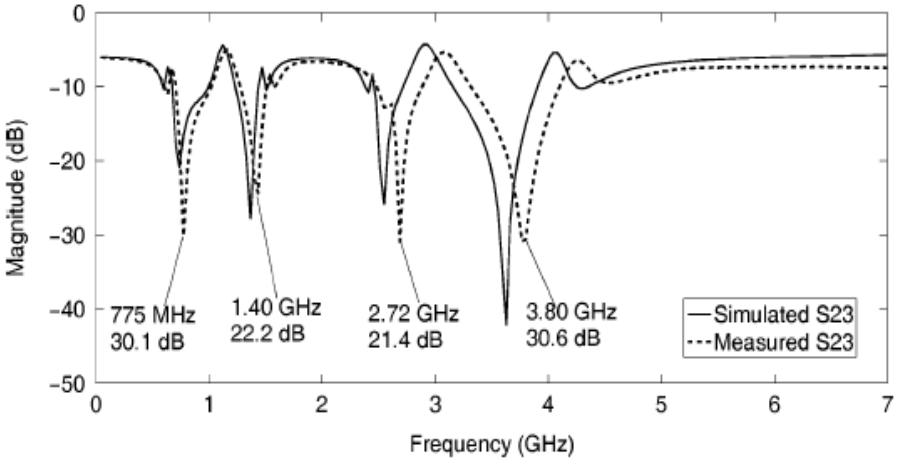


**Figure 2-14: Simulated and Measured S23 Output Port Isolation**

### 2.3.3 Power Divider with Multilayer Slot line

In this section, a novel ultra-wideband multilayer slot line power divider with bandpass filtering response will be presented. This structure was proposed by Kaijun Song.

According to his design, a single isolation resistor is properly placed between two output ports. By applying the transmission line equivalent circuit method, the proposed design was derived with even and odd mode analysis. Concepts regarding design of ultra wide band power dividers from various papers were applied to finalize this research. Here, Kaijun introduces multilayer microstrip line slot line coupling structure that can divide, combine power of microwave signals as well as rejecting unwanted frequency signals. The configuration of his design is shown in figure 2-15 and figure 2-16.

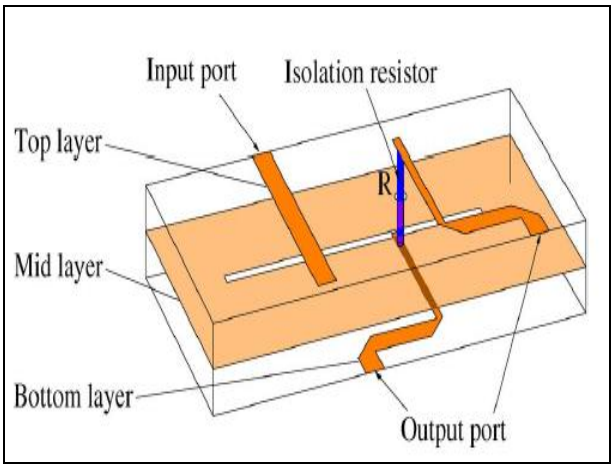


**Figure 2-15: 3D view of UWB multilayer slot line power divider**

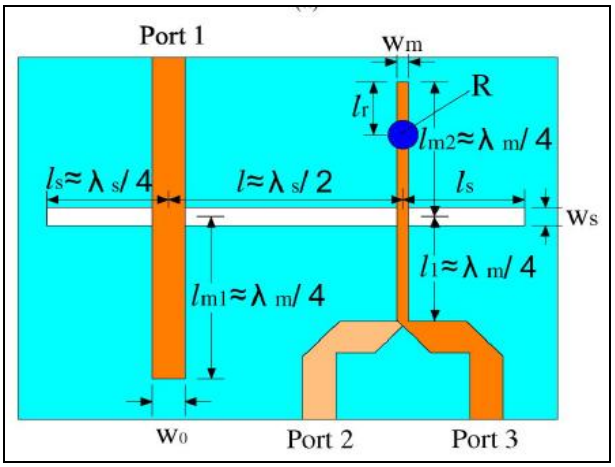


**Figure 2-16: Top view of UWB multilayer slot line power divider**

Using even and odd mode analysis, even and odd equivalent circuits are illustrated.

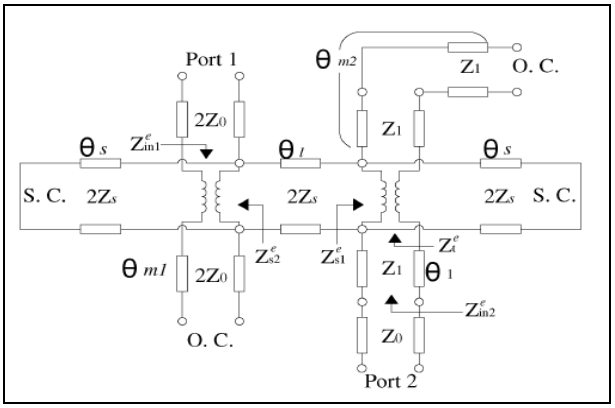


**Figure 2-17: Even-mode circuit mode**

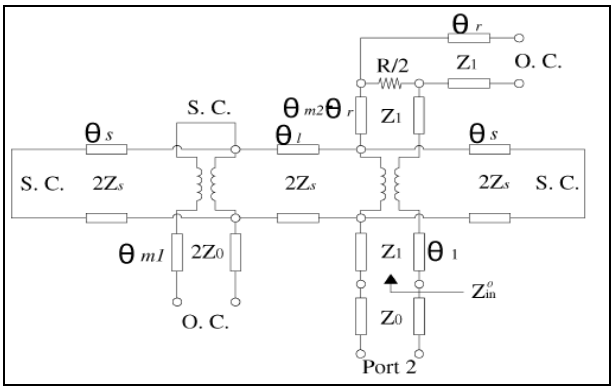


**Figure 2-18: Odd-mode circuit model**

After performing the calculations, the proposed design performances are measured. Figure below illustrates the performances and the fabricated device.

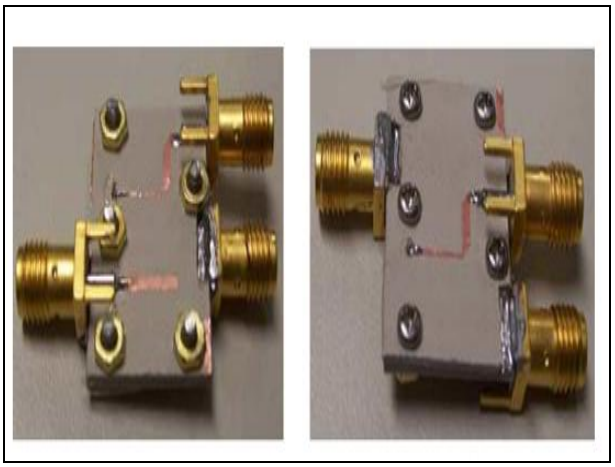

**Figure 2-19: Top and Bottom view of fabricated UWB multilayer slot line power divider**

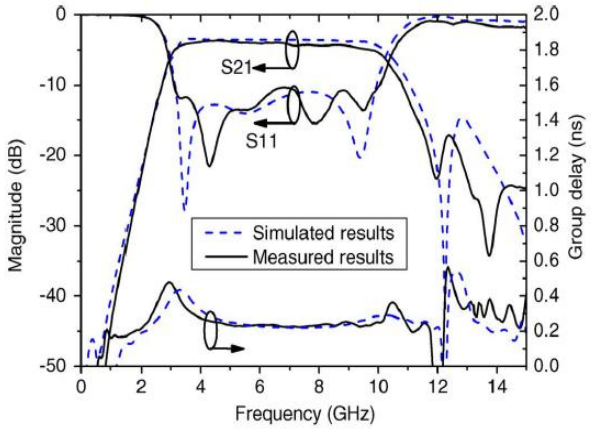


**Figure 2-20: Amplitude Response of UWB multilayer slot line power divider**

## 2.4 Introduction of Simulation Tools

In this project, two simulation tools are used to simulate the amplitude response and the phase response of the design. Through this software, the author is able to estimate the characteristics and performance of the design before performing any actual experiments.

### 2.4.1 High Frequency Simulation Structure

HFSS software is the industry-standard simulation tool for 3-D full-wave electromagnetic field simulation and is essential for the design of high-frequency and high-speed component design. HFSS offers multiple state-of the-art solver technologies based on either the proven finite element method or the well-established integral equation method. With HFSS, engineers can extract scattering matrix parameters (S, Y, Z parameters), visualize 3-D electromagnetic fields (near- and far-field) and generate ANSYS Full-Wave SPICE models that link to circuit simulations. Signal integrity engineers use HFSS within established EDA design flows to evaluate signal quality, including transmission path losses, reflection loss due to impedance mismatches, parasitic coupling and radiation. Each HFSS solver is based on a powerful, automated solution process where you are only required to specify geometry, material properties and the desired output.

### 2.4.2 Microwave Office

Microwave Office RF/microwave design software is the industry's fastest growing microwave design platform. Microwave Office has revolutionized the communications design world by providing users with a superior choice. Built on the unique AWR high-frequency design environment platform with its unique unified data model™, Microwave Office offers unparalleled intuitiveness, powerful and innovative technologies, and unprecedented openness and interoperability, enabling integration with best-in-class tools for each part of the design process.

Microwave Office design suite encompasses all the tools essential for high-frequency IC, PCB and module design, including:

a. Linear circuit simulators
b. Non-linear circuit simulators
c. Electromagnetic (EM) analysis tools
d. Integrated schematic and layout
e. Statistical design capabilities
f. Parametric cell libraries with built-in design-rule check (DRC).

# CHAPTER 3

# PATCH POWER DIVDER

## 3.1 Background

Power dividers can be classified into two types depending on the phase difference between the two output ports for a 2 way divider (J.-X. Chen, Z.-H.Bao, Q.Xue, 2009). They are classified as in-phase or out-of-phase power divider. One well known divider which offers a one to two equal dividing function is the Wilkinson power divider (Wai-Kai Chen, 2005). According to J.-X Chen *etal*., the most general design method to achieve an out of phase characteristic between the two output ports is to use a 180 degree electric length delay such as a ring hybrid. Recently, many researchers have developed several out of phase dividers using balanced transmission lines. In this chapter, two designs of power dividers will be presented by the author. Both dividers are designed using rectangular patch resonators. In the first section, the in-phase divider will be discussed followed by the out of phase.

## 3.2 In-Phase Patch Power Divider

### 3.2.1 Configuration

In this section, the author will illustrate the configuration of the in-phase patch power divider. Based on the configuration shown in figure 3.1, the in-phase power divider consists of three ports, which are numbered as Port 1, Port 2, and Port 3. Port 1 is the

input port. Both Port 2 and Port 3 are the output ports. All ports are connected to 50 ohm microstrip feed lines. The power divider model is non-symmetrical.

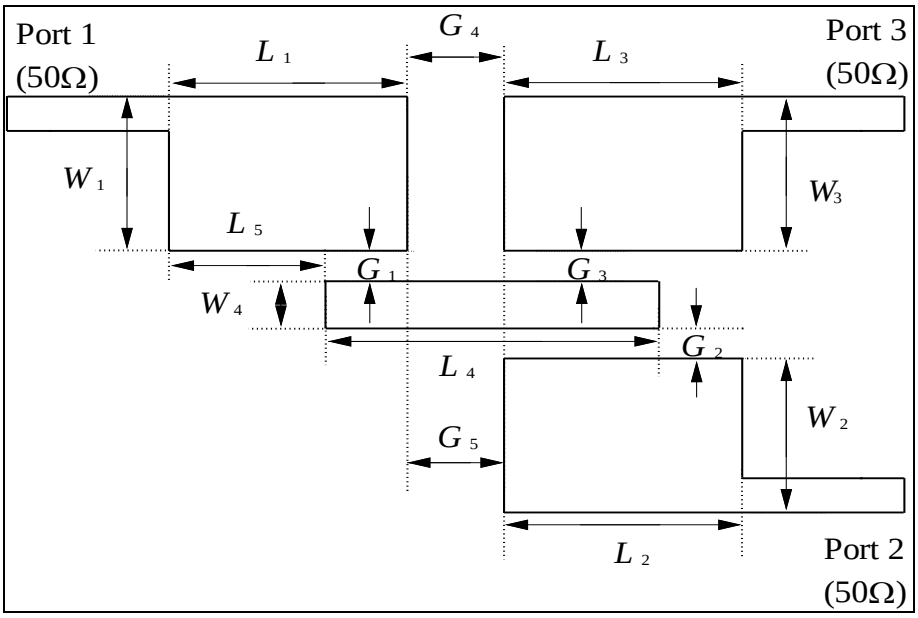


**Figure 3-1: Configuration of In-Phase Power Divider**

Here, the author emphasised on implementing rectangular patches as resonators. In this design, there are four rectangular patches in total. The 3 side rectangular patches which are connected to the input/output ports by 50 ohm feed lines have identical length and width. Each of the 3 side patches has an area of 24.8mm x 10.0mm = 248 $mm^2$. The rectangular patch in the centre has an area of 24.5mm x 1.0mm = 24.5$mm^2$. The area of the entire in-phase power divider is 41.4mm x 85.0mm = 3591.0$mm^2$.

The substrate used in implementing this design has a dielectric constant of 2.33 and a thickness of 1.57mm. In the following, the design dimensions of the entire configuration will be presented. L, W and G represent the parameters of length, width and gap respectively.

$L_1$ = 24.8mm, $L_2$ = 24.8mm, $L_3$ = 24.8mm, $L_4$ = 24.5mm, $L_5$ = 13.8mm, $W_1$ = 10.0mm, $W_2$ =10.0mm, $W_3$= 10.0mm, $W_4$ = 1.0mm, $G_1$ = 0.2mm, $G_2$ = 0.2mm, $G_3$ = 0.2mm, $G_4$ = 5.0mm, $G_5$ = 5.0mm

Figure 3.2 illustrates the top view configuration of the power divider in HFSS, Figure 3.3 display the configuration in 3D view, and Figure 3.4 is the photograph of the fabricated in-phase power divider.

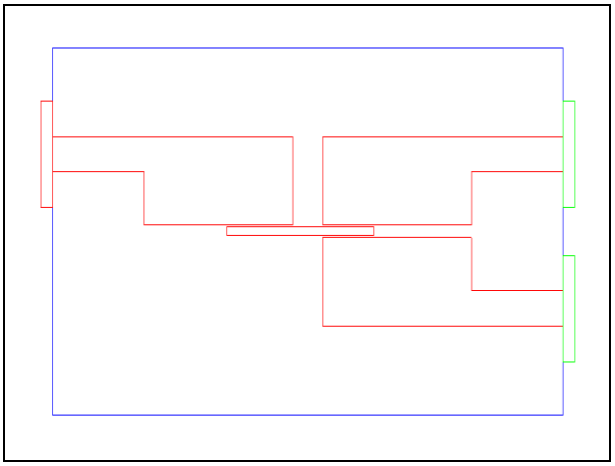

**Figure 3-2: In-Phase Power Divider (Top View)**

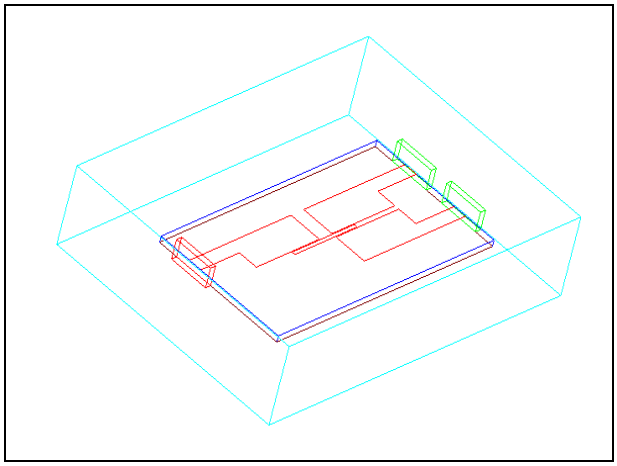

**Figure 3-3: In-Phase Power Divider (3D view)**

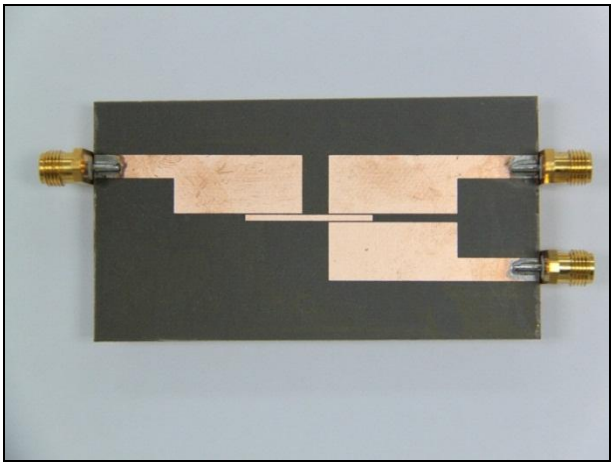

**Figure 3-4Photograph of In-Phase Power Divider**

### 3.2.2 Transmission Line Model

The previous section illustrated on the design configuration of the in-phase power divider. Here, the author will present the transmission line model that corresponds to the equivalent circuit of the proposed in-phase power divider. Figure 3.5 shows the transmission line model of the proposed device.

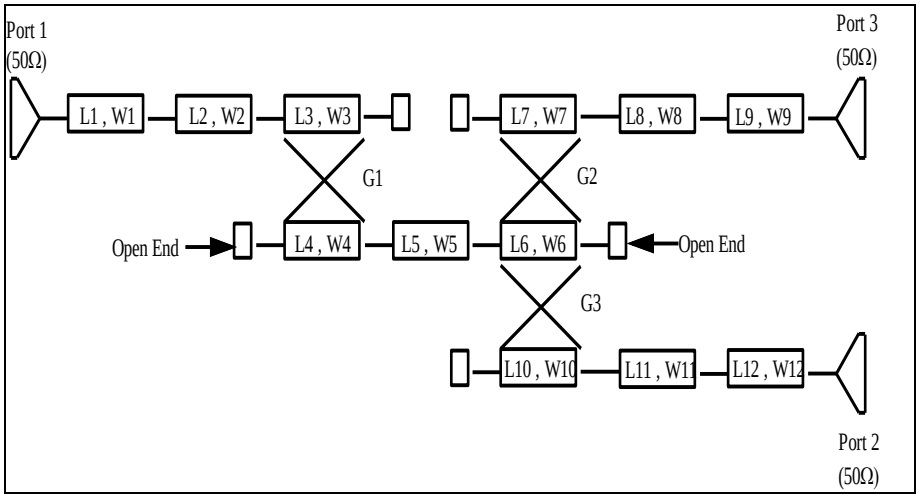


**Figure 3-5: Transmission Line Model of In-Phase Power Divider**

The table below shows the dimension of each element representation.

| LENGTH | (mm) |
|---|---|
| L1 | 15.2 |
| L2 | 13.8 |
| L3 | 11.0 |
| L4 | 11.0 |
| L5 | 5.0 |
| L6 | 8.5 |
| L7 | 8.5 |
| L8 | 16.3 |
| L9 | 15.2 |
| L10 | 8.5 |
| L11 | 16.3 |
| L12 | 15.2 |

| WIDTH | (mm) |
|---|---|
| W1 | 4.0 |
| W2 | 10.0 |
| W3 | 10.0 |
| W4 | 1.0 |
| W5 | 1.0 |
| W6 | 1.0 |
| W7 | 10.0 |
| W8 | 10.0 |
| W9 | 4.0 |
| W10 | 10.0 |
| W11 | 10.0 |
| W12 | 4.0 |

| GAP | (mm) |
|---|---|
| G1 | 0.2 |
| G2 | 0.2 |
| G3 | 0.2 |

**Table 3-1: Element Parameters for In-Phase Power Dividers**

Based on the transmission line model shown above, the triangular shape objects are used to represent passive circuit termination that applies a load specified by impedance. In this case, they represent the input (Port 1) and output ports (Port 2 and Port 3) of the device. It is a convention for all ports to be set as 50 ohms.All rectangular boxes filled incorporated with index characters represent the microstrip transmission lines. Both L and W represent the strip length and width respectively. During the implementation of the microstrip line component, the transmission model assumes a Quasi-TEM mode of propagation and incorporates the effects of dielectric and conductive losses. The highlighted sections in figure 3.6 represents the 50 ohm feed lines that connect between the ports and rectangular patches.

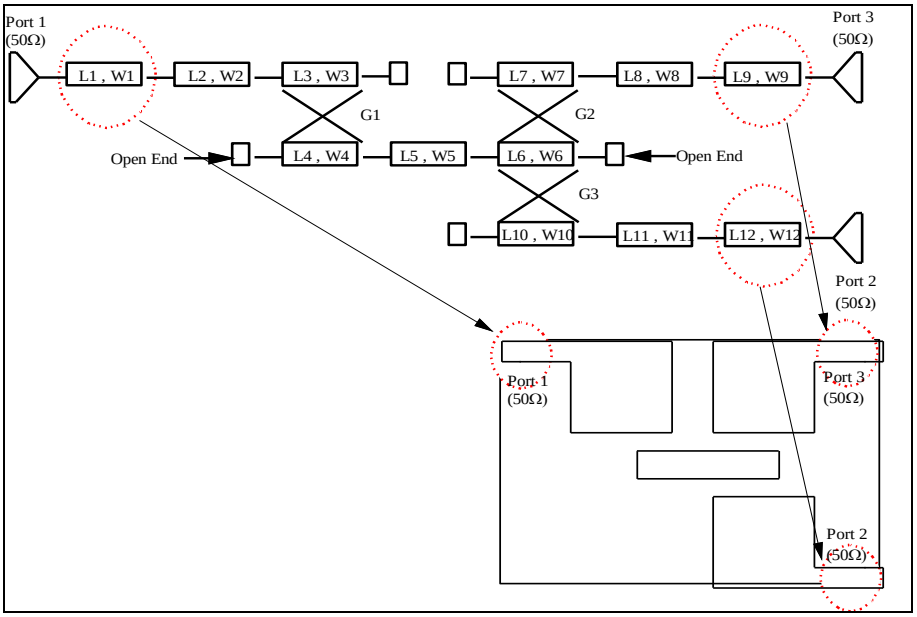


**Figure 3-6: Feed lines representation**

All side rectangular patches are represented by elements highlighted in figure 3.7. A rectangular patch is represented in two distinct parts because part of the rectangular patch is separated from the centre patch by a small gap of 0.2mm.Therefore, the coupling of mircostrip lines must be taken into consideration.

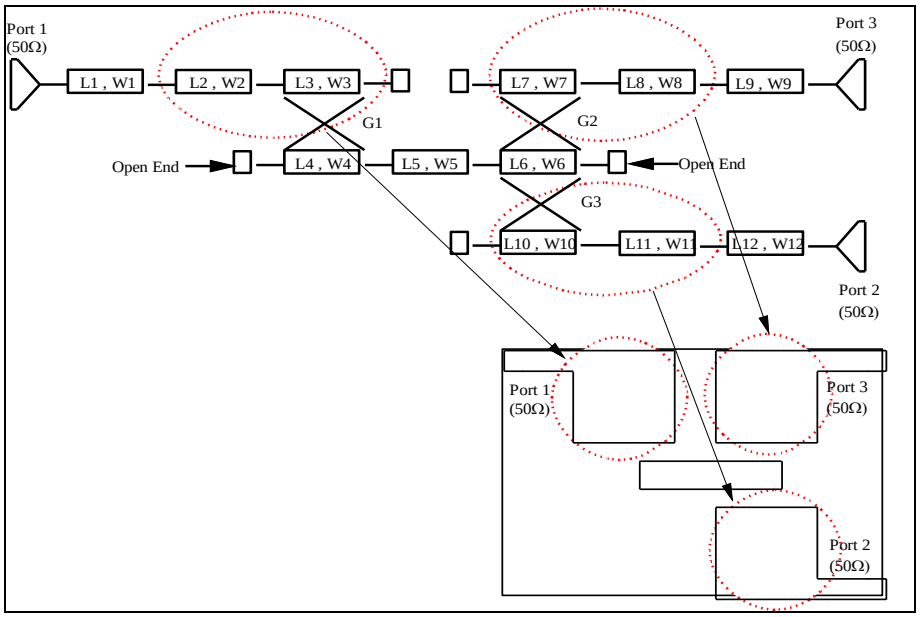


**Figure 3-7: Rectangular patches representation**

Two rectangular boxes connected in parallel by an "X" figure denote two microstrip lines that are coupled together. It is shown in figure 3.8. G represents the gap that separates both the microstrip lines. Same theory applies to three rectangular boxes that are connected in parallel. However, this time it represents 3 microstrip lines being coupled together.

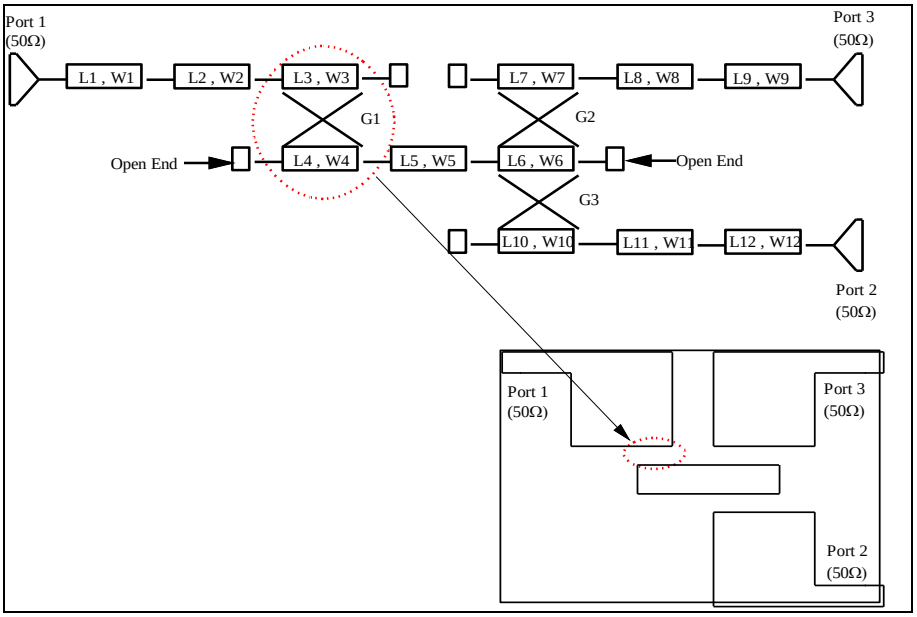


**Figure 3-8: Coupled Microstrip Lines Representation**

The 3 rectangular boxes connected in series represent the centre rectangular patch of the power divider, shown in figure 3.9.

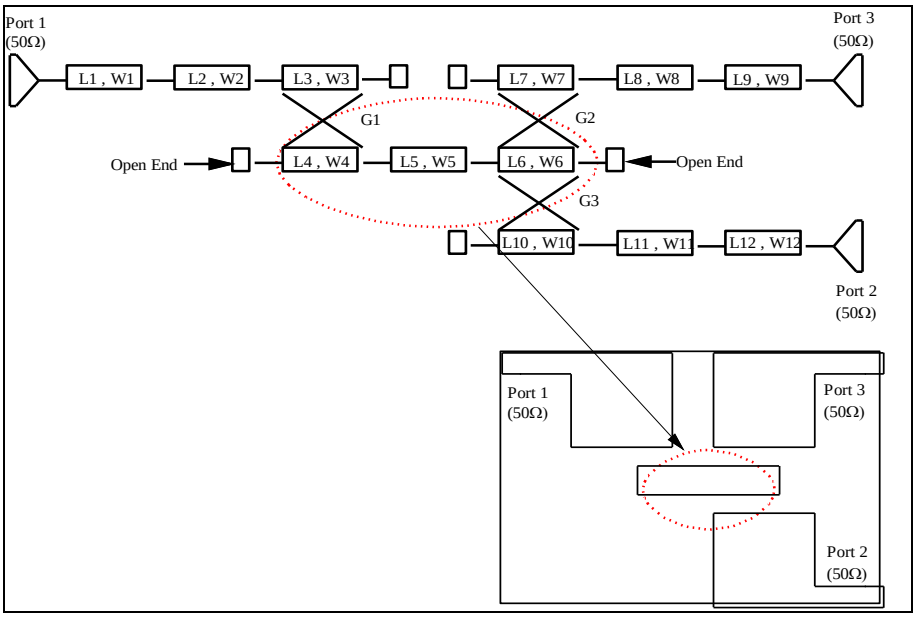


**Figure 3-9: Centre Rectangular Patch Representation**

Lastly, all open ends are represented by MOPEN which is known as microstrip open circuit with end effect.

### 3.2.3 Results

Now, all work results for the in-phase power divider are presented. Based on the proposed design configurations, an experiment was carried out to measure the performance of the divider. All simulation results were obtained from HFSS and all measurement results on the fabricated divider were acquired using an Agilent Vector Network Analyser (VNA). From the amplitude response and phase response graphs shown below, the experimental result exhibits good agreement with the simulation.

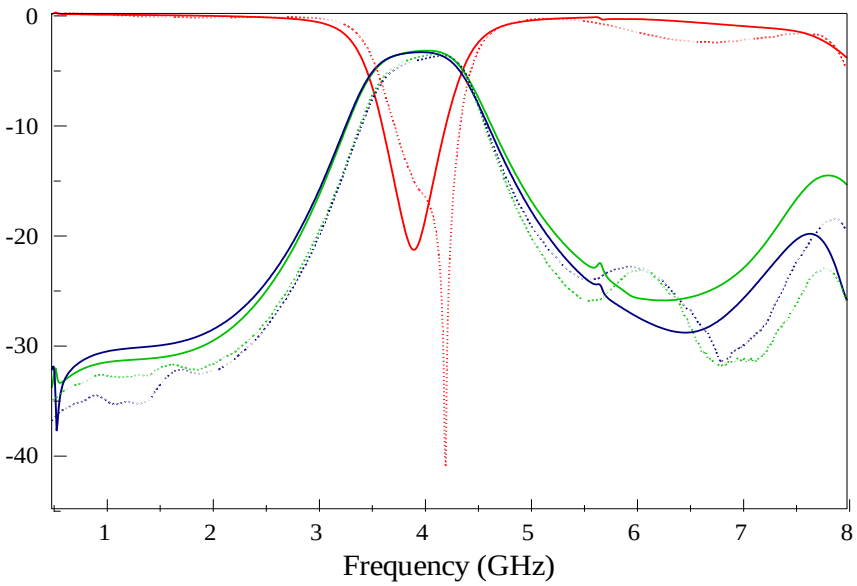


Figure 3-10: Amplitude Response of In-Phase Power Divider (Simulation VS Experiment)

It can be observed from the simulated amplitude response curve that the power divider has a passband from 3.61GHz to 4.21GHz, thus providing a passband bandwidth of 0.6GHz. The centre frequency is at 3.91GHz. Therefore, this corresponds to fractional bandwidth of 15.3%.

From the measured response curve, we can observe a slight shift in centre frequency. The passband of the fabricated divider is now approximately between 3.75GHZ to 4.25GHz, which provides passband bandwidth of 0.6GHz as well. This shows that both simulation and measurement have approximately equal operating bandwidth. The fractional bandwidth is 15%. However, lower frequency components seem to have poorer return loss due to impedance mismatch cause by minor defects during fabrication. Meanwhile, there is a good roll-off incorporated by the divider.

Both the simulated and measured S21 and S31 are approximately -3.5dB and virtually flat at the passband. This corresponds to equally divided input power to the outputs at all operating bands. Moreover, the $2^{nd}$ harmonics due to the fundamental frequency are deeply supressed. The error between the simulated and measured is 2.25%.

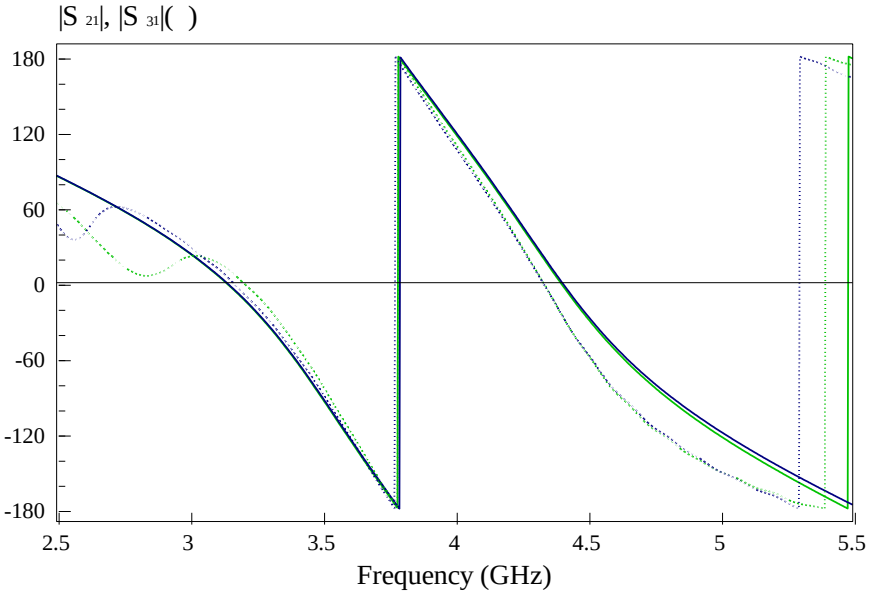


**Figure 3-11: Phase Response of In-Phase Power Divider (Simulation VS Experiment)**

Figure 3.11 illustrates the phase response of the in-phase power divider. It can be seen that both outputs are in-phase at all frequencies.

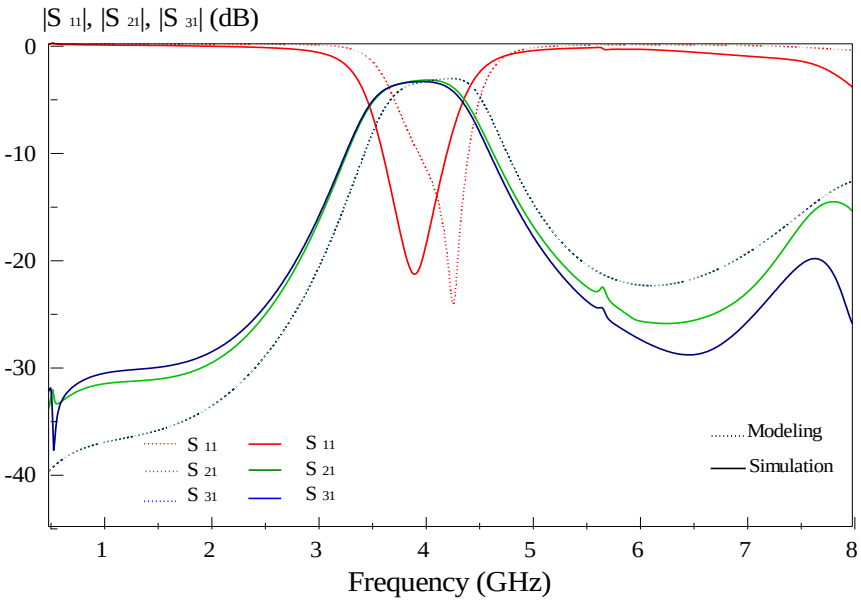


**Figure 3-12: Amplitude Response of In-Phase Power Divider (Simulation VS Modelling)**

Here, the modelling results are compared with the simulation results. All modelling values are acquired from Microwave Office. From figure 3.12, the modelling amplitude response curve demonstrates that the divider is able to operate

at frequencies between 3.9GHz to 4.4GHz, thus resulting a smaller passband bandwidth. At this point, the centre operating frequency of the transmission model divider is 4.15GHz which provides fractional bandwidth of 12%. The return loss is -24.1dB while the insertion loss is -3.39dB on average for both outputs.

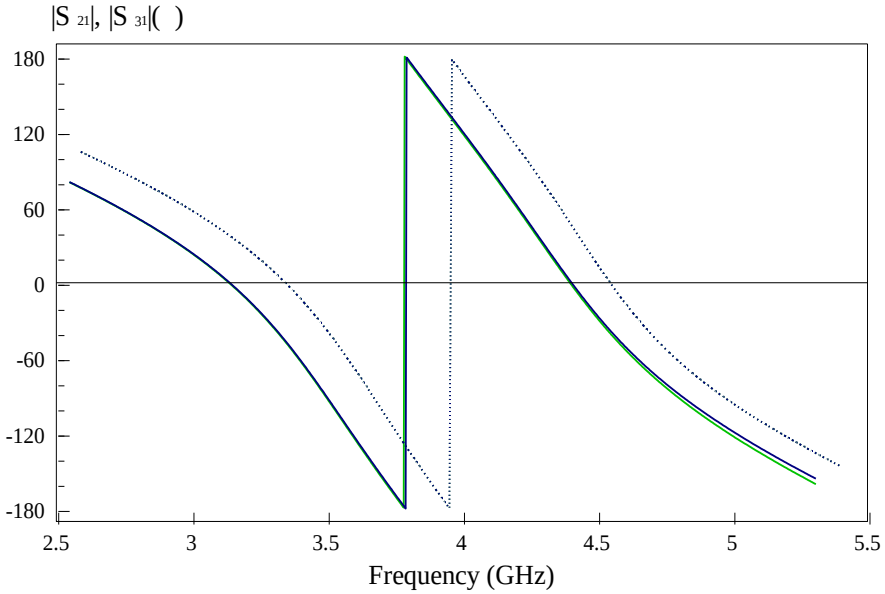


**Figure 3-13: Phase Response of In-Phase Power Divider (Simulation VS Modelling)**

Figure 3.13 illustrates the phase response of the in-phase power divider based on modelling. It can be seen that both outputs are in-phase at all frequencies.

### 3.2.4 Parametric Analysis

Parametric Analysis is a process of investigating the characteristics of the device by changing individual design parameters such as length, width, capacitance, inductance and etc. Based upon the characteristics obtained from the investigation, it allows us to understand the behaviour of the design parameters, thus enabling us to modify the design in order to achieve certain specifications.

In this section, the effects of each parameter are revealed by the author. Figure 3.14 displays the proposed design configurations together with the original dimensions.

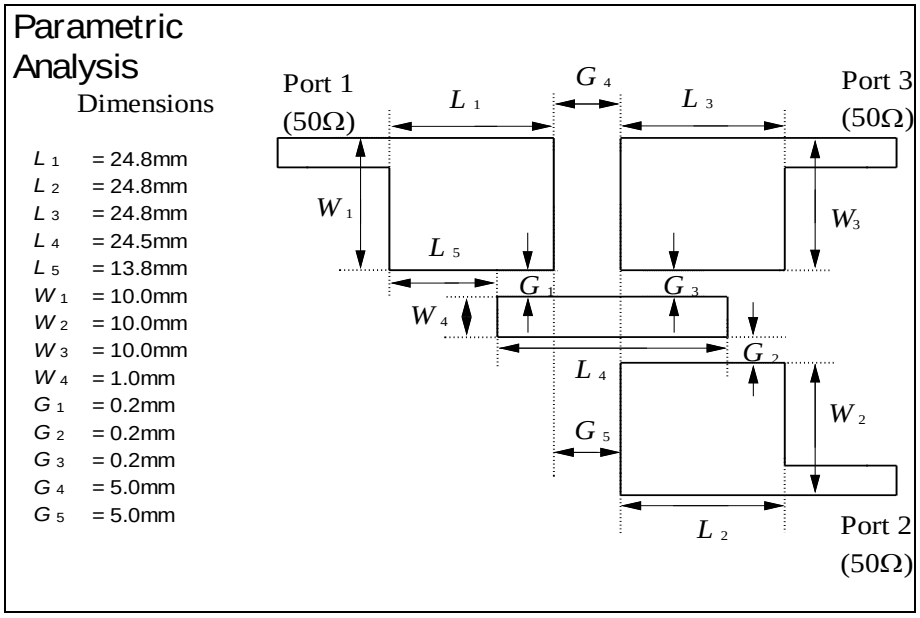


**Figure 3-14: Dimensions of proposed In-Phase Power Divider**

Case 1: Uniform variation of gaps

$G_1 = G_2 = G_3 = 0.1mm$

$G_1 = G_2 = G_3 = 0.2mm$

$G_1 = G_2 = G_3 = 0.3mm$

Results

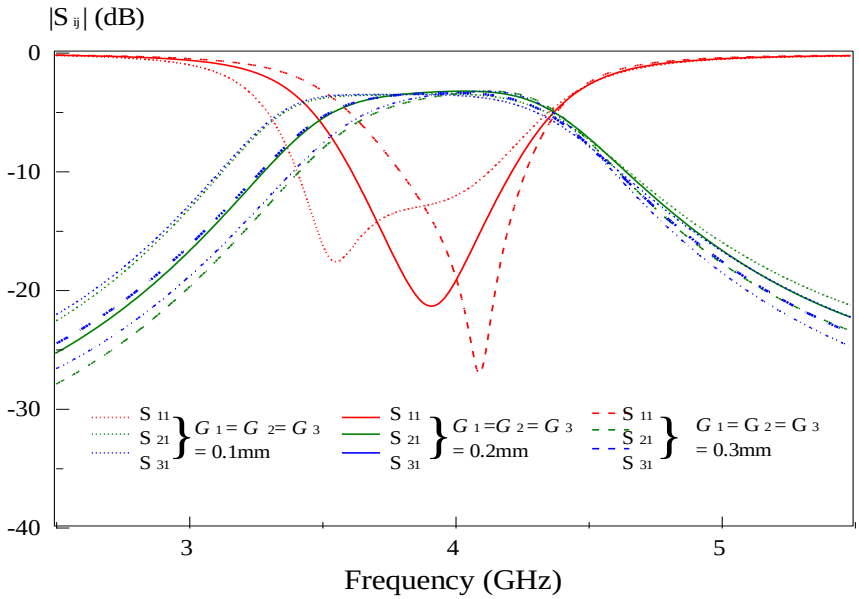


**Figure 3-15: Amplitude Response due to uniform variation of gaps**

Observation

Based on figure 3.15, we can observe that variation in gaps between patches (resonators) affects the return loss of the divider. The poles are shifted to the left for smaller gaps while shifted to the right when gaps are larger. Moreover, the return loss is much poorer at higher frequency components for smaller gaps while the return loss is much poorer at lower frequency components for larger gaps. Bandwidth of the passband and insertion loss approximately remains the same. Both outputs remain in phase.

Case 2: Variation of gap 1

$G_1$ = 0.1mm, $G_2$ = $G_3$= 0.2mm

$G_1$ = 0.2mm, $G_2$ = $G_3$= 0.2mm

$G_1$ = 0.3mm, $G_2$ = $G_3$= 0.2mm

Results

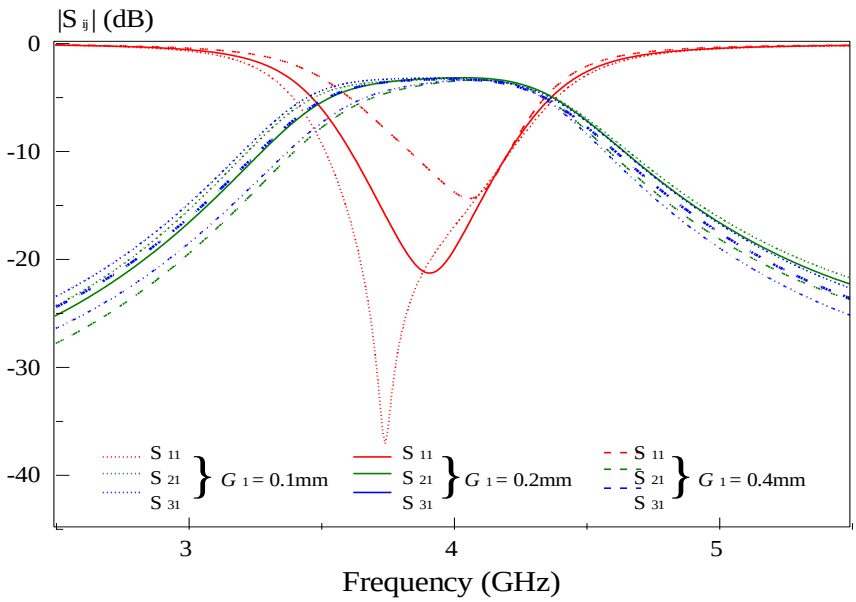


**Figure 3-16: Amplitude Response due to variation in gap 1**

Observation

From the amplitude response in figure 3.16, smaller gap exhibits better return loss (-38 dB) while larger gap causes poorer return loss (-15dB). Poles are shifted to the right when gaps are increased. Larger gap also leads to smaller bandwidth of passband. Both outputs still remain in-phase.

Case 2: Variation of gap 2

$G_2$ = 0.1mm, $G_1$ = $G_3$= 0.2mm

$G_2$ = 0.2mm, $G_1$ = $G_3$= 0.2mm

$G_2$ = 0.3mm, $G_1$ = $G_3$= 0.2mm

Results

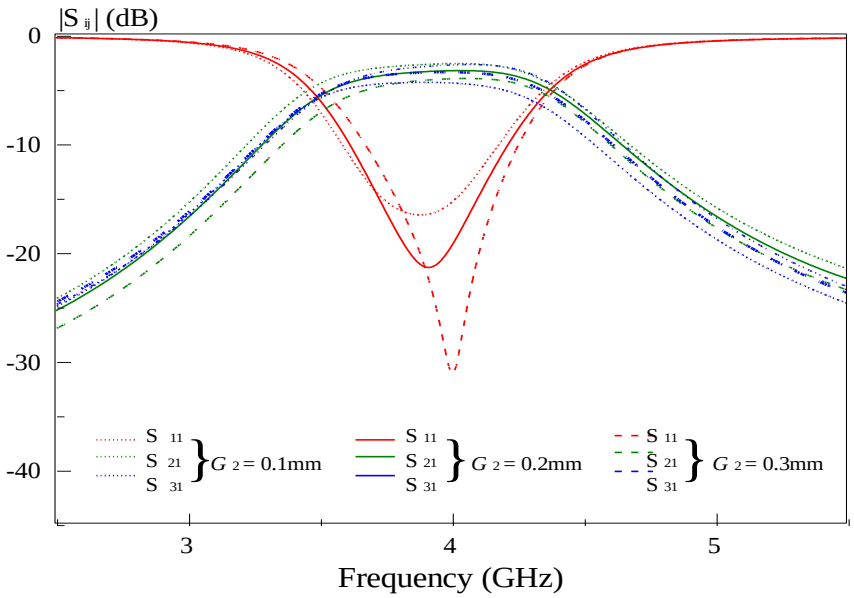


**Figure 3-17: Amplitude Response due to variation in gap 2**

Observation

We can observe the variation in gap 2 affects the return loss of the divider. Smaller gap exhibits higher return loss while larger gap displays smaller return loss. However, the insertion loss is much lower for larger gap. Poles position remains almost unchanged. Outputs signals remain in-phase.

Case 3: Variation of gap 3

$G_3$ = 0.1mm, $G_1$ = $G_2$ = 0.2mm

$G_3$ = 0.2mm, $G_1$ = $G_2$ = 0.2mm

$G_3$ = 0.3mm, $G_1$ = $G_2$ = 0.2mm

Results

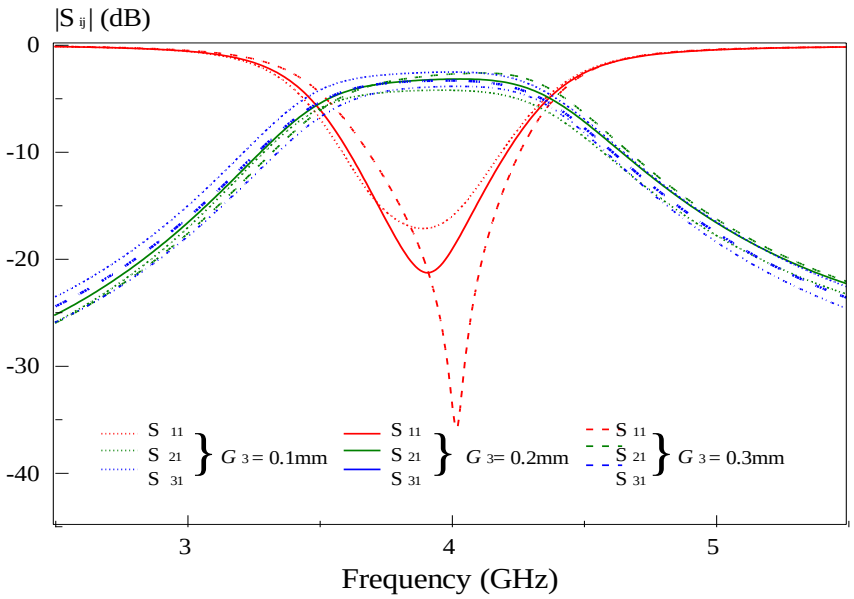


**Figure 3-18: Amplitude Response due to variation in gap 3**

Observation

Based on amplitude response shown in figure 3.18, it can observe that the variation in gap 3 affects the return loss of the divider most. Smaller gap exhibits higher return loss while larger gap displays smaller return loss. The passband bandwidth is slightly reduced when gap 3 is increased. Outputs signals remain in-phase.

Case 4: Variation of gap 4 and 5

$G_4 = G_5 = 4.0mm$

$G_4 = G_5 = 5.0mm$

$G_4 = G_5 = 6.0mm$

Results

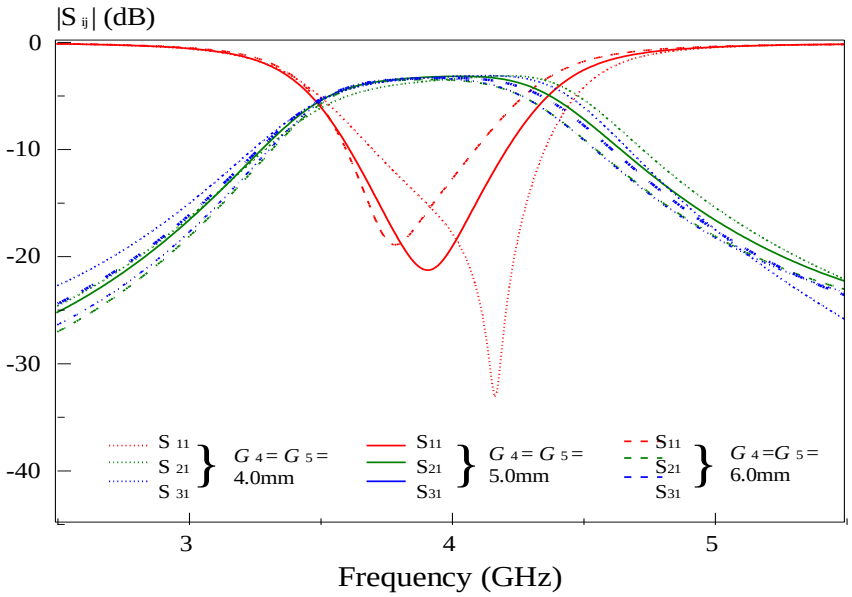


**Figure 3-19: Amplitude Response due to variation in gap 4 and 5**

Observation

Smaller gap between the left and right rectangular patches provides better return loss. Wider gap leads to poorer return loss. However, insertion loss remains unchanged. Poles position is shifted. Passband bandwidth decreases as gaps widen. Output signals remain in-phase.

Case 4: Uniform Variation of Patch Length

$L_1 = L_2 = L_3 = 22.0mm$

$L_1 = L_2 = L_3 = 24.8mm$

$L_1 = L_2 = L_3 = 27.0mm$

Results

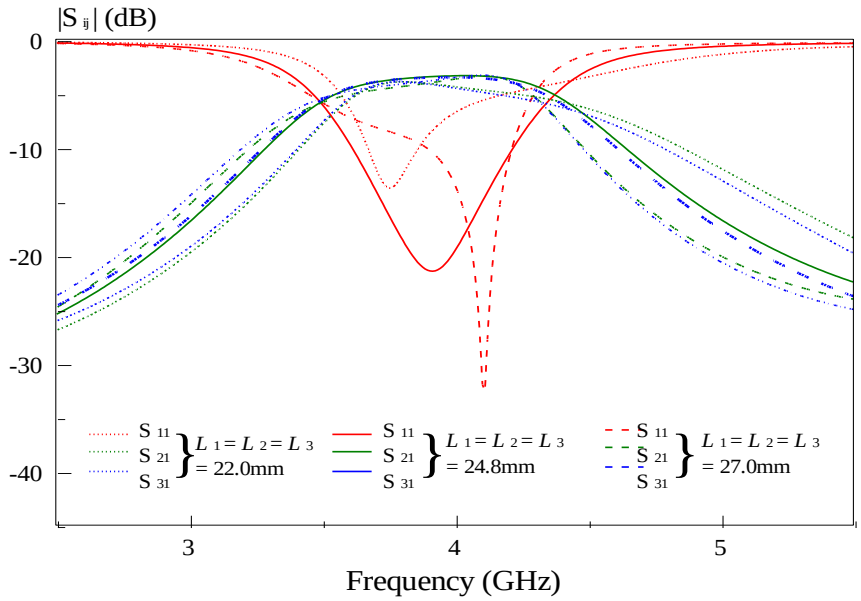


**Figure 3-20: Amplitude Response due to uniform patch length variation**

Observation

Through this investigation, we can notice that the rectangular patch length plays a major impact on the return loss of the divider. Patch length that is too short causes S11 to increase, thus reducing the divider performance. The passband bandwidth is significantly reduced and S21 and S23 are not flat. This causes output power to be non-constant at different frequencies. Patch length that is too long also causes poor return loss at the lower frequencies of the passband. Nevertheless, there is no variation in phase between outputs.

Case 5: Variation of Patch Length L1

$L_1$ =22.0mm, $L_2$ = $L_3$ = 24.8mm

$L_1$ =24.8mm, $L_2$ = $L_3$ = 24.8mm

$L_1$ =27.0mm, $L_2$ = $L_3$ = 24.8mm

Results

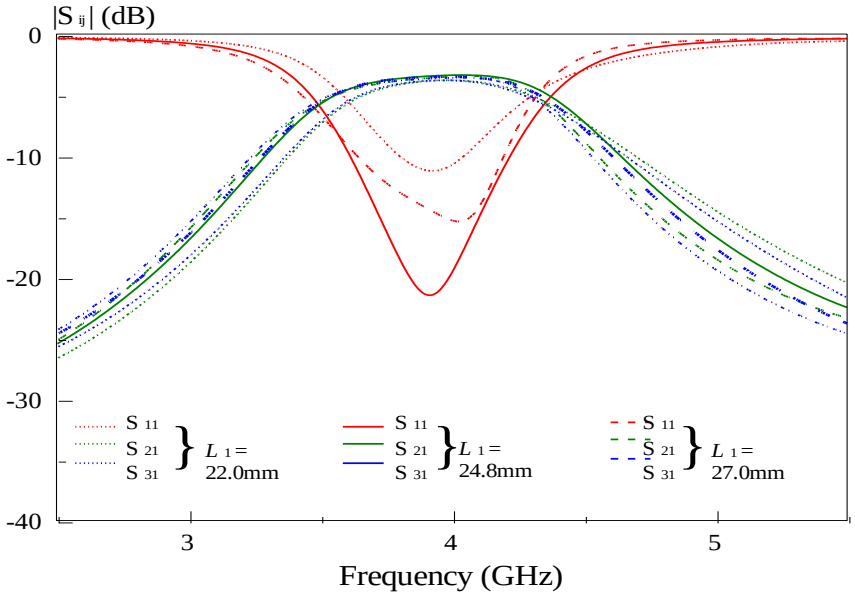


**Figure 3-21: Amplitude Response due to patch length 1 variation**

Observation

By varying a single patch length which in this case, is patch 1, the only significant change is the deepness of S11. Patch length that is between a certain ranged will exhibit good return loss. Other performance parameters remain constant.

Case 6: Variation of Patch Length L2

$L_2$ =22.0mm, $L_1 = L_3$ = 24.8mm

$L_2$ =24.8mm, $L_1 = L_3$ = 24.8mm

$L_2$ =27.0mm, $L_{21} = L_3$ = 24.8mm

Results

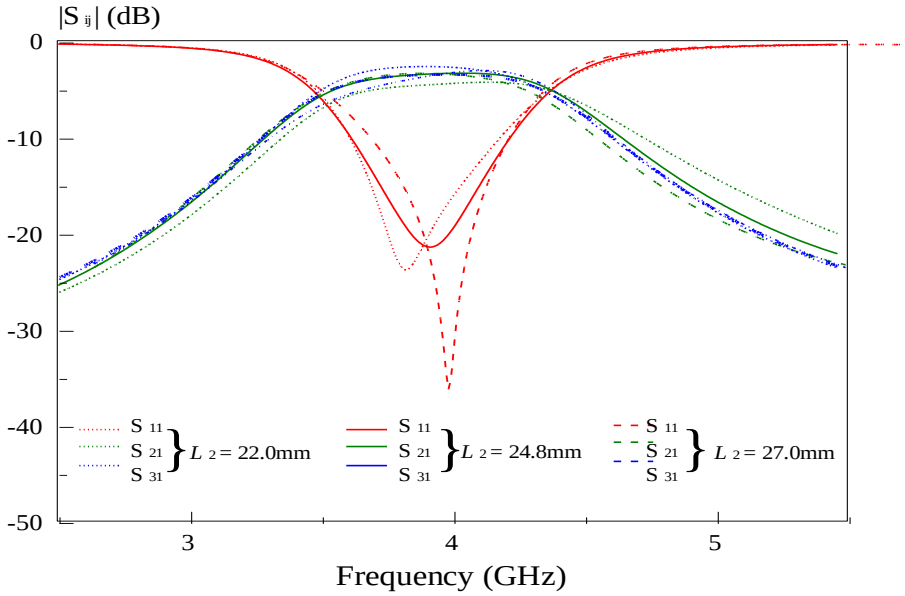


**Figure 3-22: Amplitude Response due to patch length L2 variation**

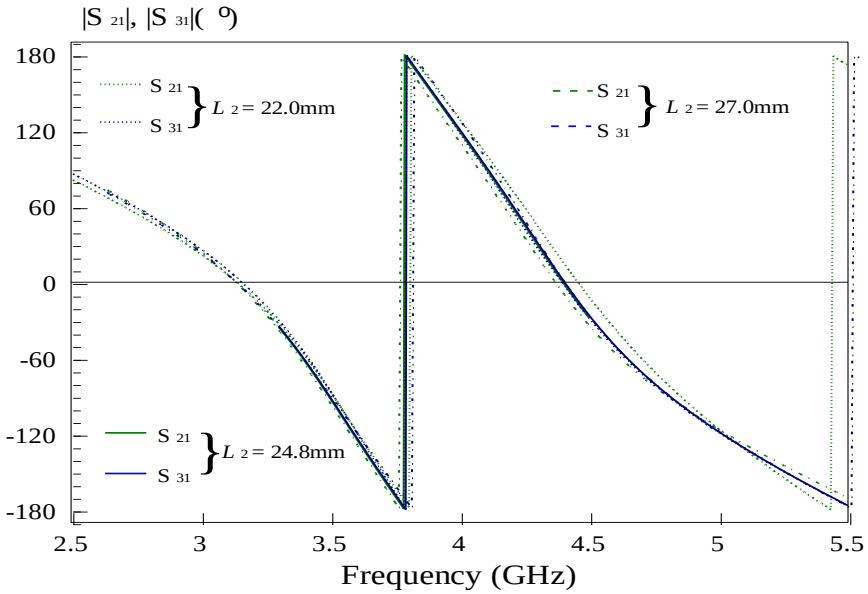


**Figure 3-23: Phase Response due to patch length L2 variation**

Observation

The variation of patch length L2 or L3 affects the return loss of the device. The major difference for this two particular variation is that the output signals are no longer in-phase.

Case 7: Variation of Patch Length L3

$L_3$ =22.0mm, $L_1 = L_2$ = 24.8mm

$L_3$ =24.8mm, $L_1 = L_2$ = 24.8mm

$L_3$ =27.0mm, $L_{21} = L_2$ = 24.8mm

Result

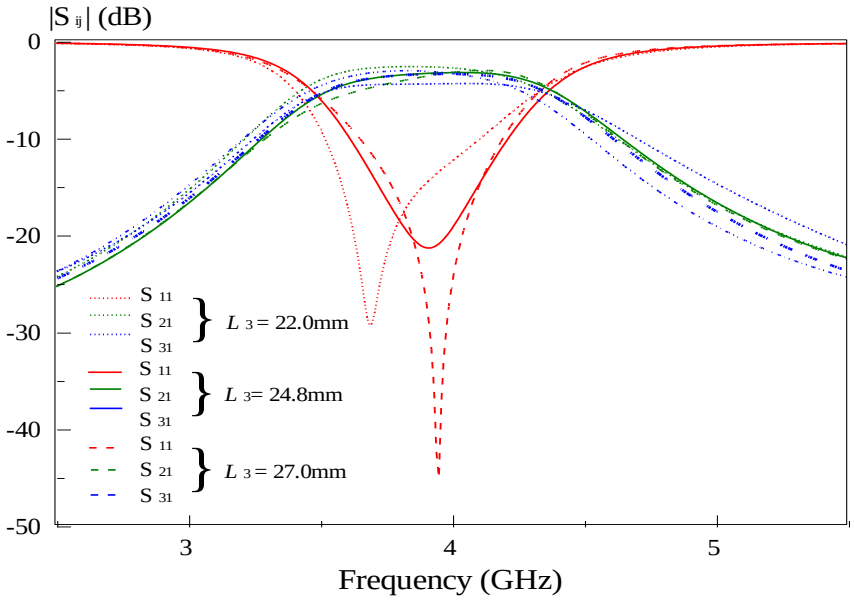


**Figure 3-24: Amplitude Response due to patch length L3 variation**

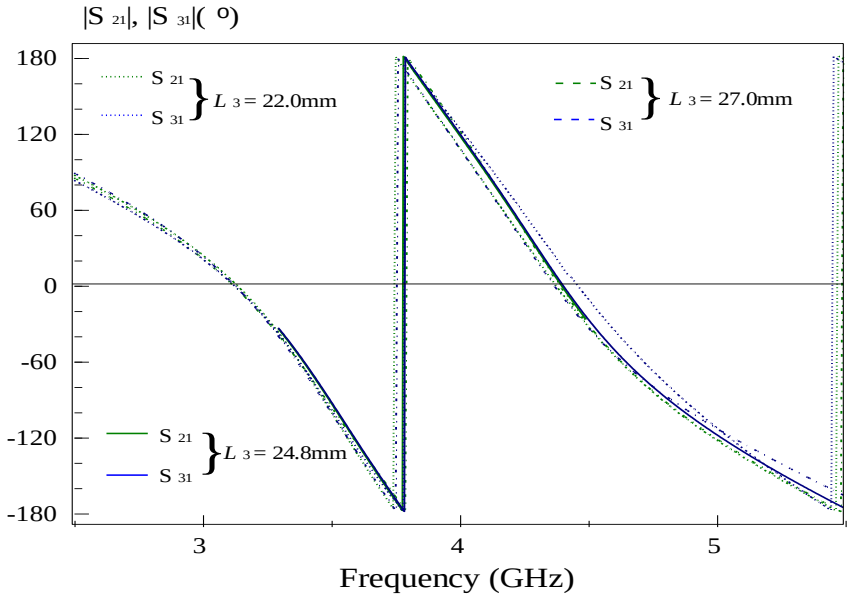


**Figure 3-25): Phase Response due to patch length L3 variation**

Observation

The effects shown here is similar to case 6 studied.

Case 8: Variation of Patch Length L4

$L_4$ =23.5mm

$L_4$ =24.5mm

$L_4$ =26.5mm

Result

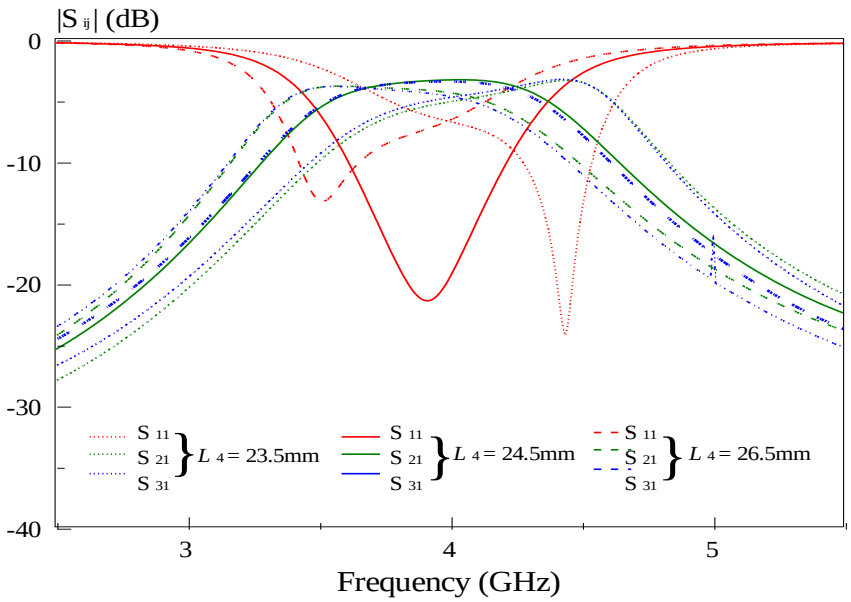


**Figure 3-26: Amplitude Response due to patch length L4 variation**

Observation

Based on the result shown in figure above, varying the patch length L4 will cause the pole position to change significantly. In addition to that, it affects the bandwidth of the operating band as well as the return loss. The insertion loss of the device is also significantly affected. Thus, this parameter is one of the most essential ones during the design process.

Case 9: Variation of Patch Length L5

$L_4$ =22.0mm,

$L_4$ =24.8mm

$L_4$ =27.0mm

Result

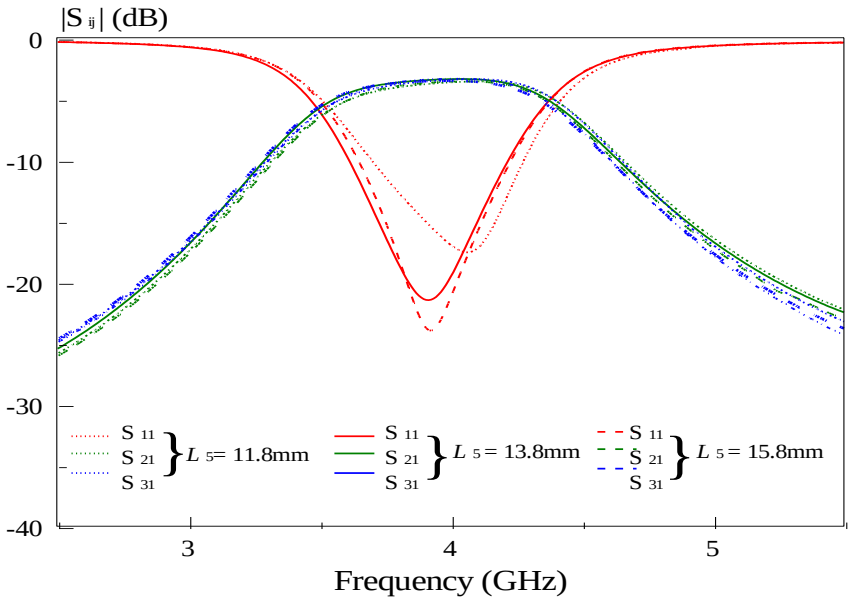


**Figure 3-27: Amplitude Response due to patch length L5 variation**

Observation

The outcome due to variation of patch length L5 is similar to Case 5 where there is no significant change in performance. Only return loss is affected slightly.

Case 10: Uniform Variation of Patch Width

$W_1 = W_2 = W_3 = 9.0mm$

$W_1 = W_2 = W_3 = 10.0mm$

$W_1 = W_2 = W_3 = 12.0mm$

Result

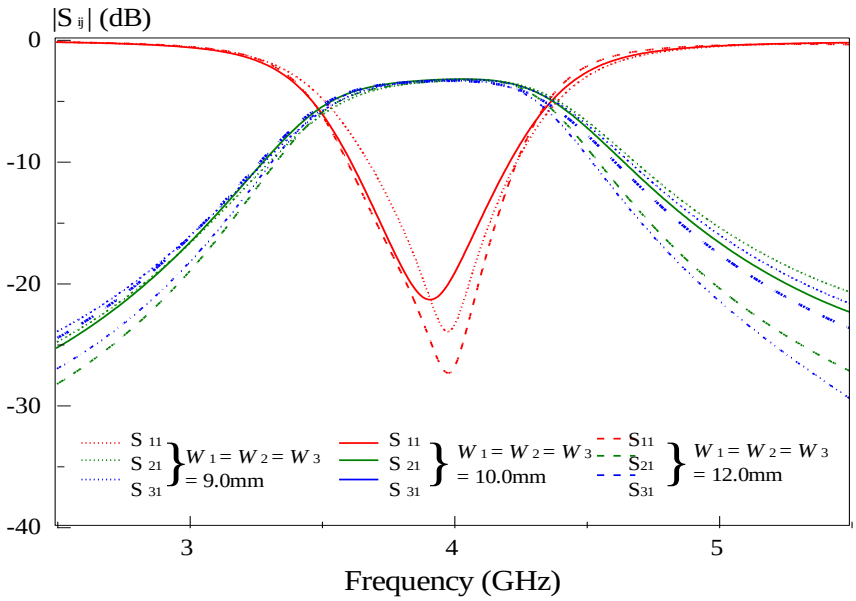


**Figure 3-28: Amplitude Response due to uniform variation of patch width**

Observation

Change in all side rectangular patches width does not exhibit much effect. Only return loss of the in-phase power divider is affected. Output remains in phase.

Case 11: Variation of Patch Width W1

$W_1$ =9.0mm, $W_2 = W_3$ = 10.0mm

$W_1$ =10.0mm, $W_2 = W_3$ = 10.0mm

$W_1$ =11.0mm, $W_2 = W_3$ = 10.0mm

Result

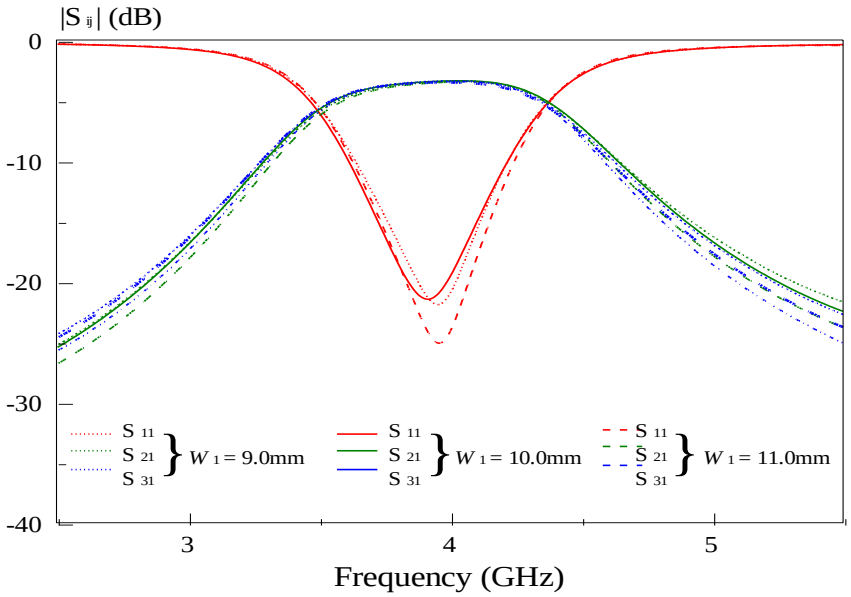


**Figure 3-29: Amplitude Response due to variation of patch width W1**

Observation

From the amplitude response graph, the change in patch width W1 varies the return loss of the device. Insertion loss remains approximately at -3.5 dB. Poles and zeroes positions does not change. Both output signals remain in-phase.

Case 12: Variation of Patch Width W2

$W_2$ =9.0mm, $W_1 = W_3$ = 10.0mm

$W_2$ =10.0mm, $W_1 = W_3$ = 10.0mm

$W_2$ =11.0mm, $W_1 = W_3$ = 10.0mm

Result

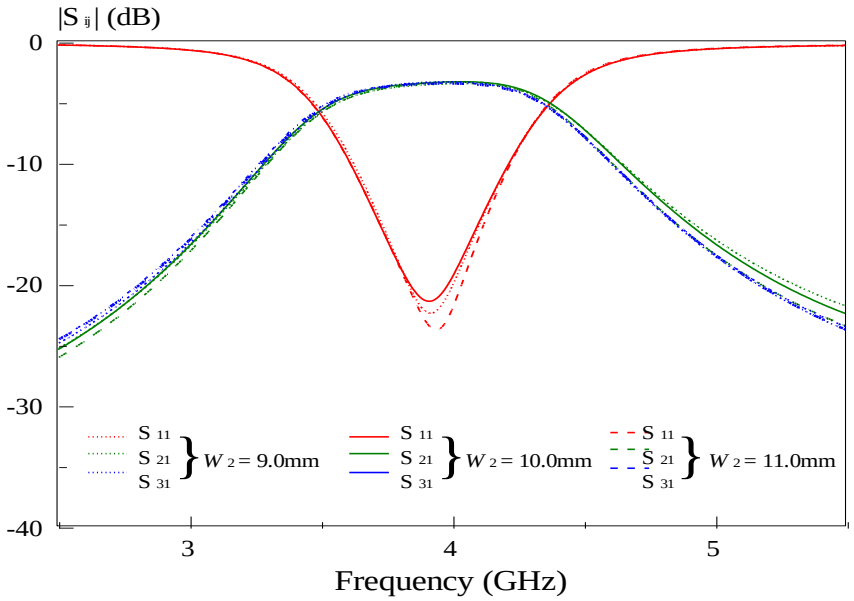


**Figure 3-30: Amplitude Response due to variation of patch width W2**

Observation

The effect due to change in patch width W2 is similar with case 11 whereby the variation will affect the return loss of the device. Insertion loss remains approximately at -3.5 dB. Poles and zeroes positions does not change. Both output signals remain in-phase.

Case 13: Variation of Patch Width W3

$W_3$ =9.0mm, $W_1 = W_2$ = 10.0mm

$W_3$ =10.0mm, $W_1 = W_2$ = 10.0mm

$W_3$=11.0mm, $W_1 = W_2$ = 10.0mm

Result

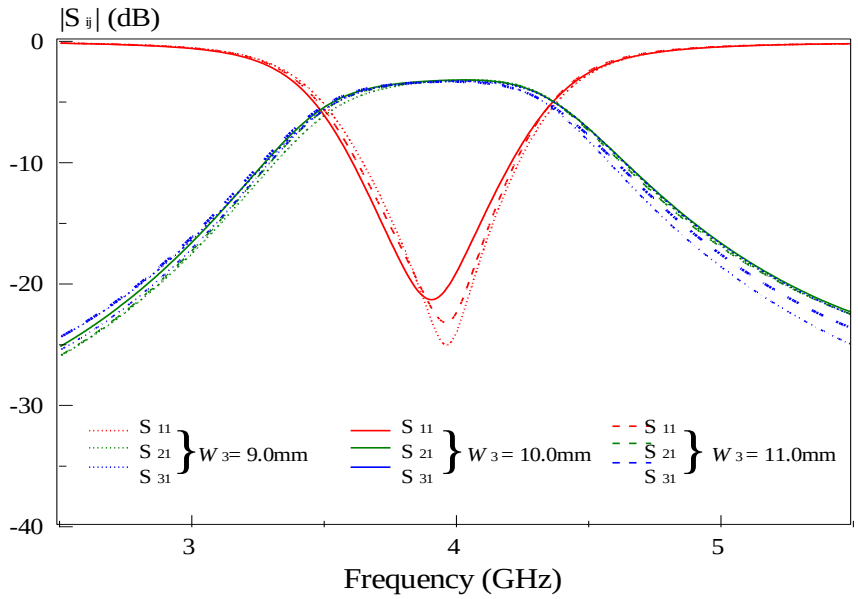


**Figure 3-31: Amplitude Response due to variation of patch width W3**

Observation

Based on the effects shown above, variation of W3 exhibits identical effects shown in case 11 and 12. Outputs (S21 and S31) remains flat within the passband. Insertion loss remains approximately at -3.5 dB. Poles and zeroes positions does not change. Both output signals remain in-phase.

Case 14: Variation of Patch Width W4

$W_4 = 0.5mm$

$W_4 = 1.0mm$

$W_4 = 2.0mm$

Result

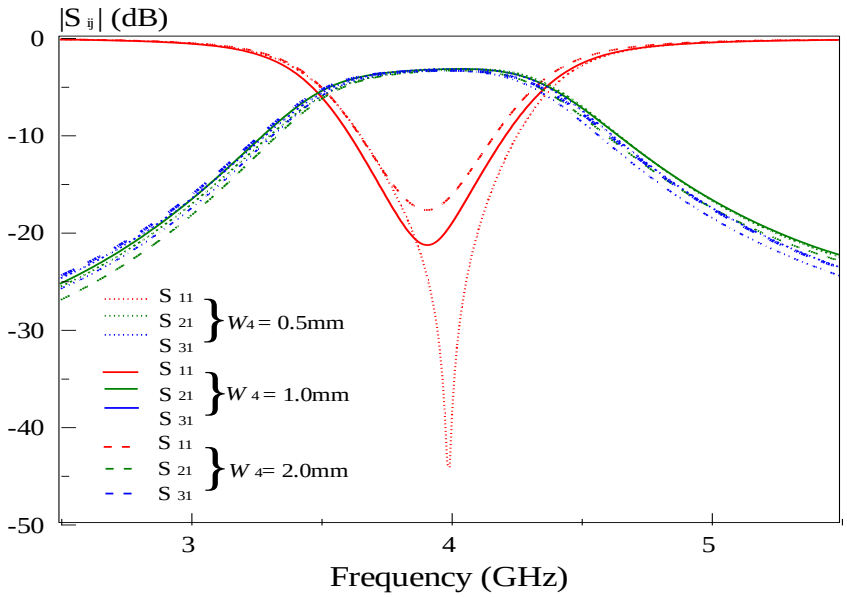


**Figure 3-32: Amplitude Response due to variation of patch width W4**

Observation

As the centre patch width W4 increases, the return loss of the divider becomes poorer. Passband bandwidth and insertion loss remains almost unchanged. Both output powers is still in phase.

## 3.3 Out-of-Phase Power Divider

### 3.3.1 Configuration

In this section, the author will illustrate the configuration of the out-of-phase patch power divider. Based on the configuration shown below in figure 3.33, the proposed power divider consists of three ports, which are numbered as Port 1, Port 2, and Port 3. In this design, Port 3 is the input port. Both Port 1 and Port 2 are the output ports. All ports are connected to 50 ohm microstrip feed lines. Similarly like the in-phase divider, this power divider model is non-symmetrical.

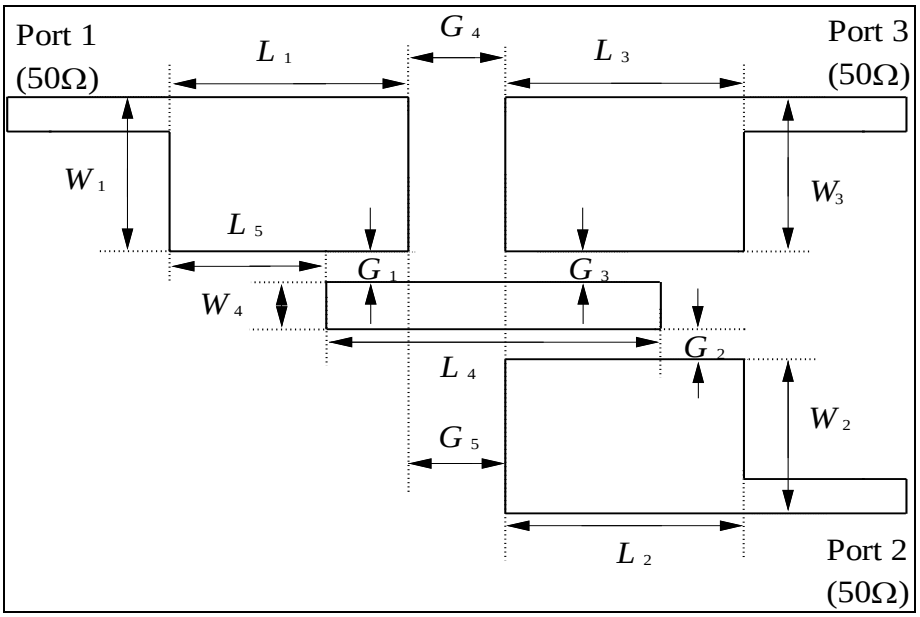


**Figure 3-33: Configuration of out-of-phase power divider**

The 3 rectangular patches which are connected to the input/output ports by 50 ohm feed lines have identical length and width. Each of the 3 patches mentioned has an area of 25.0mm x 12.0mm = 300 $mm^2$. The rectangular patch in the centre has a different length and width compared to the 3 previous mentioned rectangular patches. It has an area of 25.3mm x 3.0mm = 75.9$mm^2$. The area of the entire out-of-phase power divider is 43.0mm x 89.0mm = 3827.0$mm^2$.

The substrate used in implementing this design has a dielectric constant of 2.33 and a thickness of 1.57mm. In the following, the design dimensions of the entire configuration will be presented. L, W and G represent the parameters of length, width and gap respectively.

$L_1$ = 25.0mm, $L_2$ = 25.0mm, $L_3$ = 25.0mm, $L_4$ = 25.3mm, $L_5$ = 16.0mm, $W_1$ = 12.0mm, $W_2$ =12.0mm, $W_3$= 12.0mm, $W_4$ = 3.5mm, $G_1$ = 0.5mm, $G_2$ = 0.5mm, $G_3$ = 0.2mm, $G_4$ = 2.0mm, $G_5$ = 2.0mm

Figure 3.34 illustrates the top view configuration of the power divider in HFSS, Figure 3.35 display the configuration in 3D view, and Figure 3.36 is the photograph of the fabricated out-of-phase power divider.

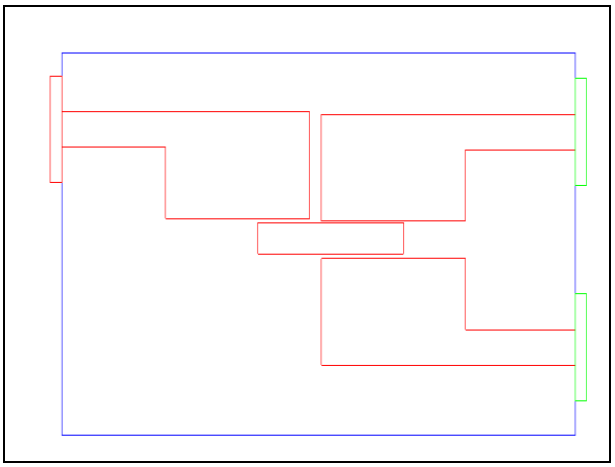

**Figure 3-34: Out-of-phase power divider (Top View)**

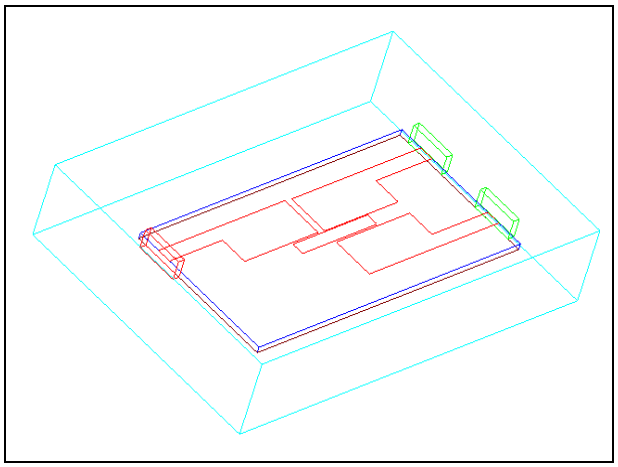

**Figure 3-35: Out-of-phase power divider (3D View)**

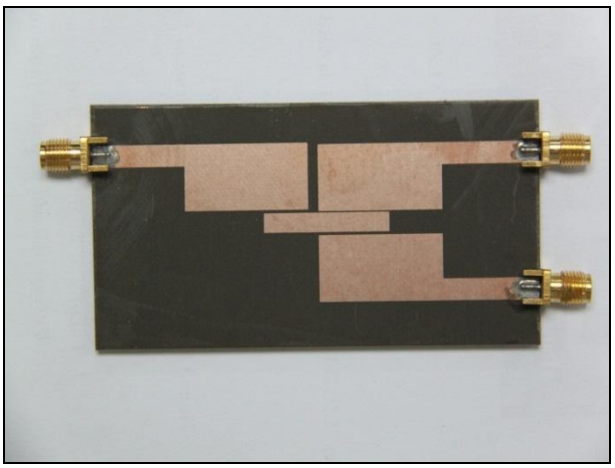

**Figure 3-36: Photograph of fabricated Out-of-Phase Power Divider**

### 3.3.2 Transmission Line Model

In section 3.3.2, the transmission line model of the out-of-phase power divider will be presented. Figure 3.37 shows the equivalent circuit model of the divider. This transmission line model concept is similar to the in-phase one but with different width, length and gap. Therefore, a non-comprehensive discussion will be presented here.

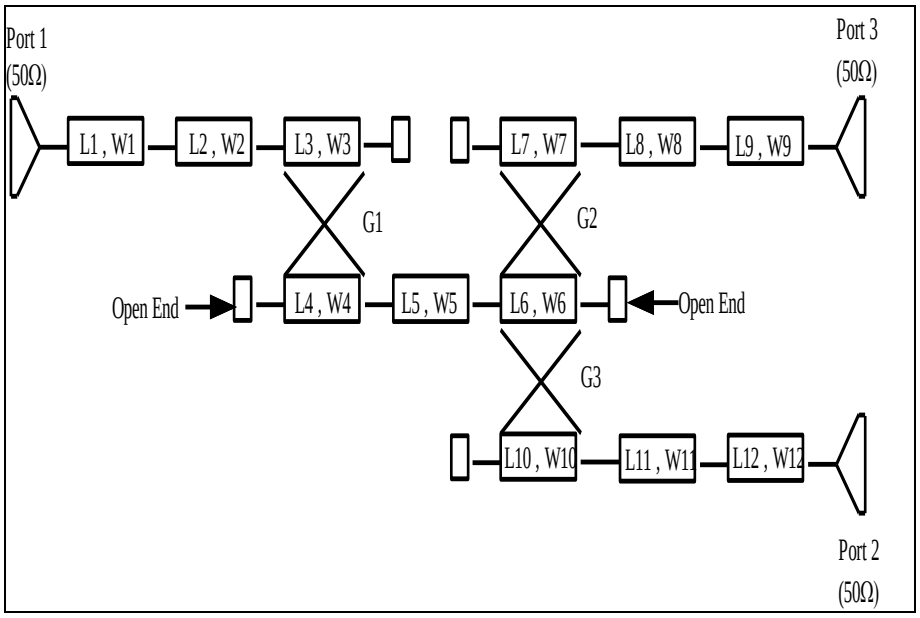


**Figure 3-37: Transmission Line Model for Out-of-Phase Power Divider**

| LENGTH | (mm) |
|---|---|
| L1 | 18.0 |
| L2 | 16.0 |
| L3 | 11.0 |
| L4 | 11.0 |
| L5 | 3.5 |
| L6 | 13.0 |
| L7 | 13.0 |
| L8 | 10.7 |
| L9 | 19.0 |
| L10 | 13.0 |
| L11 | 10.7 |
| L12 | 19.0 |

| WIDTH | (mm) |
|---|---|
| W1 | 4.0 |
| W2 | 12.0 |
| W3 | 12.0 |
| W4 | 3.5 |
| W5 | 3.5 |
| W6 | 3.5 |
| W7 | 12.0 |
| W8 | 12.0 |
| W9 | 4.0 |
| W10 | 12.0 |
| W11 | 12.0 |
| W12 | 4.0 |

| GAP | (mm) |
|---|---|
| G1 | 0.5 |
| G2 | 0.2 |
| G3 | 0.5 |

**Table 3-2: Element Parameters for Out-Phase Divider**

Table 3-2 shows the parameters of each element. Based on the proposed design configuration, the out-of-phase power divider consists of 3 ports which are symbolized by the triangular objects displayed in figure 3.37. All input and output ports are conventionally fixed as 50ohms.

All rectangular boxes denote the microstrip transmission lines of the divider. L and W indicate the length and width of each transmission line respectively. Rectangular boxes which are aligned in parallel signify the strip lines which are coupled together. In practical, these microstrip lines are separated with a gap. G denotes the gap of the coupled lines. Open circuit configurations are represented by open end element.

### 3.3.3 Results

In section 3.3.3, the performance of the out-of-phase power divider will be demonstrated. All simulation, measured, and modelling results are acquired through HFSS, Agilent Network Analyser and Microwave Office respectively.

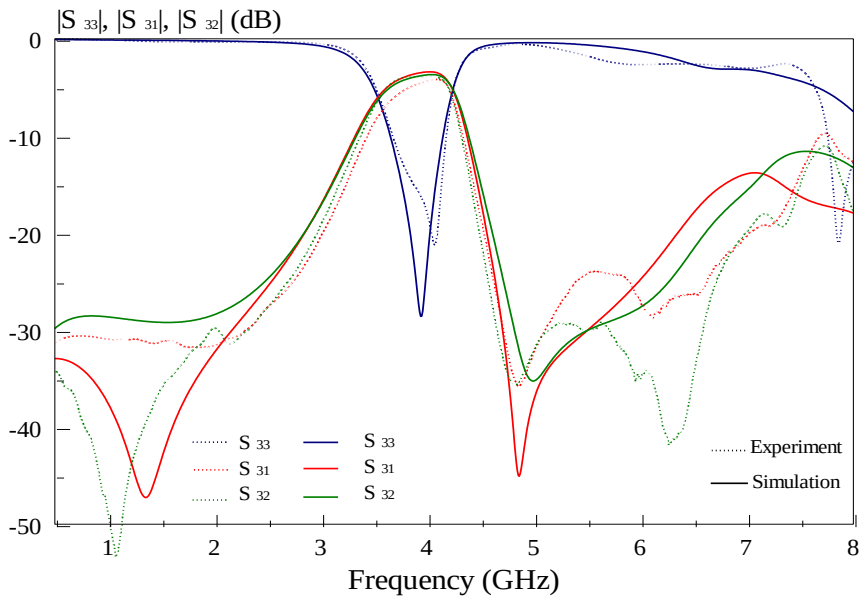


**Figure 3-38: Amplitude Response of Out-of-Phase Power Divider (Simulation VS Experiment)**

Based on figure 3.38 , the simulation amplitude response curve shows that the divider is able to operate at frequencies between 3.655GHz to 4.142GHz, thus providing a passband bandwidth of 0.486GHz. The centre operating frequency of the divider is at 3.896GHz. Hence, the fractional bandwidth of the device is 27%. In addition to that, the return loss (S33) of the out-of-phase divider is -28.636 dB and the insertion loss (S31 and S32) are both approximately -4dB. Furthermore, there is a good roll-off shown by the divider.

Meanwhile, the measured amplitude response curve shows that the divider is also able to operate at frequencies between 3.655GHz to 4.142GHz, thus providing a passband bandwidth of 0.486GHz as well. However, the return loss (S33) is much lower especially at the lower frequencies of the passband, thus affecting the output powers of the divider. We can observe that the insertion losses are higher at the lower frequencies of the passband. Still, simulation and measured results shows good agreement overall.

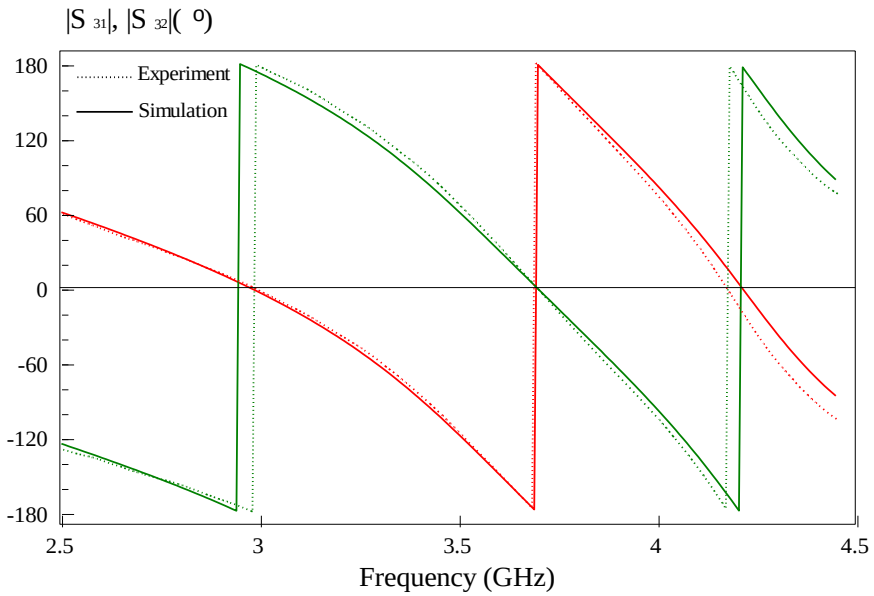


**Figure 3-39: Phase Response of Out-of-Phase Power Divider (Simulation VS Experiment)**

Based on figure 3.39, the simulation phase response shows that the two output signals are almost 180 degree out of phase at passband. The measured phase response also displays good matching with the simulated results.

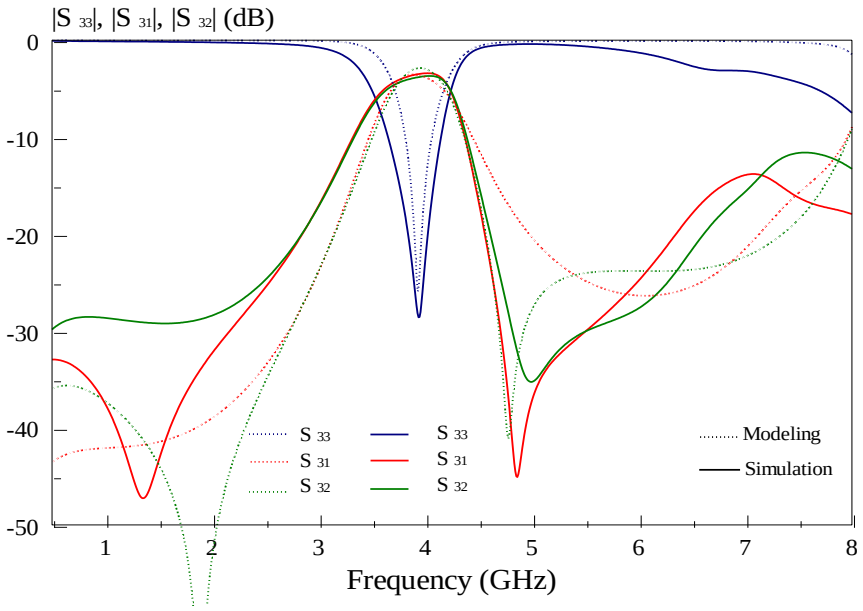


**Figure 3-40: Amplitude Response of Out-of-Phase Power Divider (Simulation VS Modeling)**

Here, the modelling results are compared with the simulation results. From figure 3.40, the modelling amplitude response curve demonstrates that the divider is able to operate at frequencies between 3.81GHz to 4.06GHz, thus resulting a smaller passband bandwidth. At this point, the centre operating frequency of the transmission model divider is 3.935GHz which provides fractional bandwidth of 6%. The return loss is -25.87dB while the insertion loss is -3.686dB on average for both outputs.

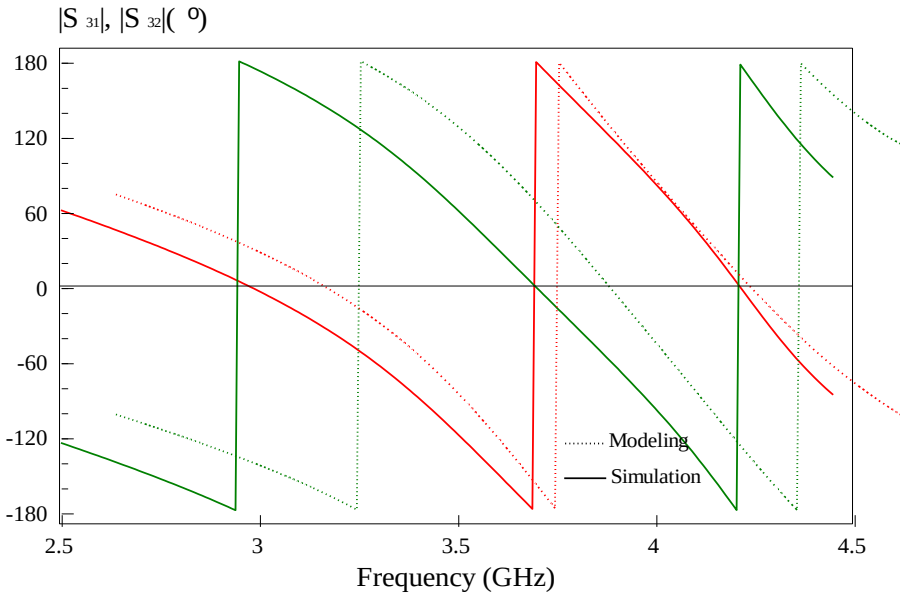


**Figure 3-41: Phase Response of Out-of-Phase Power Divider (Simulation VS Modelling)**

Based on figure 3.41, the modelling phase response shows that the two output signals are almost 180 degree out of phase at passband. However, there is a slight shift in frequencies.

### 3.3.4 Parametric Analysis

As previously discussed in section 3.2.4, the purpose of parametric analysis is to observe the characteristics and responses of the design by changing certain parameters such as length, width, gap, capacitance, inductance and etc.

Here, the effects of each parameter of the out-of-phase divider will be revealed by the author. To begin with, Figure 3.42 displays the proposed design configurations together with the original dimensions.

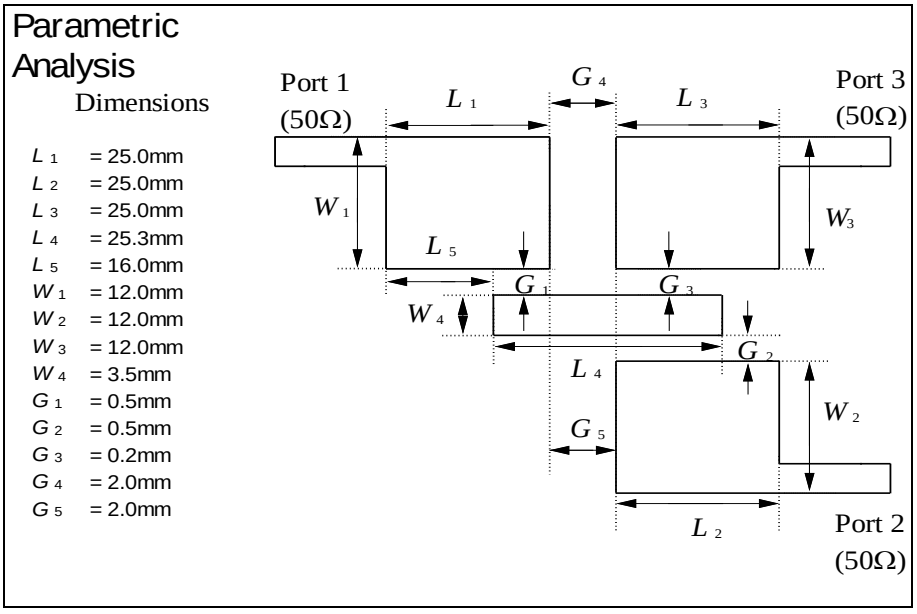


**Figure 3-42: Dimensions of proposed Out-of-Phase Power Divider**

Case 1: Uniform variation of gap

$G_1 = G_2 = 0.4mm, G_3 = 0.1mm$

$G_1 = G_2 = 0.5mm, G_3 = 0.2mm$

$G_1 = G_2 = 0.6mm, G_3 = 0.3mm$

Result

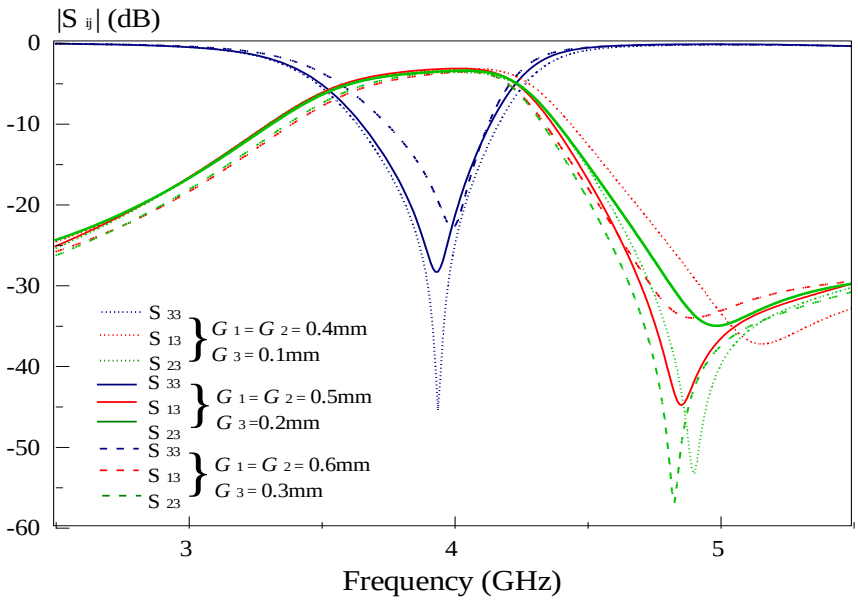


**Figure 3-43: Amplitude Response due to uniform gap variation**

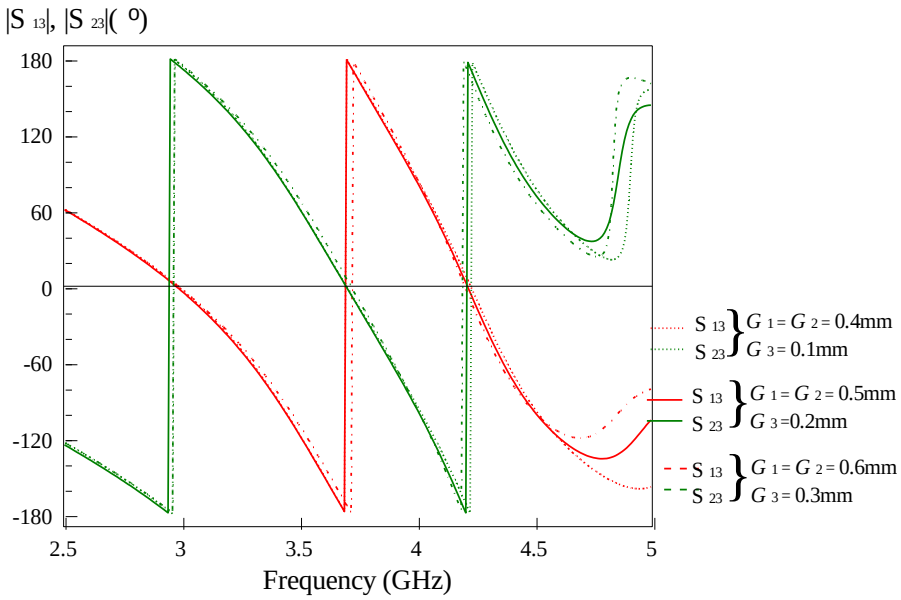


**Figure 3-44: Phase Response due to uniform gap variation**

Observation

Based on figure 3.43, decreasing all gaps by 0.1mm does not provide any significant change. However, this process enables to improve the return loss by a further 60% which slightly improves the insertion loss of the divider. Meanwhile, the original configuration of the divider provides operating frequencies between 3.655GHz to 4.142GHz, thus providing a passband bandwidth of 0.486GHz. Increasing all gaps by 0.1mm not only decreases the return loss but also the passband bandwidth of the device. The passband bandwidth is 0.482GHz which implies a

decrease in 17.28% in bandwidth. In terms of phase response, there is not much variation and is still on average, 180 degrees out of phase at all passband.

Case 2: Variation of gap 1

$G_1$ = 0.3mm

$G_1$ = 0.5mm

$G_1$ = 0.6mm

Result

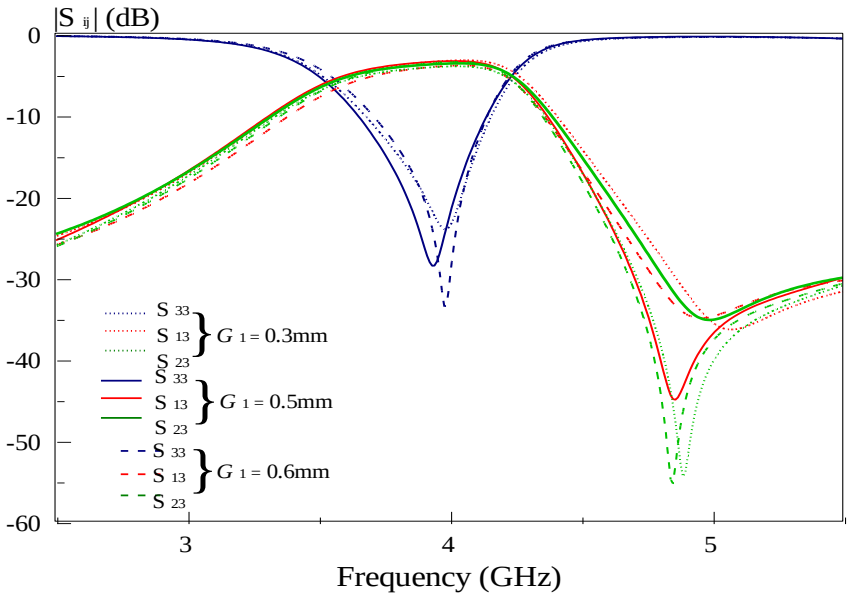


**Figure 3-45: Amplitude Response due to variation of gap 1**

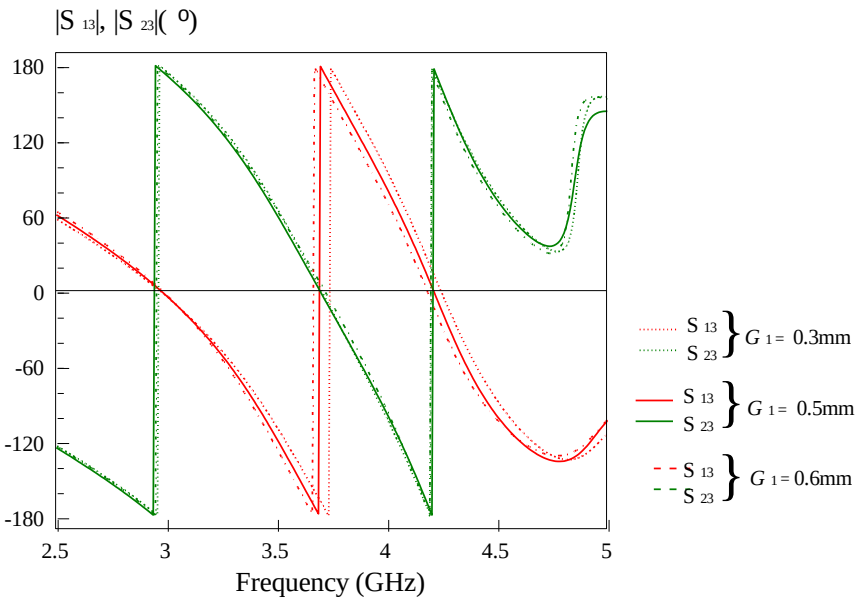


**Figure 3-46: Phase response due to variation of gap 1**

Observation

Here, the variation of a single parameter $G_1$ does not provide any significant effect in the performance of the divider. In figure 3.39, the only noticeable change is the return loss of the divider alongside a very small change is passband bandwidth (<3%). Decrease in gap causes lower return loss while increasing the gap provides better return loss. The output phase difference is still able to produce a difference of 180 degress at all passband.

Case 3: Variation of gap 2

$G_2$ = 0.3mm

$G_2$ = 0.5mm

$G_2$ = 0.6mm

Result

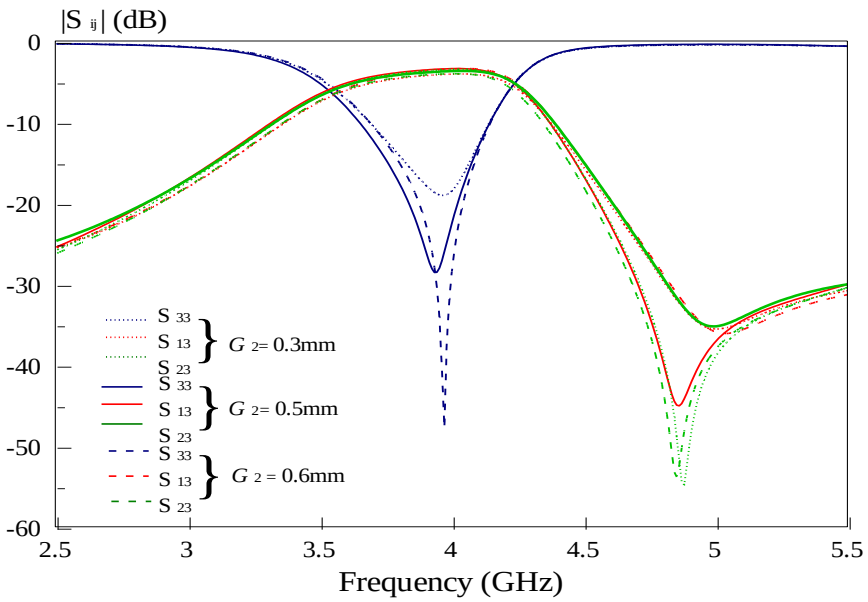


**Figure 3-47Amplitude Response due to variation of gap 2**

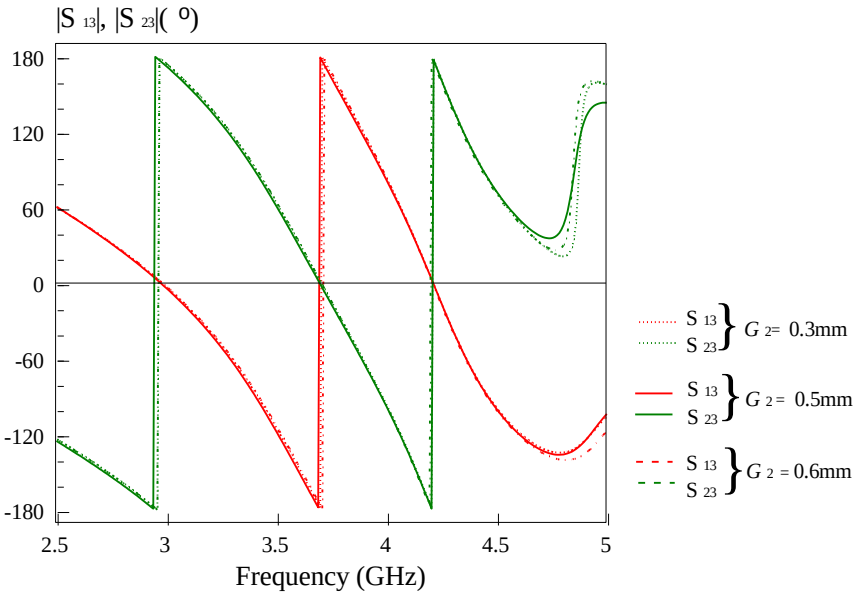


**Figure 3-48: Phase Response due to variation of gap 2**

Observation

The effect of varying $G_2$ is similar to the one illustrated in case 2. No major change is exhibited by changing a single parameter $G_2$. Increasing the gap by 0.1mm improves the matching, thus increasing the return loss of the divider. Decreasing the gap by 0.1mm only degrades the matching which provides poorer return loss. Insertion loss is still approximately at -4dB. Moreover, no drastic change in phase response was seen.

Case 4: Variation of gap 3

$G_3$ = 0.1mm

$G_3$ = 0.2mm

$G_3$ = 0.3mm

Result

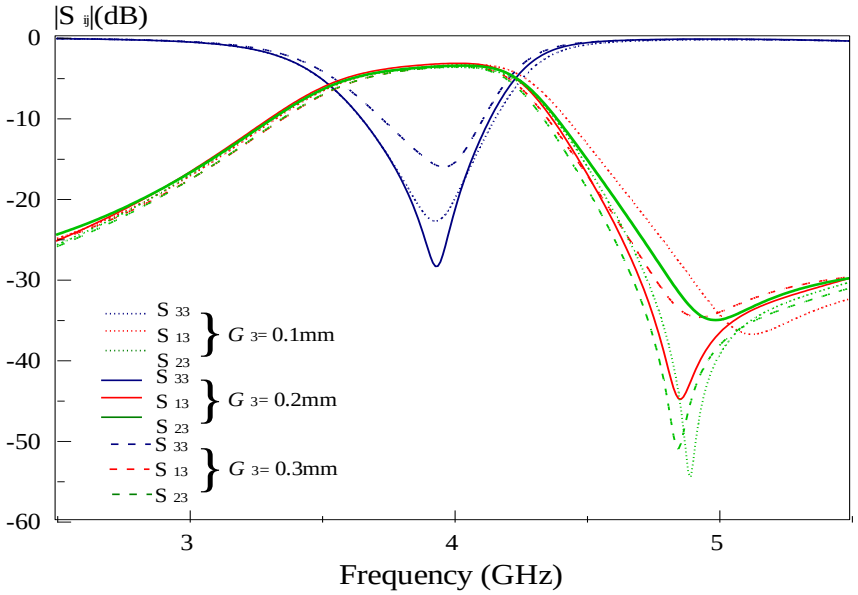


**Figure 3-49: Amplitude Response due to variation of gap 3**

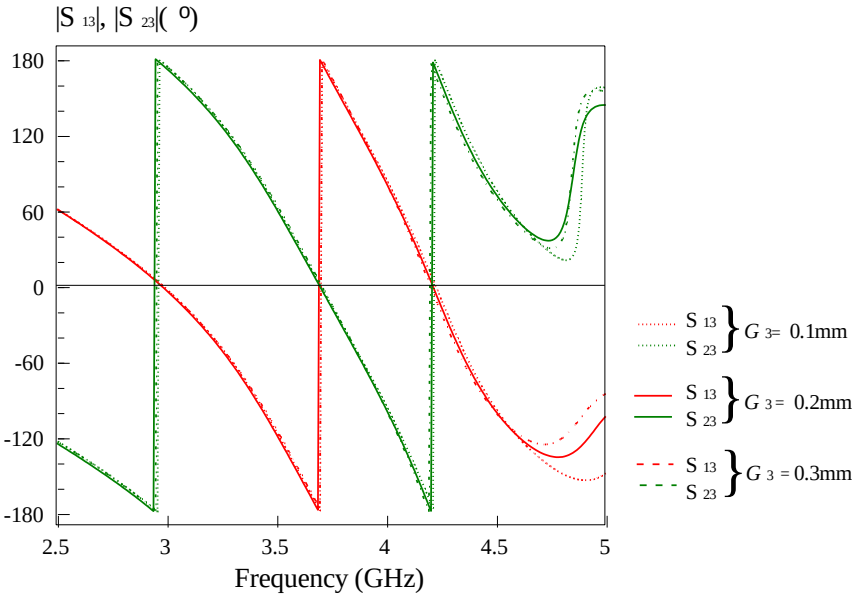


**Figure 3-50: Phase Response due to variation of gap 3**

Observation

Figure 3.49 and figure 3.50 illustrates the amplitude response and phase response respectively due to the variation of gap 3. The process of widening and reducing the gap 3 mostly affects the matching of the transmission lines, thus affecting the return loss of the power divider. From the graph, reducing the gap by 0.1mm causes 11.3% decrease in return loss. Similarly, widening the gap by 0.1mm causes a drop of more than 50%. Passband bandwidth and fractional bandwidth are not significantly affected. However, increasing the gap by 0.1mm shows a minor

decrease in both passband and fractional bandwidth (<2%). Phase response remains unchanged.

Case 5: Variation of gap 4 and gap 5

$G_4 = G_5 = 1.0mm$

$G_4 = G_5 = 2.0mm$

$G_5 = G_5 = 3.0mm$

Result

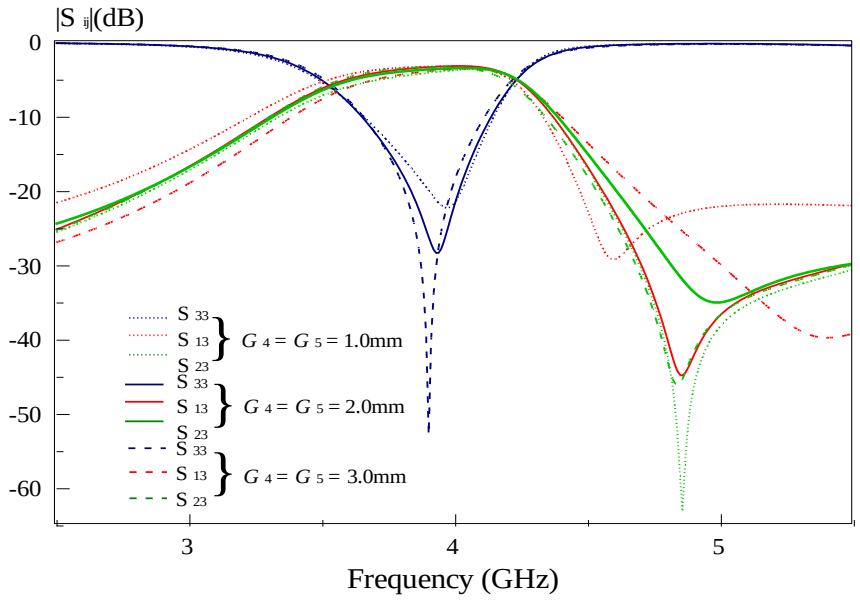


**Figure 3-51Amplitude Response due to variation of gap 4 and gap 5**

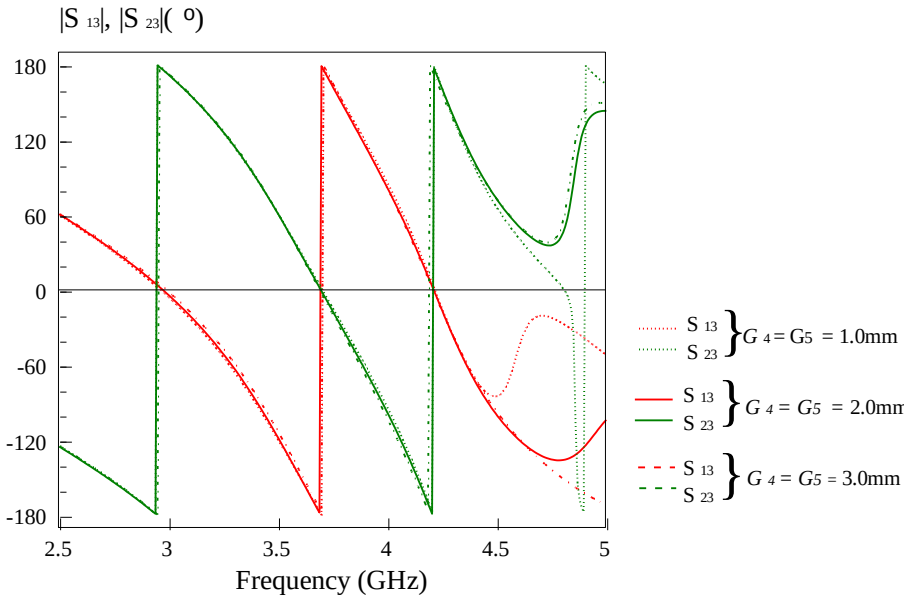


**Figure 3-52: Phase response due to variation of gap 4 and gap 5**

Observation

Case 5 studies on the response of the device by varying both $G_4$ and $G_5$ parameters concurrently. Similarly like all other gaps variations, no significant effects are seen besides the return loss of the divider. Smaller gap leads to poorer return loss while larger gap provides better return loss. Outputs are still 180 degrees out of phase on average at all passband.

Case 6: Uniform variation of patch length

$L_1 = L_2 = L_3 = 22.0mm$

$L_1 = L_2 = L_3 = 25.0mm$

$L_1 = L_2 = L_3 = 27.0mm$

Result

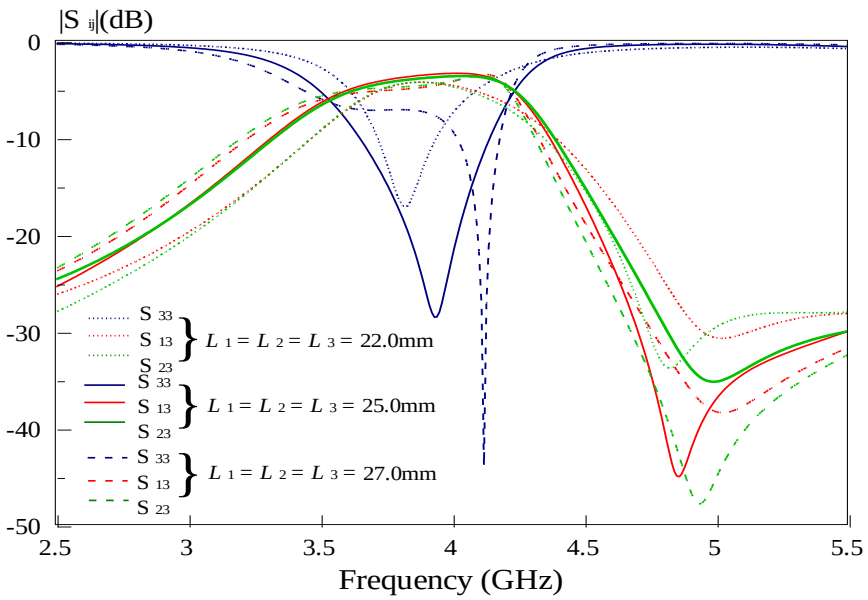


**Figure 3-53: Amplitude Response due to uniform variation of patch length**

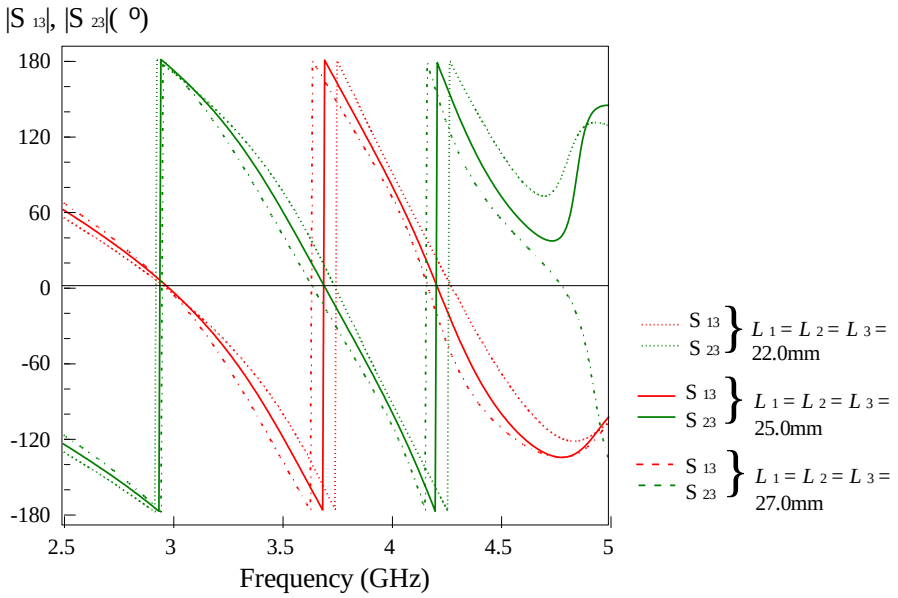


**Figure 3-54: Phase Response due to uniform variation of patch length**

Observation

Based on the amplitude response curve, the length of the rectangular patches is an essential parameter need to be taken into consideration when designing the divider. From figure 3.7, patches with length = 22.0mm operates only at frequencies between 3.72GHz to 3.94GHz, thus providing a bandwidth of 0.22GHz. The centre frequency is now 3.83GHz which exhibits a fractional bandwidth of 5%. Here, we can observe a drastic decrease in passband bandwidth (45.26%) and fractional bandwidth (22%). Meanwhile, return loss is much lower (-17.21dB). S31 and S32 are not flat within the passband. However, the phase differences for all passbands are still within 175-185 degrees range. Patches with length= 27.0 mm causes pole to shift to the upper frequency spectrum. In this case, the divider has only a passband bandwidth of 0.142GHz with fractional bandwidth equalling to 3%. Most of the outputs phase difference at passband is less than 175 degrees.

Case 7: Variation of patch length L1

$L_1$ = 22.0mm

$L_1$ = 25.0mm

$L_1$ = 27.0mm

Result

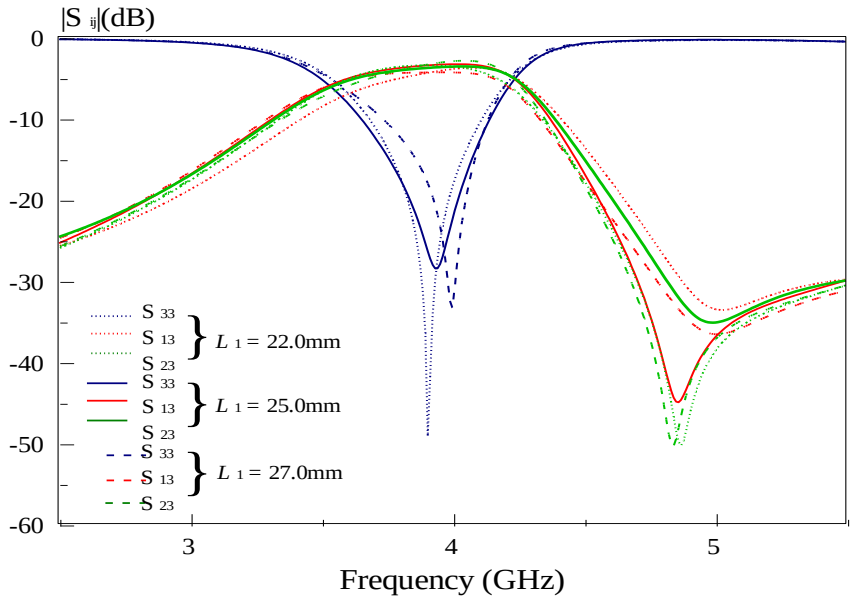


**Figure 3-55: Amplitude Response due to variation of patch length L1**

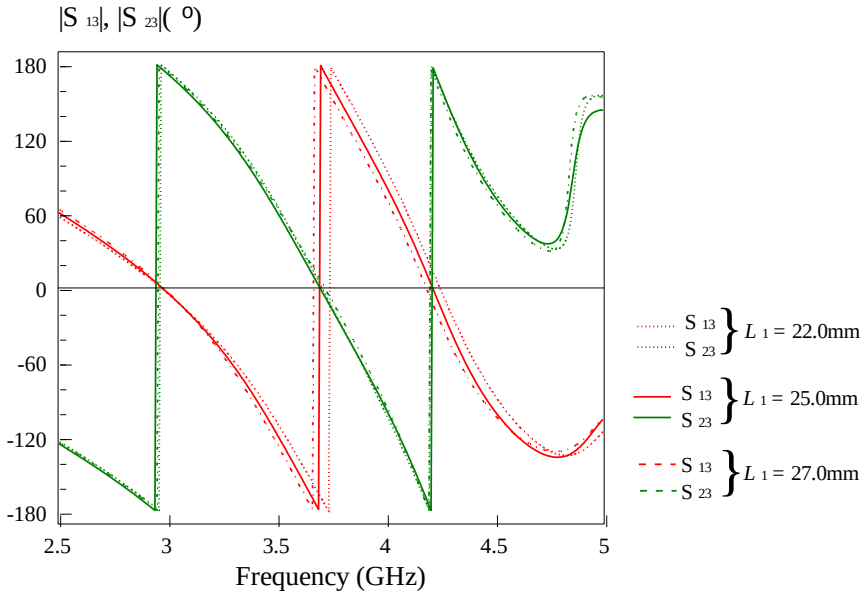


**Figure 3-56: Phase Response due to variation of patch length L1**

Observation

Here, the variation of a single parameter $L_1$ does not provide any significant effect in the performance of the divider. In figure 3.55, the only noticeable change is the return loss of the divider alongside a very small change is passband bandwidth (<3%). Decrease in length causes better return loss while increasing the length provides poorer return loss. Poles are shifted to the lower frequency spectrum when length is reduces while poles are shifter to the upper frequency spectrum when length is increases. The output phase difference is still able to produce a difference of 180 degree at all passband.

Case 8: Variation of patch length L2

$L_2$ = 22.0mm

$L_2$ = 25.0mm

$L_2$ = 27.0mm

Result

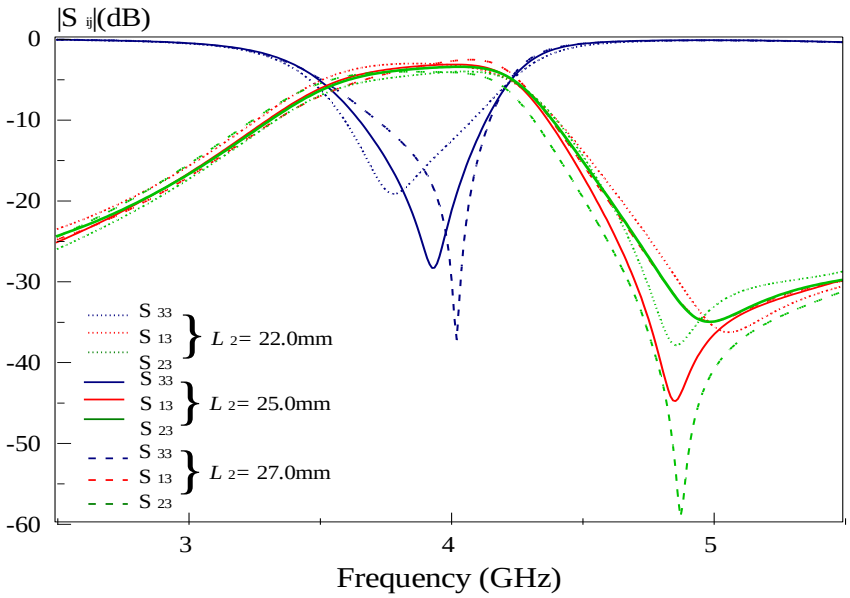


**Figure 3-57: Amplitude Response due to variation of patch length L2**

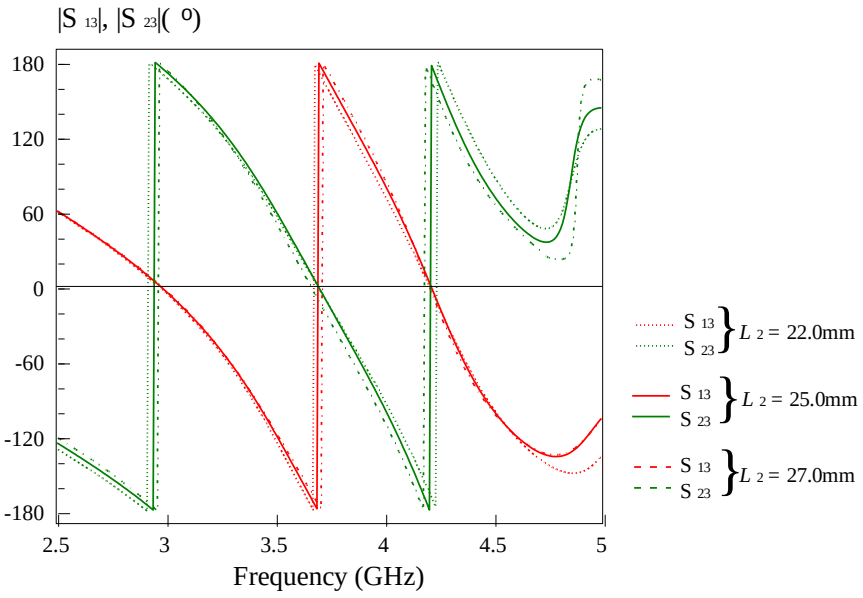


**Figure 3-58: Phase Response due to variation of patch length L2**

Observation

In figure 3.57, poles are shifted to the left of the spectrum when patch length is reduces while they are shifter right when patch length is increases. Shorter patch length exhibits better return losses at the lower frequencies while longer patches show better return losses at the upper frequencies. However, the passband and fractional bandwidth are approximately the same for all changes. Both outputs signals are still 180 degrees out of phase at all passband.

Case 9: Variation of patch length L3

$L_3$ = 22.0mm

$L_3$ = 25.0mm

$L_3$ = 27.0mm

Result

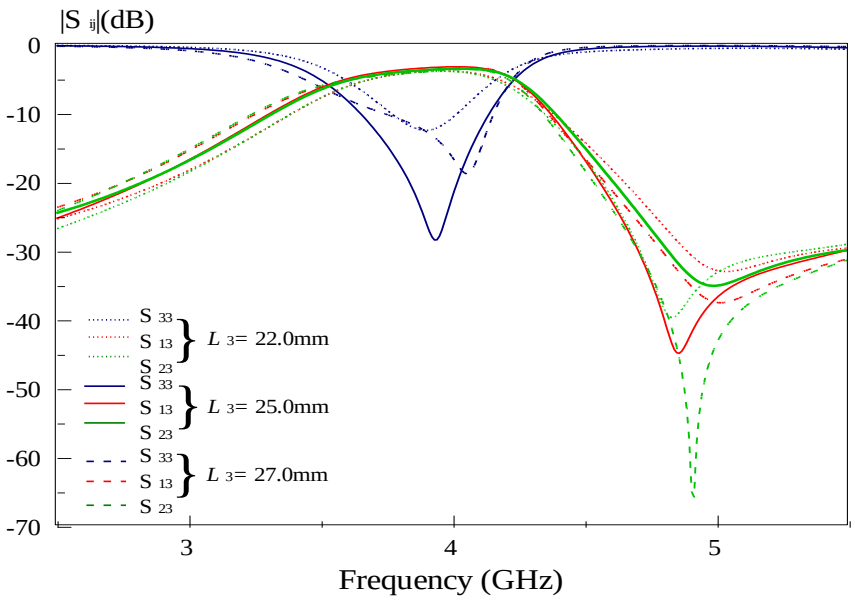


**Figure 3-59: Amplitude Response due to variation of patch length L3**

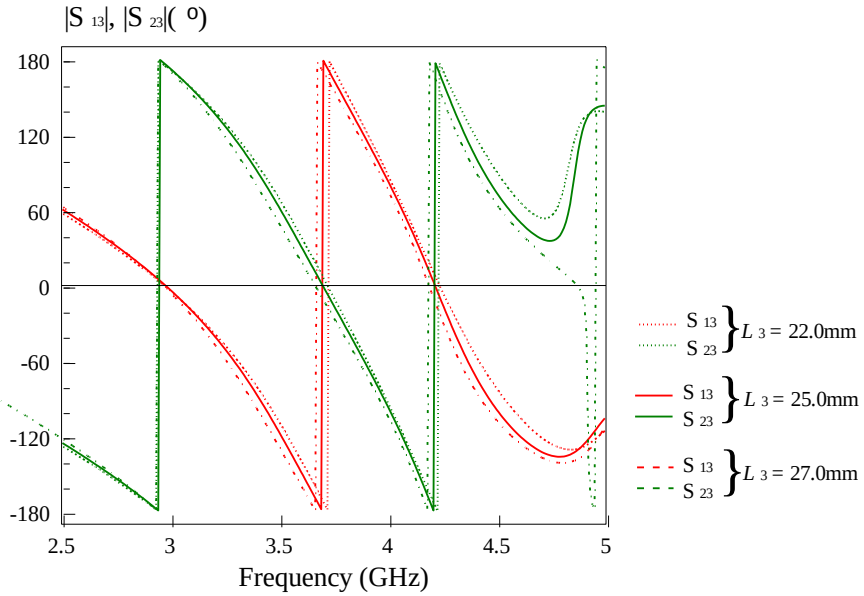


**Figure 3-60: Phase Response due to variation of patch length**

Observation

In figure 3.60, the amplitude response curve shows that when patch length L3 is reduced from 25.0mm to 22.0mm, the passband bandwidth is reduced from 0.486GHz to 0.262GHz. This implies a 53.9% reduction in bandwidth. As a result, the fractional bandwidth is 6.7%. The lowest S33 point is at -12.64dB, indicating that the return loss is much poorer. However, the phase difference of the output signals is still 180 degrees out of phase in the new passband. When patch length L3 is increased from 25.0mm to 27.0mm, the passband bandwidth is 0.430GHz, indicating a slightly smaller bandwidth compared the patch length L3 at 25.0mm. Therefore, the fractional bandwidth will be similar to the one when L3 equals to 25.0mm. Besides that, we can also observe that the lower frequencies of the passband have much poorer return loss compared to those at the higher frequencies. This implies that the pole of the curve is shifted to the upper frequency spectrum. Both output signals phase difference still lies in the range of 175-185 degrees.

Case 10: Variation of patch length L4

$L_4$ = 23.3mm

$L_4$ = 25.3mm

$L_4$ = 27.3mm

Result

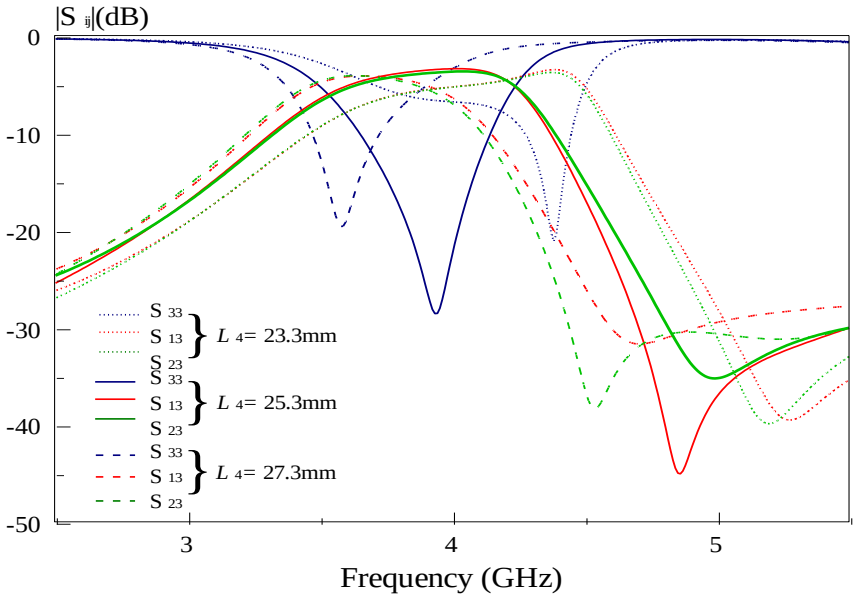


**Figure 3-61: Amplitude Response due to variation of patch length L4**

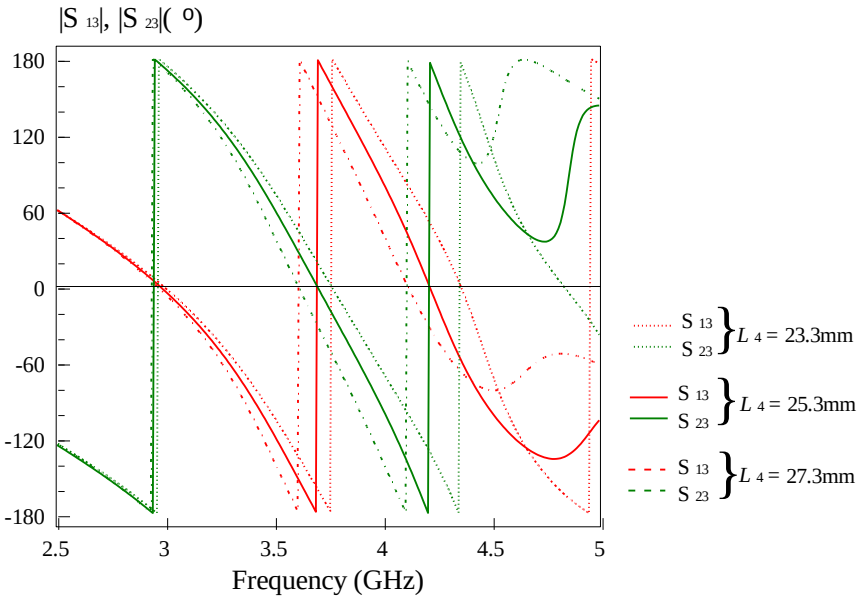


**Figure 3-62: Phase Response due to variation of patch length L4**

Observation

In this section, the centre patch length is investigated. By observing the amplitude response curve, reducing the patch length shifts the pole of the S33 curve to the upper frequency spectrum. The centre frequency for $L_4$ = 23.3mm is 4.36GHz and the operating passband range spans from 4.27GH to 4.45GHz. Therefore, the operating bandwidth of the divider is reduced by 65%. In this configuration, the divider has insertion loss of -3.5dB. Meanwhile, both outputs at frequency outside the passband range do not have phase difference of 180 degree. Similarly, when

patch length is increased to $L_4$= 27.3mm, the pole of the S33 curve is shifted to the lower frequency spectrum. The increment also leads to bandwidth reduction, which in this case by 48.1%. The insertion loss is approximate -4.27dB. All passband stills produce outputs that are out of phase.

Case 11: Variation of patch length L5

$L_5$ = 14.0mm

$L_5$ = 16.0mm

$L_5$ = 18.0mm

Result

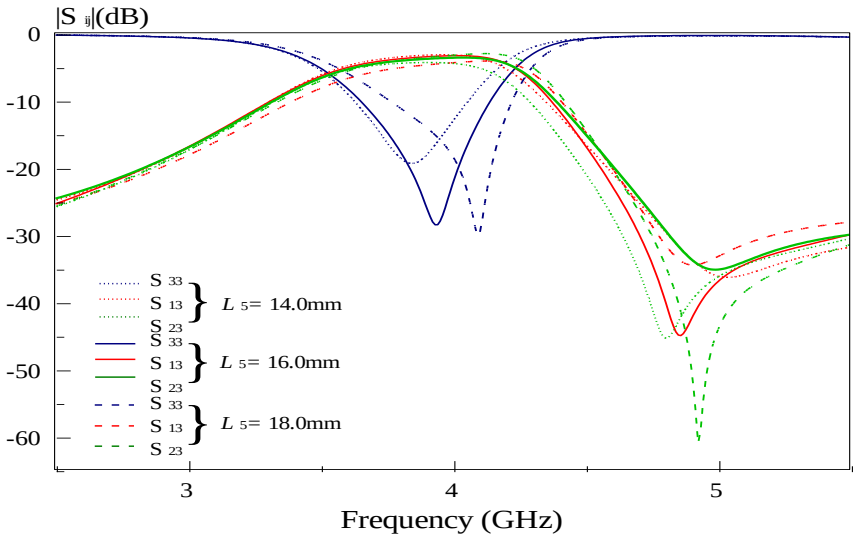


**Figure 3-63: Amplitude Response due to variation of patch length L5**

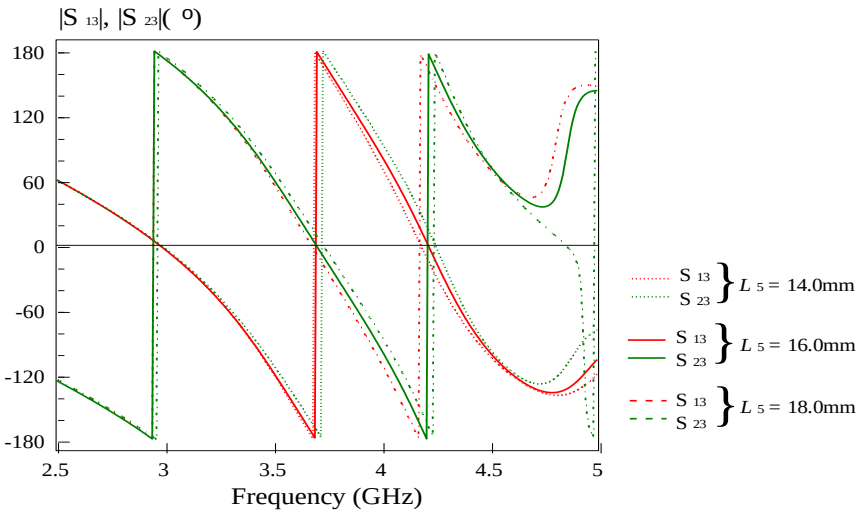


**Figure 3-64: Phase Response due to variation of patch length L5**

Observation

Figure 3.63 displays poles are shifted to the left of the spectrum when patch length is reduced while they are shifted to the right when patch length is increased. Both changes contribute to smaller passband bandwidth and fractional bandwidth. For longer patch length, the higher frequency components have larger return loss values. Both outputs signals are still 180 degrees out of phase at all passband.

Case 12: Uniform variation of patch width

$W_1 = W_2 = W_3 = 10.0mm$

$W_1 = W_2 = W_3 = 12.0mm$

$W_1 = W_2 = W_3 = 13.0mm$

Result

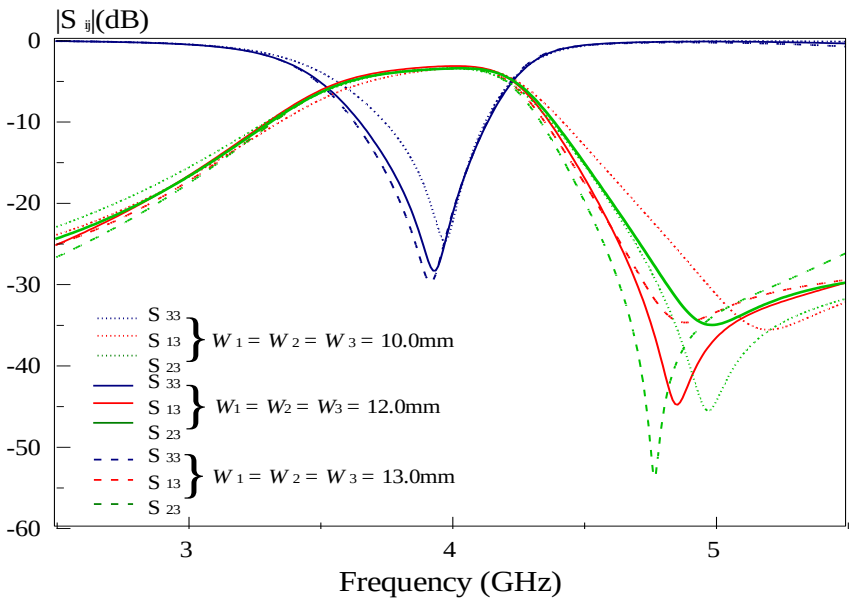


**Figure 3-65: Amplitude Response due to uniform variation of patch width**

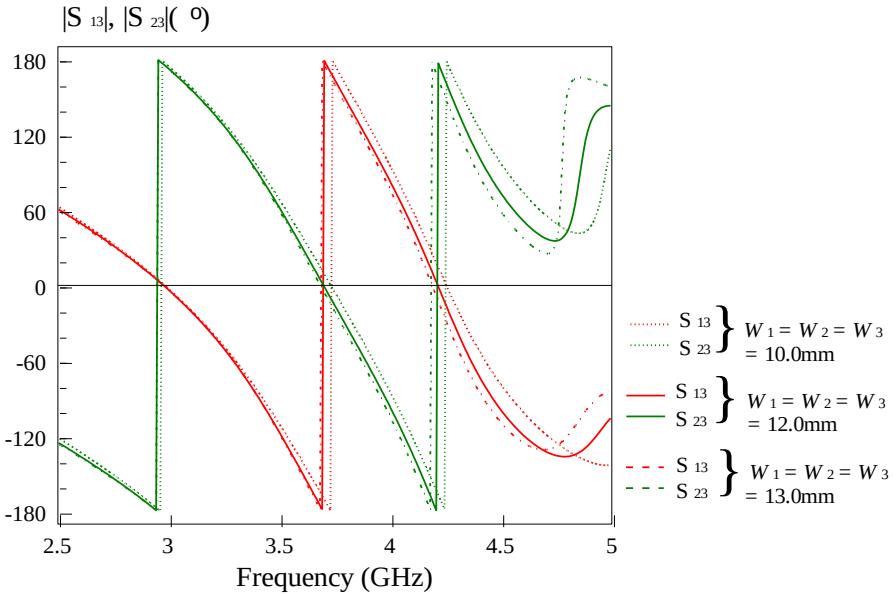


**Figure 3-66: Phase Response due to uniform variation of patch width**

Observation

In this case, there is no significant change in effects for uniform variation of all rectangular patch width. Both output phase difference remains the same.

Case 13: Variation of patch width W1

$W_1$ = 10.0mm

$W_1$ = 12.0mm

$W_1$ = 13.0mm

Result

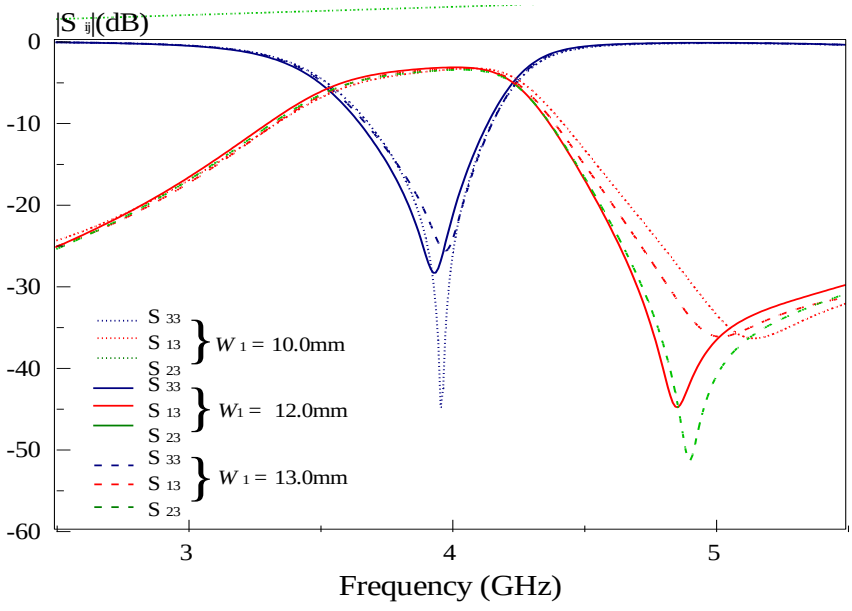


**Figure 3-67: Amplitude Response due to variation of patch width W1**

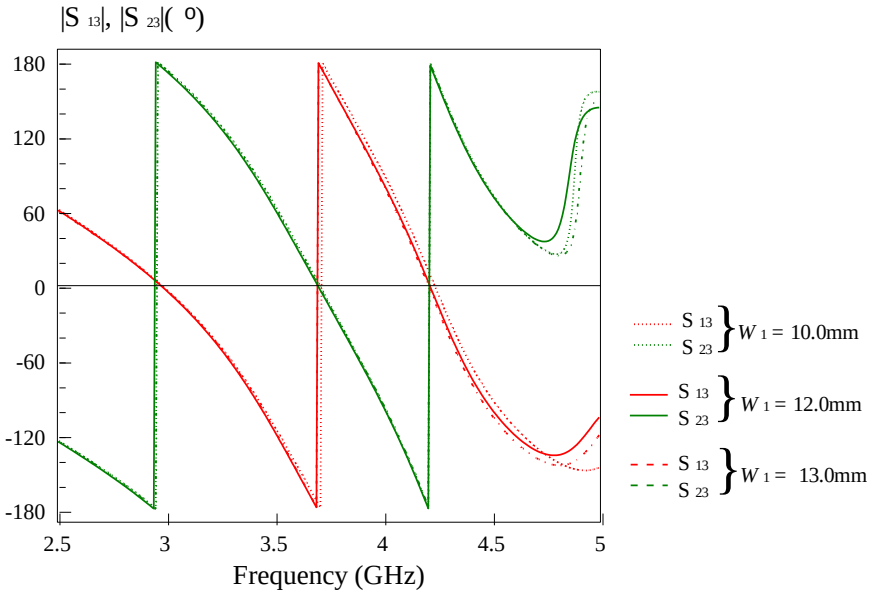


**Figure 3-68: Phase Response due to variation of patch width W1**

Observation

From the amplitude response, there is no significant change in effects due to variation of rectangular patch width W1. Only return loss factor is affected. Both output phase difference remains the same.

Case 14: Variation of patch width W2

$W_2$ = 10.0mm

$W_2$ = 12.0mm

$W_2$ = 13.0mm

Result

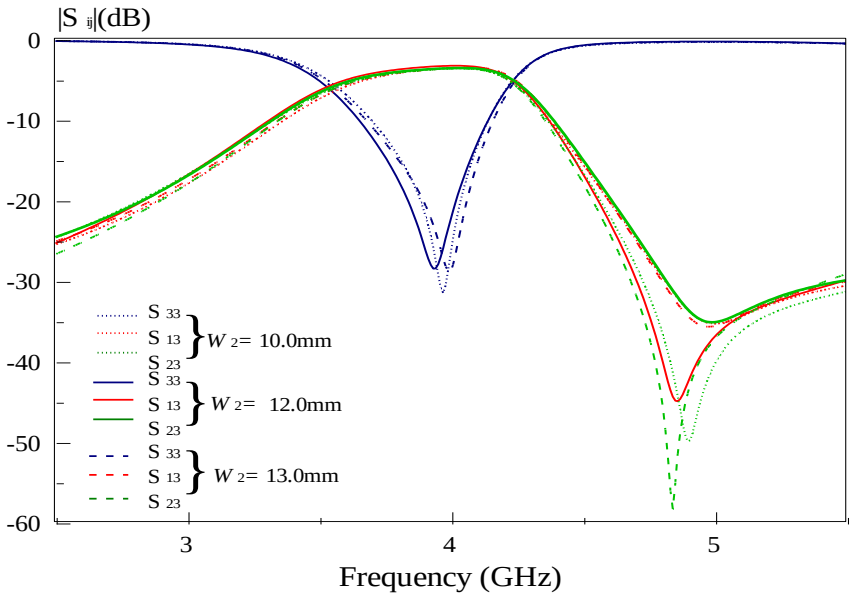


**Figure 3-69: Amplitude Response due to variation of patch width W2**

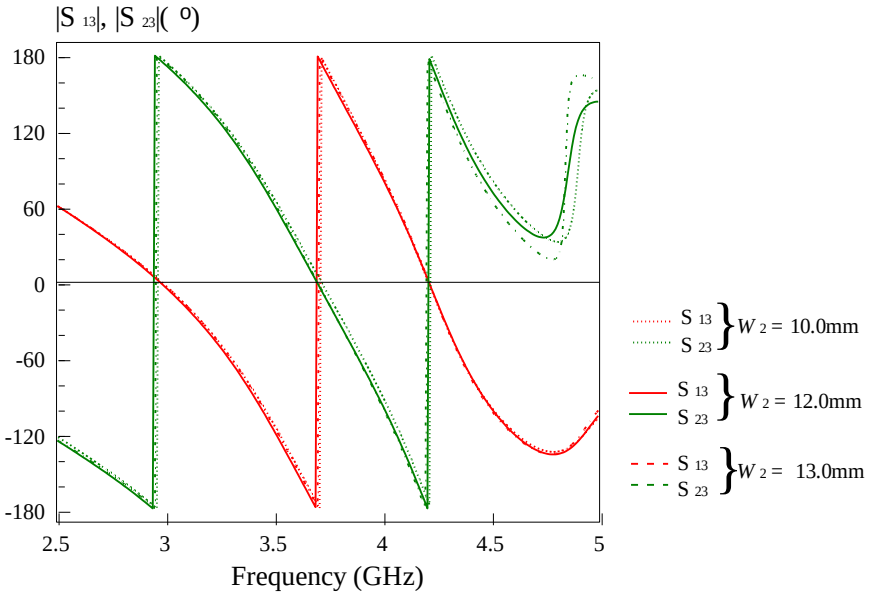


**Figure 3-70: Phase Response due to variation of patch width W2**

Observation

Similarly in case 13, there is no significant change in effects for changes of width W2. Both output phase difference remains the same.

Case 15: Variation of patch width W3

$W_3$ = 10.0mm

$W_3$ = 12.0mm

$W_3$ = 13.0mm

Result

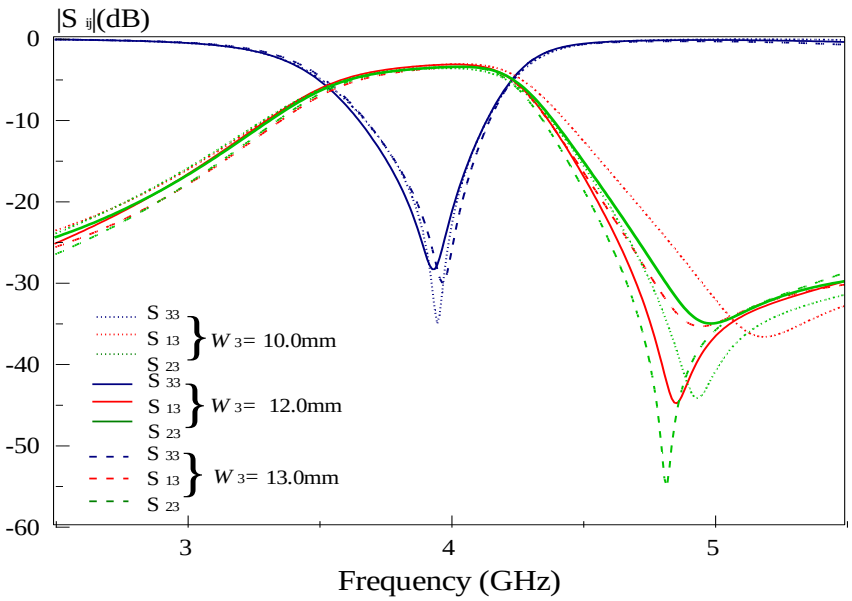


**Figure 3-71: Amplitude Response due to variation of patch width W3**

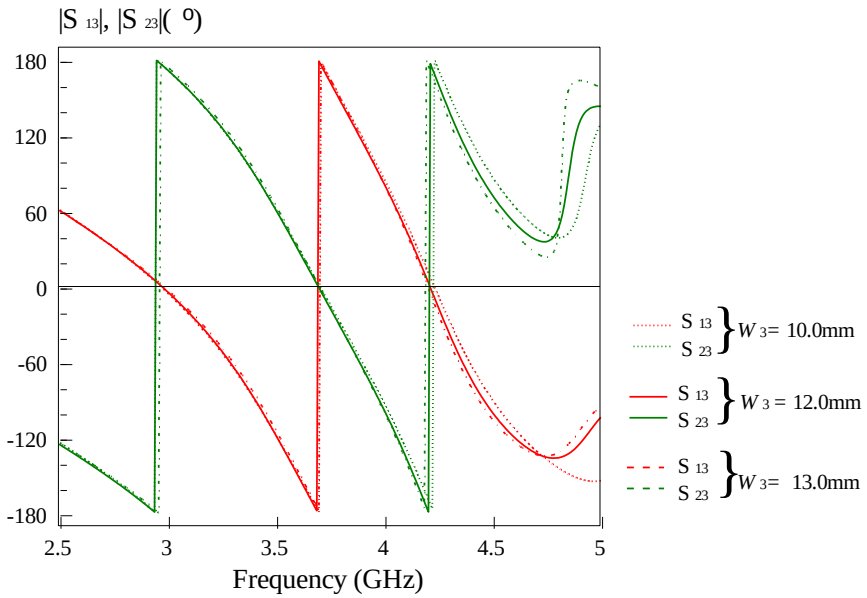


**Figure 3-72: Phase Response due to variation of patch width W3**

Observation

Similarly in case 13 and 14, there is no significant change in effects for changes of width W3. Both output phase difference remains the same.

Case 16: Variation of patch width W4

$W_4$ = 2.5mm

$W_4$ = 3.5mm

$W_4$ = 4.5mm

Result

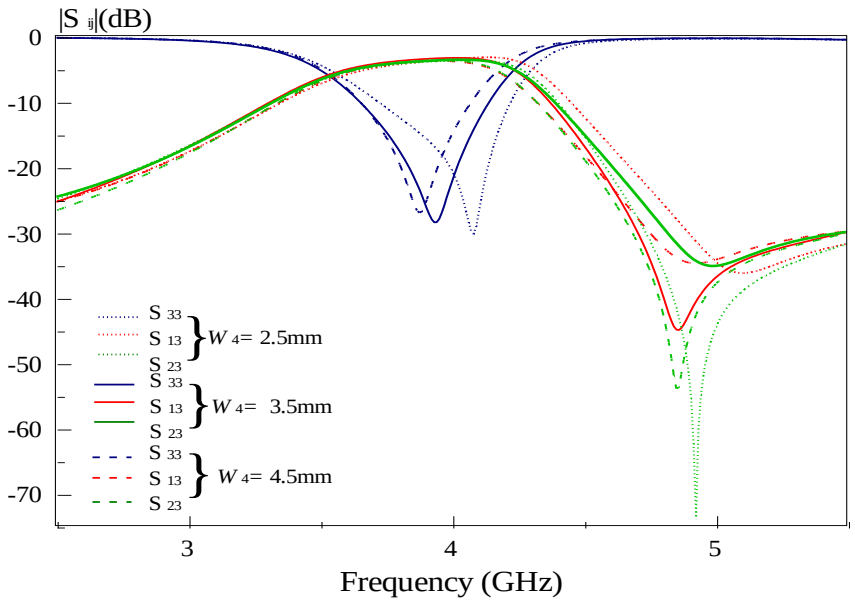


**Figure 3-73: Amplitude Response due to variation of patch width W4**

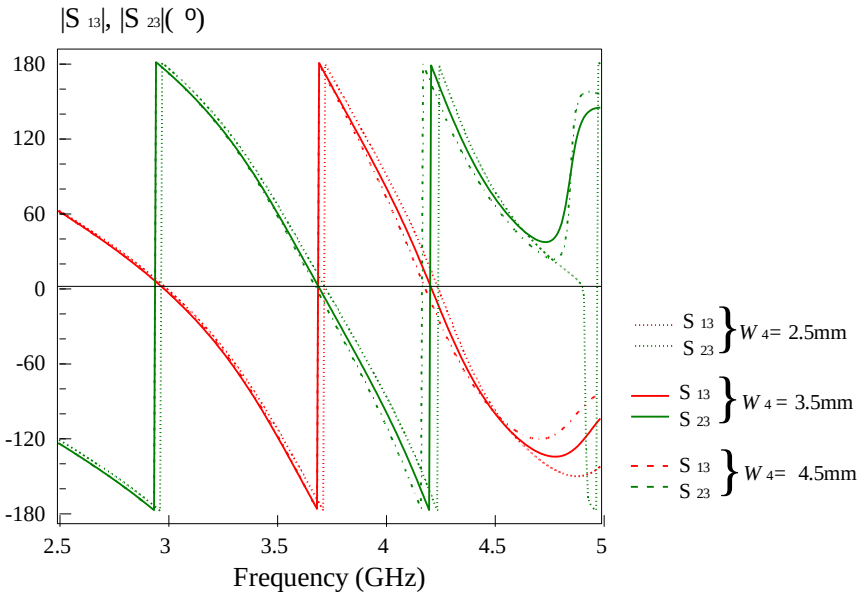


**Figure 3-74: Phase Response due to variation of patch width W4**

Observation

Based on figure 3.73, the parameter W4 affects the pole position as well as the passband bandwidth of the divider. Smaller W4 shifts the pole to the upper frequency while larger W4 shifts the pole to the lower frequency spectrum.

## 3.4 Discussion

In the passband region, we can observe that the electric field at all output ports have almost the same intensity, shown in figure 3.75 and figure 3.76. Both frequencies are within the operating bandwidth. This shows that the power divider is able to divide an input signal equally among the output ports in all operating bands because there is good impedance matching between the coupled transmission lines. Therefore, very minor reflection occurs at the input resonator.

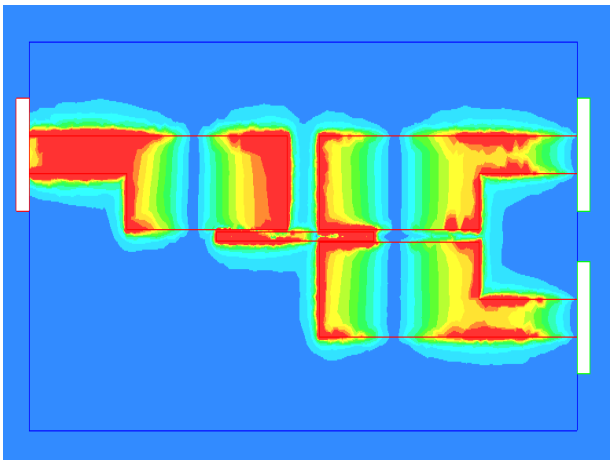

**Figure 3-75: E-Field at 5.0GHz (In-Phase Divider)**

Besides that, we can observe that the E-field strength at each point is the same at port 2 and port 3 which implies that they are moving in-phase. Beyond the passband bandwidth, we can observe that the E-field intensity at all output ports are a zero while the E-field level at the input patch is very highly concentrated. This indicates that no signal is almost able to pass through and are all reflected back to the input port. The cause of this is due to impedance mismatch between the transmission lines.

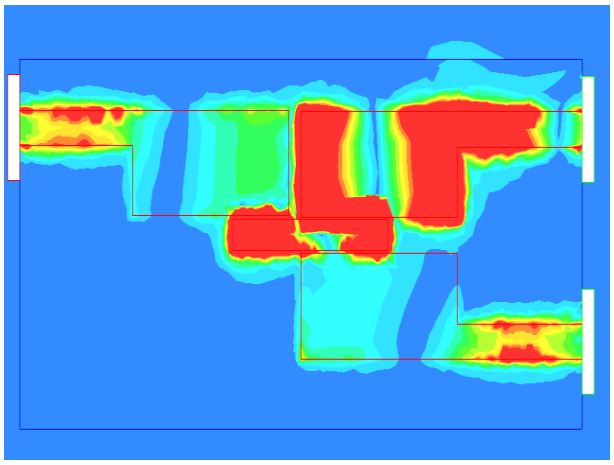

**Figure 3-76: E-Field at 3.58GHz (Out-Phase Divider)**

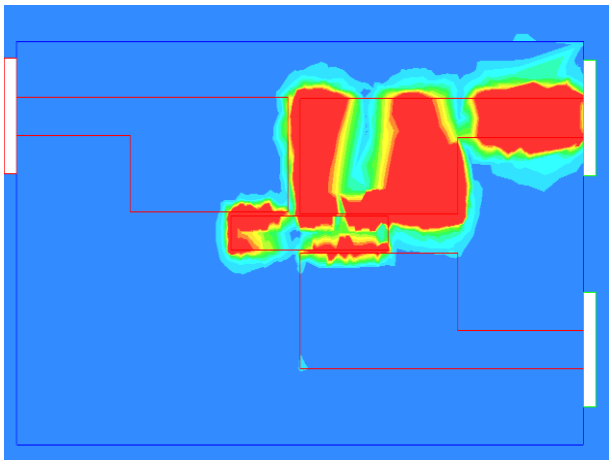

**Figure 3-77: E-Field at 5.00GHz (Out-Phase Divider)**

The same concept is applied to the out-of-phase divider. Frequency in the passband range allows signals to resonate to the output patches due to good impedance matching between the coupled lines, shown in figure 3.76. Impedance mismatch will cause reflection, thus reflecting back all the incoming signals. Therefore, no signals are detected at the output ports such as in figure 3.77. Furthermore, we can also observe that the E-field intensity variation is identical at port 1 and port 2 but at the opposite direction. This leads to a 180 degree out of phase between both ports.

# CHAPTER 4

# MULTI-WAY PATCH POWER DIVIDER

## 4.1 Background

Even today, it is still a huge challenge to design power dividers with an odd number of output ports (Jui-Chieh Chiu, Jhi-Ming Lin, Yeong-Her Wang, 2006). According to E.J Wilkinson in 1960, a divider that is used to split a signal into three parts generally requires combination of several sections of microstrip lines with addition of resistors for impedance matching. Over the years, only a few three-way power dividers have been designed and are summarized in table 3 shown below (Jui-Chieh Chiu, Jhi-Ming Lin, Yeong-Her Wang, 2006).

| Three-way power divider | Circuit length | Isolation Resistors | Circuit Dimension | DC block function |
|---|---|---|---|---|
| Wilkinson | λ/4 | Three | 3D | No |
| Recombinant | 3λ/4 | Three | 2D | No |
| Planarized | 3λ/4 | Four | 2D | No |
| Stepped-Impedance Resonators | 3λ/4 | None* | 2D | Yes |
| Modified Luzzato | λ/4 toλ/2 | Three | 3D | No |
| Sector-Shaped | λ/4 | None* | 2D | No |
| Planar N-Way | λ/4 | Two | 2D | No |
| Matched sectorial components in radial arrangement | λ/4 toλ/2 | Two | 2D | No |
| This work | λ/4 | Two | 2D | Yes |

**Table 4-1: Types of three-way power divider**

In this chapter, a novel 3-way power divider will be presented by the author. This proposed divider applies the concept of rectangular patches as resonators. Input

power is divided equally to 3 outputs ports. In section 4.2.1, the configuration of the 3-way divider will be illustrated.

## 4.2 Three-Way Patch Power Divider

### 4.2.1 Configuration

Here, the author will illustrate the configuration of the 3-way patch power divider. Based on the configuration shown below in figure 4.1, the 3-waypower divider consists of four ports, which are numbered as Port 1, Port 2, Port 3, and Port 4. Port 1 is the input port where else Port 2, 3 and 4 are the output ports. All input and output ports are connected to 50 ohm feed lines.

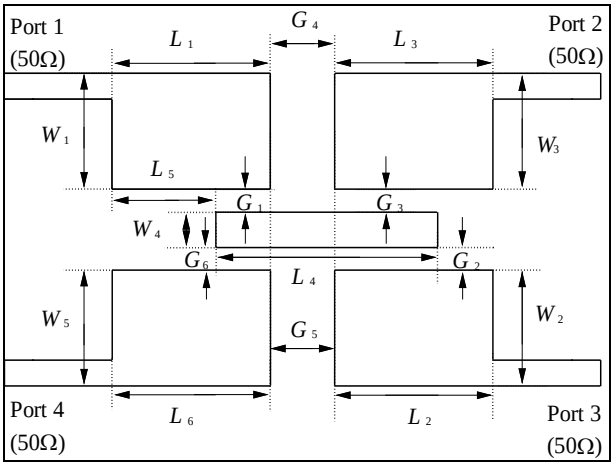


**Figure 4-1: Configuration of the 3-way power divider**

In this proposed design, the divider is developed by implementing five rectangular patches as resonators. The four side rectangular patches which are connected to the input/output ports by 50 ohm feed lines each has its own specific length and width. Overall, the area of the 3-way power divider is 42.0mm x 85.1mm = 3574.2mm$^2$.

The substrate used in implementing this design has a dielectric constant of 2.33 and a thickness of 1.57mm. In the following, the design dimensions of the multi-way divider configuration will be presented. L, W and G denotes the parameters of length, width and gap respectively.

$L_1$ = 26.1mm, $L_2$ = 26.5mm, $L_3$ = 26.5mm, $L_4$ = 27.0mm, $L_5$ = 12.0mm, L6 = 22,1mm, W1 = 12.0mm, $W_2$ =12.0mm, $W_3$= 12.0mm, $W_4$ = 1.0mm, $W_5$ = 12.0mm, $G_1$ = 0.3mm, $G_2$ = 0.7mm, $G_3$ = 0.7mm, $G_4$ = 3.0mm, $G_5$ = 1.6mm, $G_6$= 0.6mm

Figure 4.2 illustrates the top view configuration of the power divider in HFSS, Figure 4.3 display the configuration in 3D view, and Figure 4.4 is the photograph of the fabricated 3-way power divider.

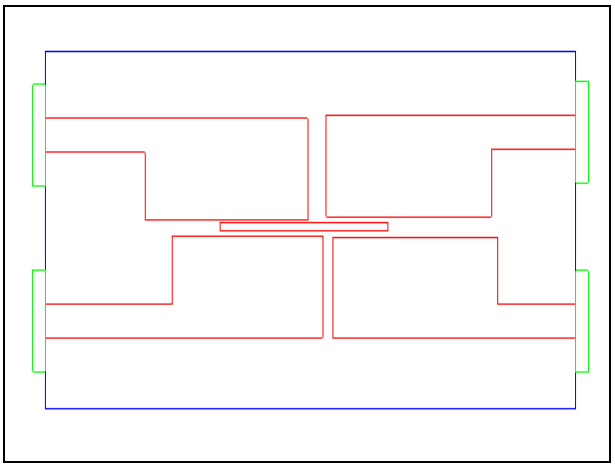

**Figure 4-2: 3-way Power Divider (Top View)**

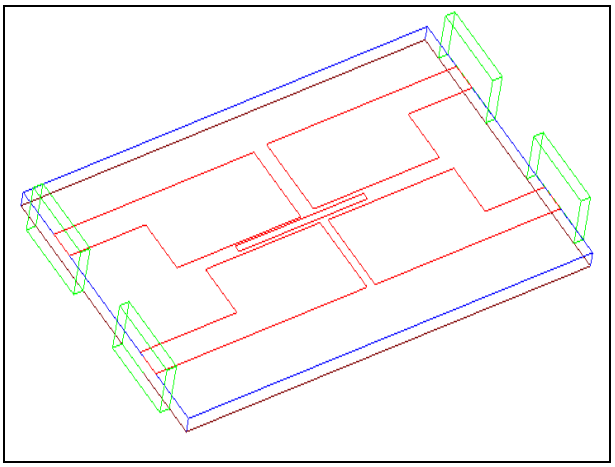

**Figure 4-3: 3-way Power Divider (3D View)**

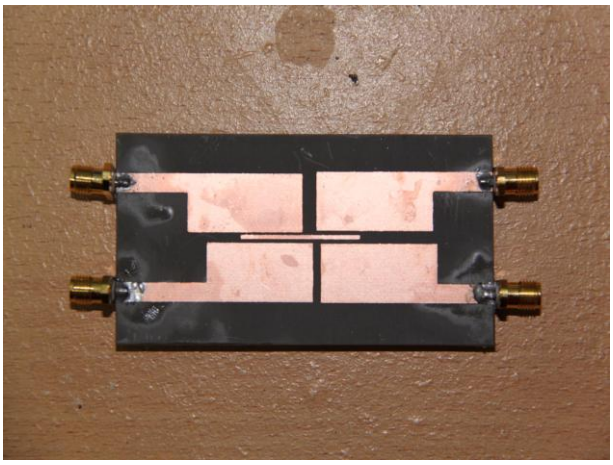

**Figure 4-4: Photograph of fabricated 3-way Power Divider**

### 4.2.2 Transmission Line Model

In section 4.2.1, the author had illustrated on the design configuration of the 3-way power divider. Here, the author will present the transmission line model that corresponds to the equivalent circuit of the proposed multi-way power divider. Figure 4.5 shows the transmission line model of the proposed device.

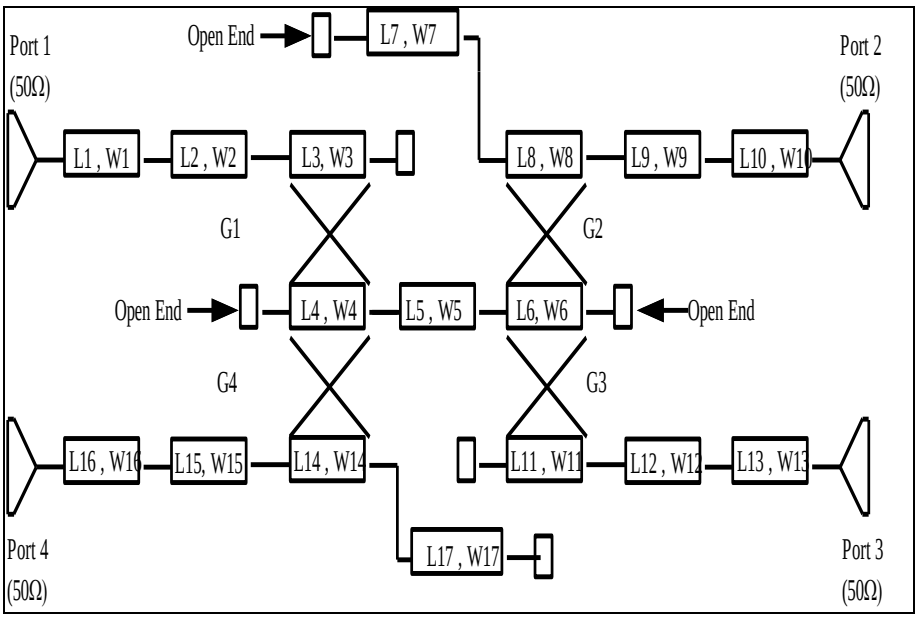


**Figure 4-5: Transmission Line Model of 3-way Power Divider**

Similarly to the in-phase and out-phase power divider transmission model, the triangular objects represent the input (Port 1) and output ports (Port 2, Port 3 and Port 4) of the device. All transmission lines are represented by rectangular boxes.

Both L and W signify the strip length and width respectively. Table below shows the length, width and gap of each represented elements

| LENGTH | (mm) |
|---|---|
| L1 | 16 |
| L2 | 12 |
| L3 | 14.1 |
| L4 | 14.1 |
| L5 | 4.0 |
| L6 | 9.4 |
| L7 | 1.0 |
| L8 | 9.4 |
| L9 | 16.6 |
| L10 | 13.5 |
| L11 | 9.4 |
| L12 | 17.6 |
| L13 | 12.5 |
| L14 | 14.1 |
| L15 | 5.6 |
| L16 | 26 |
| L17 | 2.4 |

| WIDTH | (mm) |
|---|---|
| W1 | 4 |
| W2 | 12 |
| W3 | 12 |
| W4 | 1 |
| W5 | 1 |
| W6 | 1 |
| W7 | 12 |
| W8 | 12 |
| W9 | 12 |
| W10 | 4 |
| W11 | 12 |
| W12 | 12 |
| W13 | 4 |
| W14 | 12 |
| W15 | 12 |
| W16 | 4 |
| W17 | 2.4 |

| GAP | (mm) |
|---|---|
| G1 | 0.3 |
| G2 | 0.7 |
| G3 | 0.7 |
| G4 | 0.6 |

**Table 4-2: Element Parameters for Multi-Way Power Divider**

The circled section in figure 4.6 represents the 50 ohm feed line and partial of the rectangular patch that connect is connected to the port.

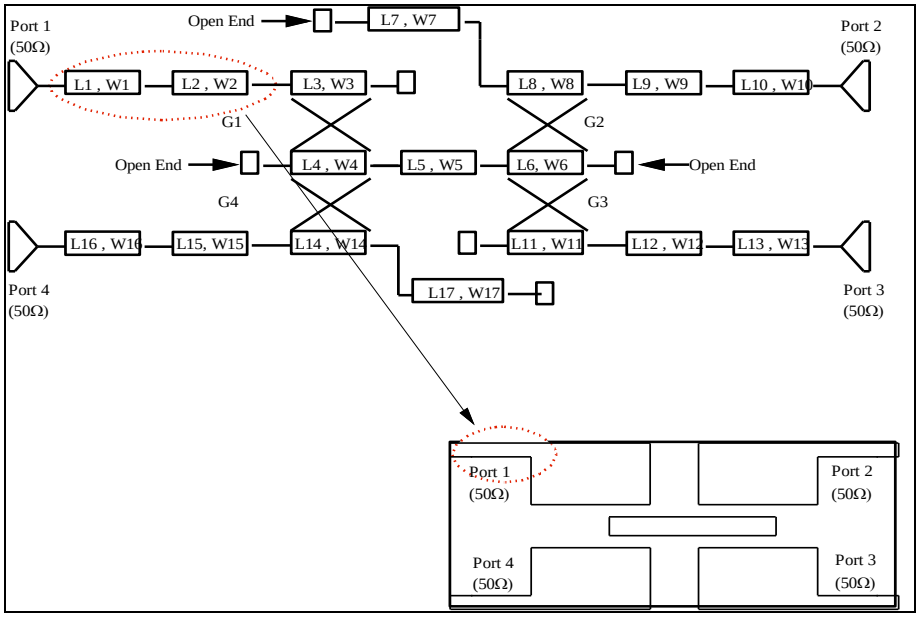


**Figure 4-6: Representation of feed line and partial rectangular patch**

Even though both constitute from microstrip lines, two elements are required since both have different widths.

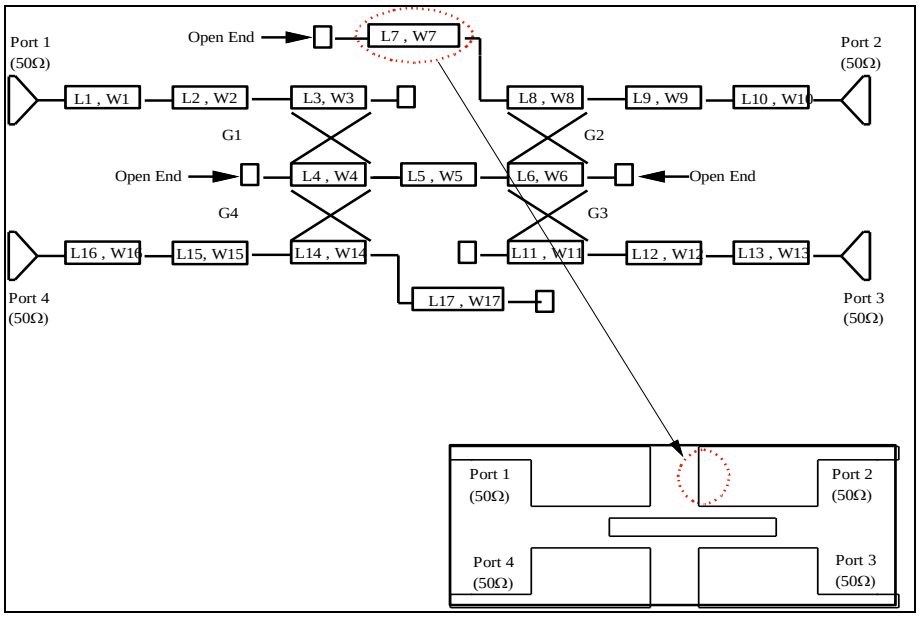


**Figure 4-7: Representation of extra part of rectangular patch**

Unlike previous transmission models, there is a partial section of the top right rectangular patch that is coupled by a single transmission line. Therefore, an extra section is added to represent that section shown in figure 4.7.

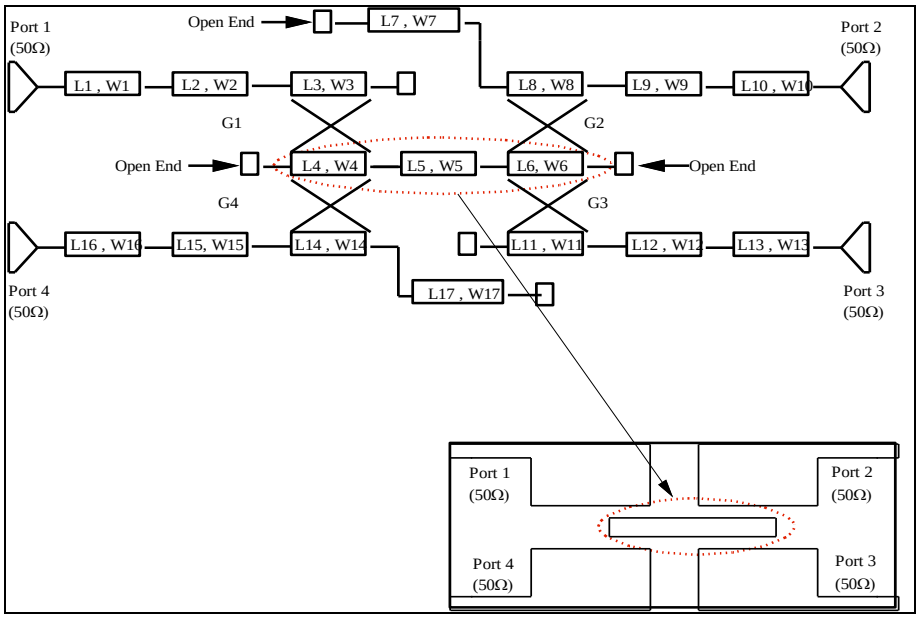


**Figure 4-8: Representation of centre patch**

The 3 rectangular boxes connected in series represent the centre rectangular patch of the divider. It is shown in figure 4.8.

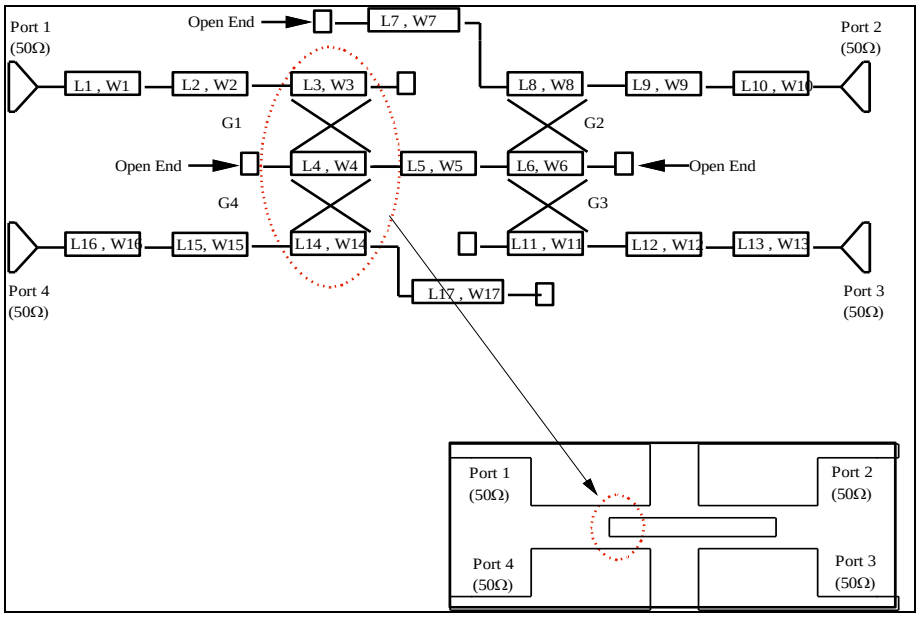


**Figure 4-9Figure 4.9: Representation of coupled lines**

The highlighted section in figure 4.9 represents the coupled lines of the transmission lines.

### 4.2.3 Results

In section 4.3, the performance of the multi-way power divider will be demonstrated. Simulation, measurement and modelling results will be compared. All simulation, measurement, and modelling results are acquired through HFSS, Agilent Network Analyser and Microwave Office respectively.

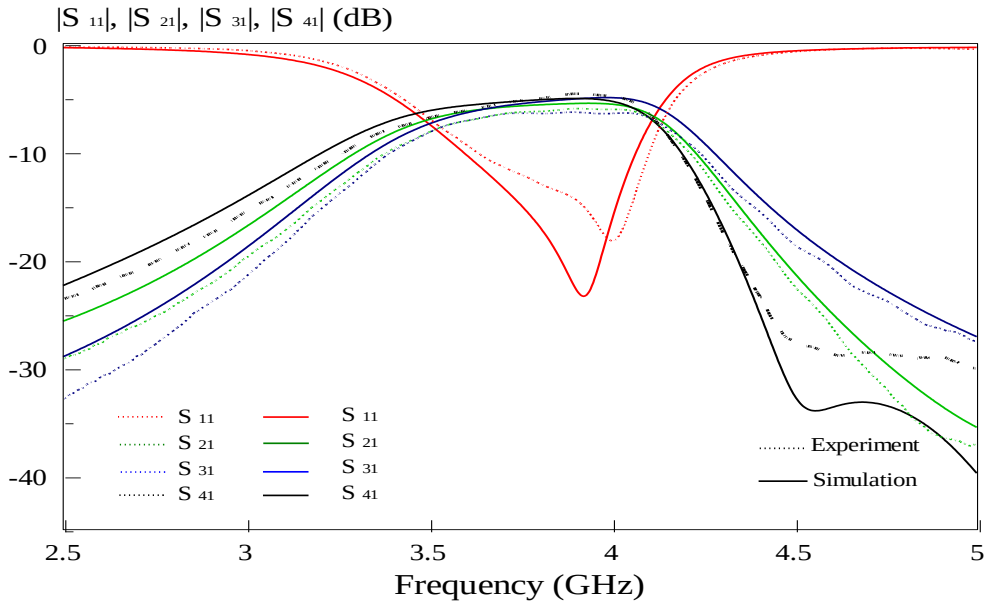


**Figure 4-10: Amplitude Response of 3-Way Power Divider (Simulated VS Measured)**

Figure 4.10 displays the comparison of simulated and measured amplitude response. From the graph shown above, the simulated amplitude response curve shows that the divider is able to perform at frequency range between 3.59GHz to 4.06GHz. Therefore, the passband bandwidth of the divider is 0.47GHz. The central frequency is 3.82GHz, thus providing a fractional bandwidth of 12%. The lowest insertion loss of the divider is -5dB while the highest insertion loss is -6.3dB. As a result, the amplitude balance based on simulation is 1.3dB.

Meanwhile, based on the measured amplitude response curve, there is a slight shift in the passband. However, the passband bandwidth and fractional bandwidth are approximately similar to the simulated one. The central frequency of the measured divider is approximately 3.9GHz. From here, the error exhibited based on the simulated and measured performance is 2% which is relatively small.

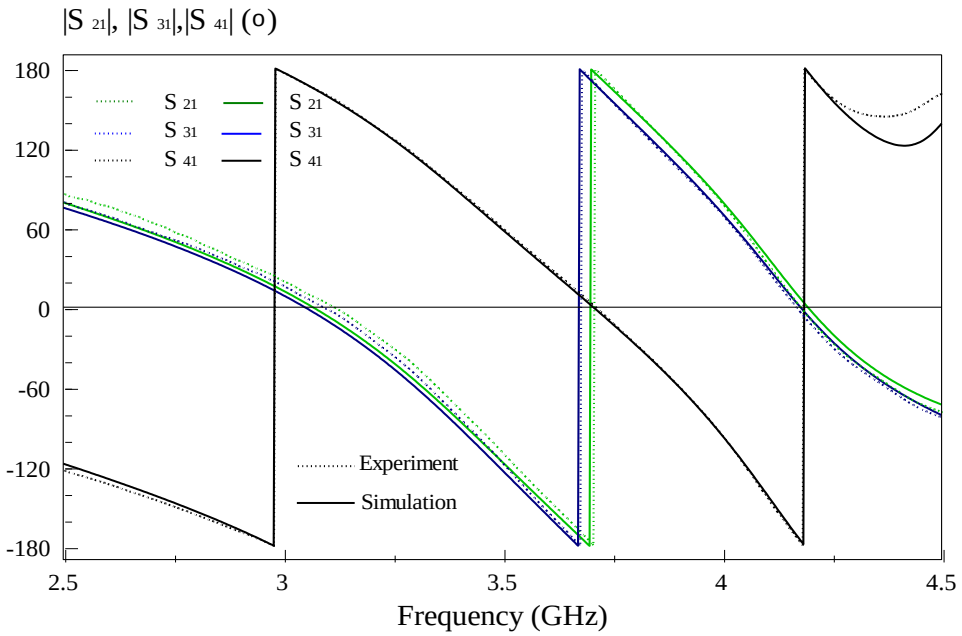


**Figure 4-11: Phase Response of 3-Way Power Divider**

Figure 4.11 illustrates the comparison of the simulated and measured phase response. Based on the graph above, we can observe that the outputs at port 2 and port 3 are in-phase while the output at port 4 relative to port 2 and port 3 is 180 degree out of phase at all working frequencies. Both response curves show good agreement between the simulated and measured results.

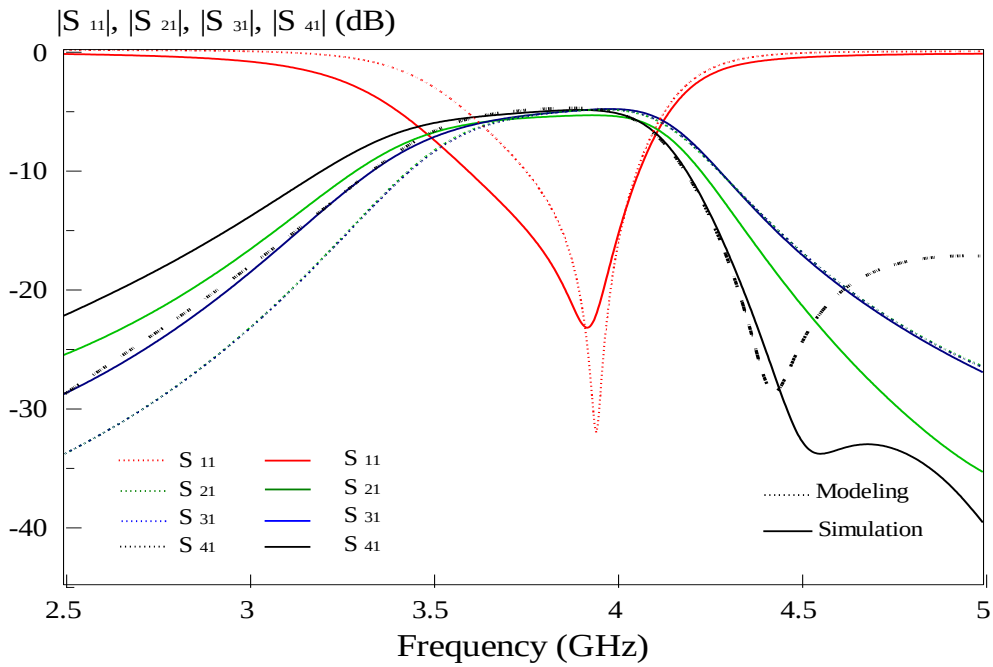


**Figure 4-12: Amplitude Response of 3-Way Power Divider (Simulated VS Modelling)**

From figure 4.12, the simulation and modelling amplitude response are compared. Based on the modelling amplitude response curve, the divider is able to perform at frequencies between 3.75GHz to 4GHz, thus having an operating bandwidth of 0.25GHz. The central frequency is 3.87GHz, which corresponds to fractional bandwidth of 6%. The insertion loss of the divider based on modelling is -5.16dB on average. Overall, the amplitude balance is less than 1dB.

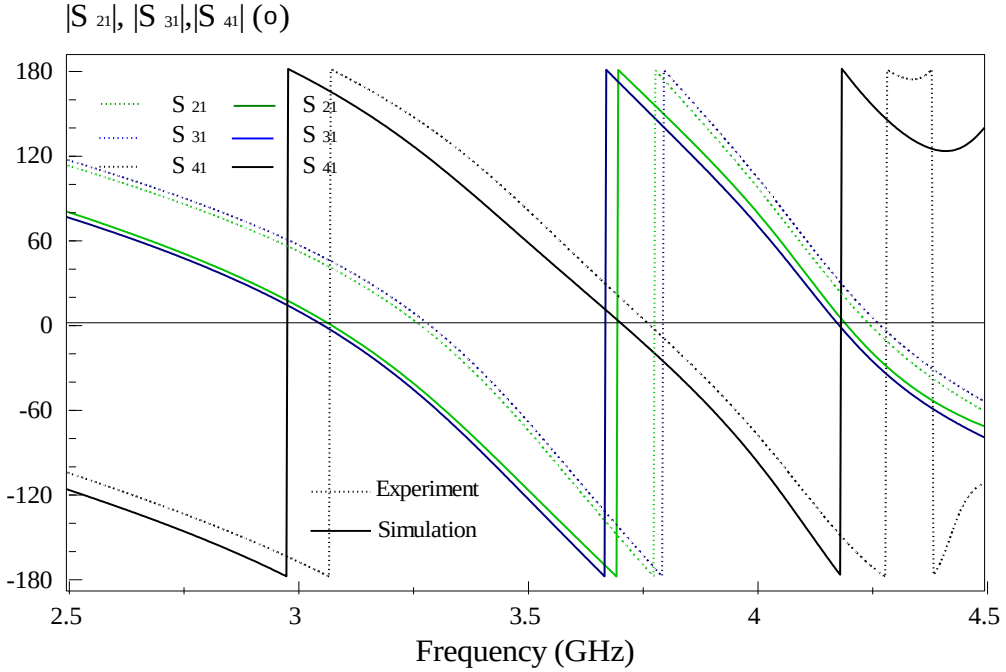


**Figure 4-13: Phase Response of 3-Way Power Divider (Simulated VS Modelling)**

Figure 4.13 illustrates the comparison of the simulated and modelled phase response. Based on the graph above, we can observe that the outputs at port 2 and port 3 are in-phase while the output at port 4 relative to port 2 and port 3 is 180 degree out of phase at all working frequencies. However, the modelling results show a shift in frequency.

### 4.2.4 Parametric Analysis

In section 4.4, the effects of each parameter of the multi-way divider will be studied. Figure 4.14 shows the proposed design configurations together with the original dimensions.

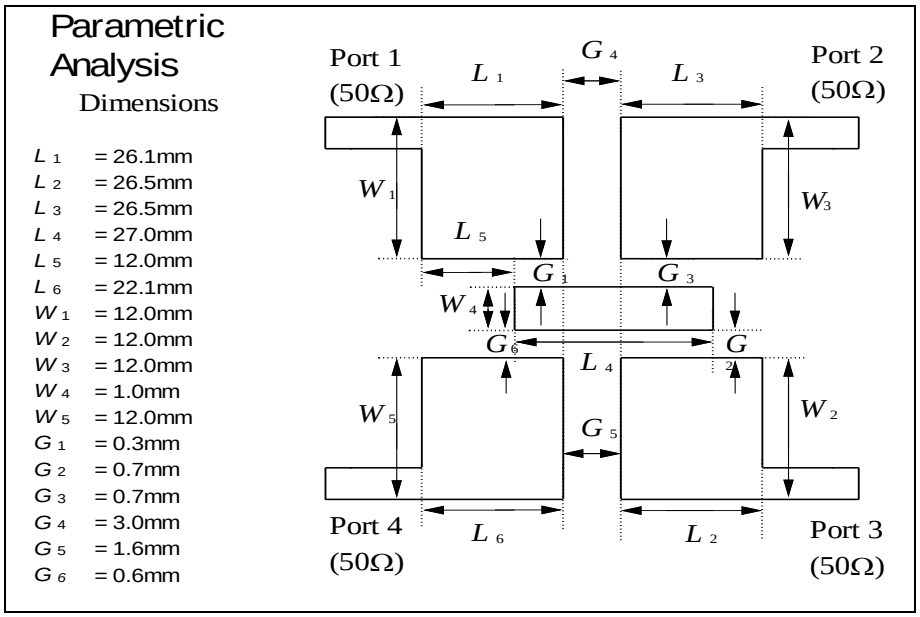


**Figure 4-14: Dimensions of proposed Multi-way Power Divider**

Case 1: Variation of length L1

$L_1$ = 22.1mm

$L_1$ = 24.1mm

$L_1$ = 26.1mm

Result

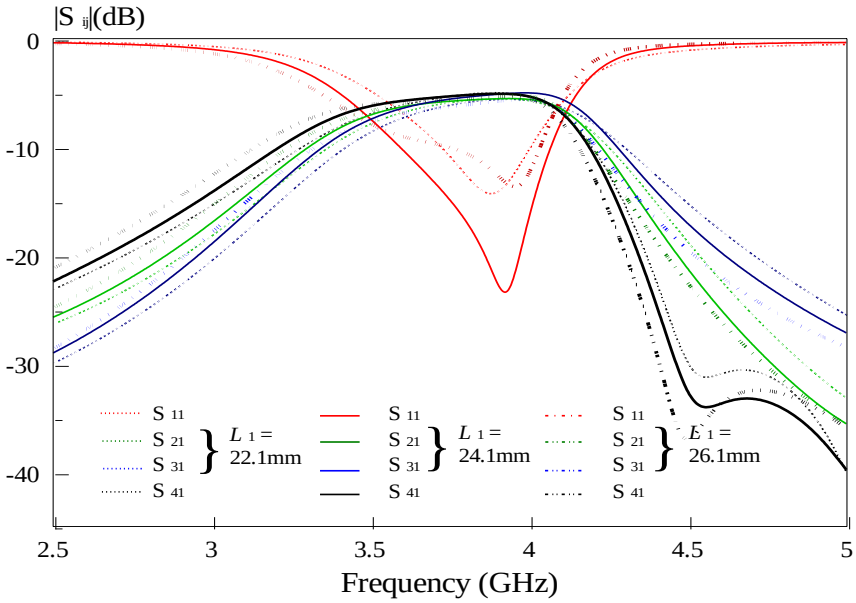


**Figure 4-15: Amplitude Response due to variation of length L1**

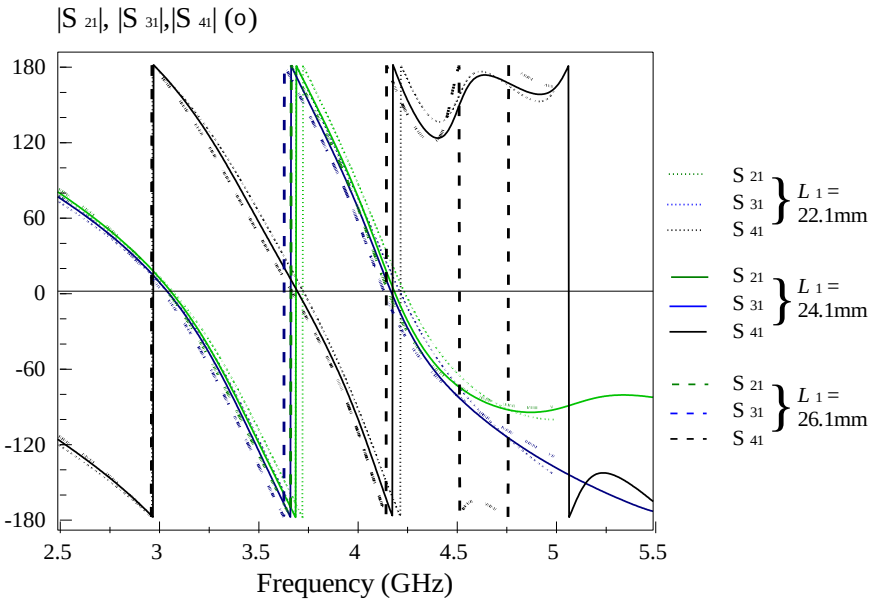


**Figure 4-16: Phase Response due to variation of length L1**

Observation

Based on the amplitude response curve shown in figure 4.15, the major effects of varying L1 are the passband bandwidth and the return loss of the multi-way divider. When L1 = 22.1mm, the divider is only able to perform at frequencies between 3.72GHz to 4.0GHz, thus providing a passband bandwidth of 0.27GHz. This shows a significant reduction in operating bandwidth of the divider. Meanwhile, the output at Port 2 and Port 3 is approximately 11 degree out of phase and only output of Port 2 and Port 4 is able to produce phase difference of 180 degree at all passband. When L1= 26.1mm, the passband bandwidth is drastically decrease as well. Similarly, the operating bandwidth is only 0.27GHz. Moreover, the performance in terms of phase response is similar to the one when L1= 22.1m.

Case 2: Variation of length L2

$L_2$ = 24.5mm

$L_2$ = 26.5mm

$L_2$ = 28.5mm

Result

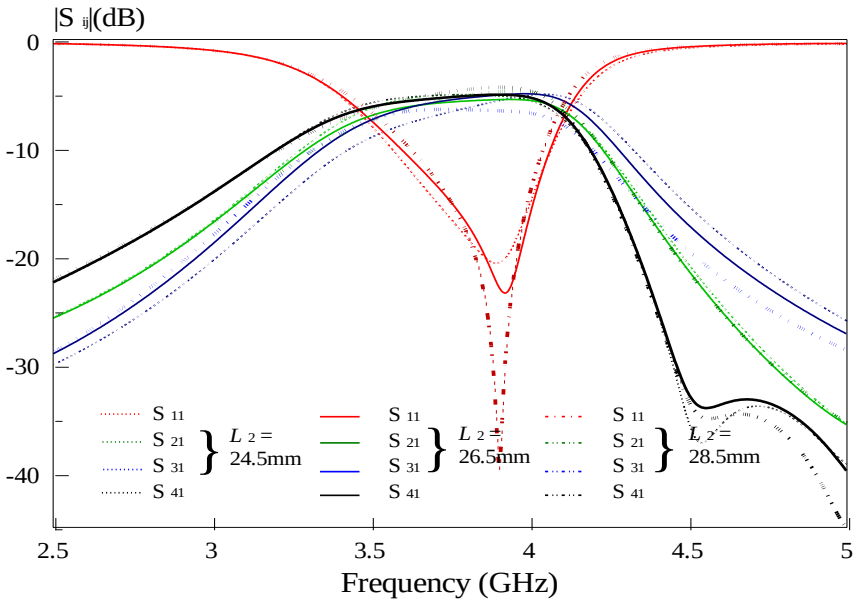


**Figure 4-17: Amplitude Response due to variation of length L2**

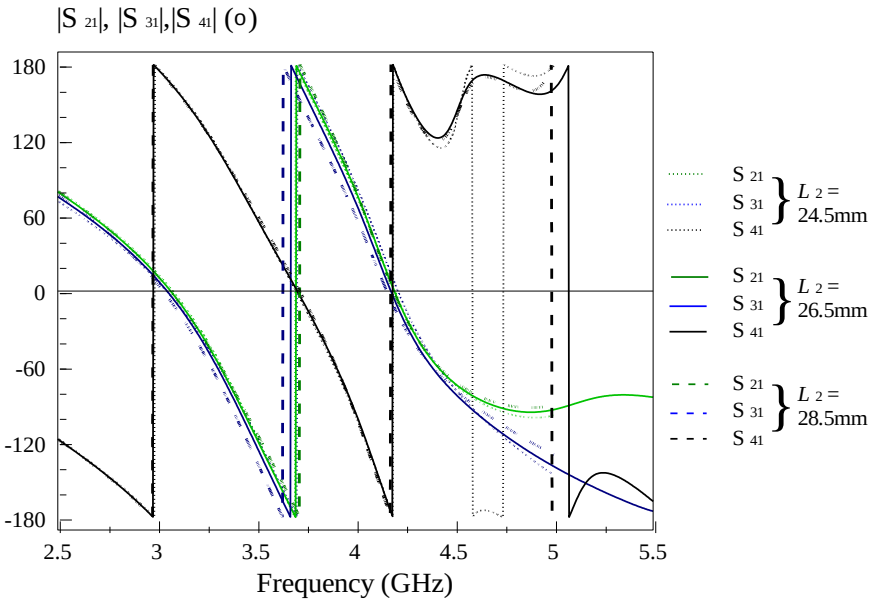


**Figure 4-18: Phase Response due to variation of length L2**

Observation

L2 is a parameter that affects the return loss and the insertion loss of the divider. Setting L2 = 24.5 mm exhibits unequal power division at the outputs. The output power at Port 3 is significantly lower compared to outputs at Port 2 and Port 4 especially at the lower frequency components of the passband. However, Port 2 and Port 3 outputs are in phase and both produce 180 degree phase difference to output at Port 4 within the passband. Setting L2= 28.5mm also shows unequal power division at the outputs. The power at Port 3 at higher frequency components of the passband

has lower power compared to Port 2 and Port 4. Outputs at Port 2 and Port 3 are not in phase. Only Port 2 and Port 4 exhibits 180 degree out of phase in the passband.

Case 3: Variation of length L3

$L_3$ = 24.5mm

$L_3$ = 26.5mm

$L_3$ = 28.5mm

Result

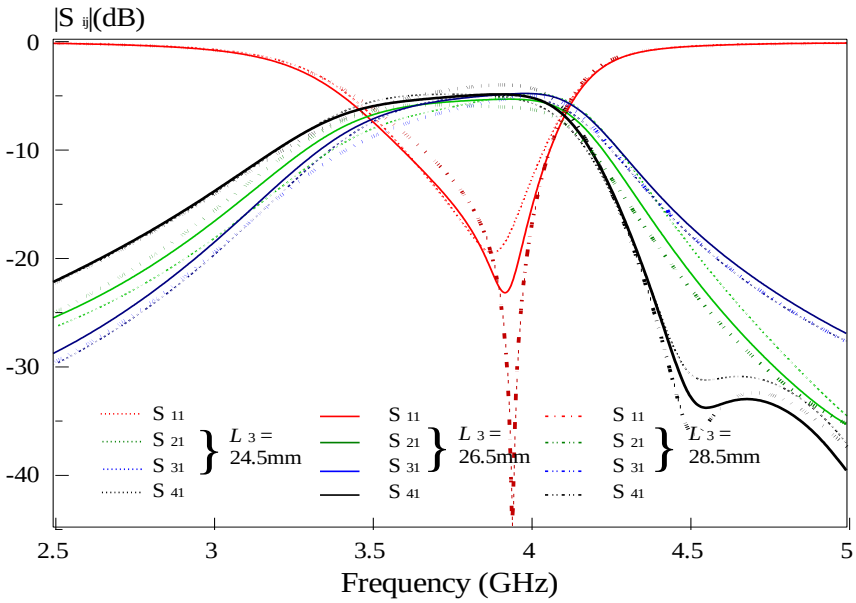


**Figure 4-19: Amplitude Response due to variation of length L3**

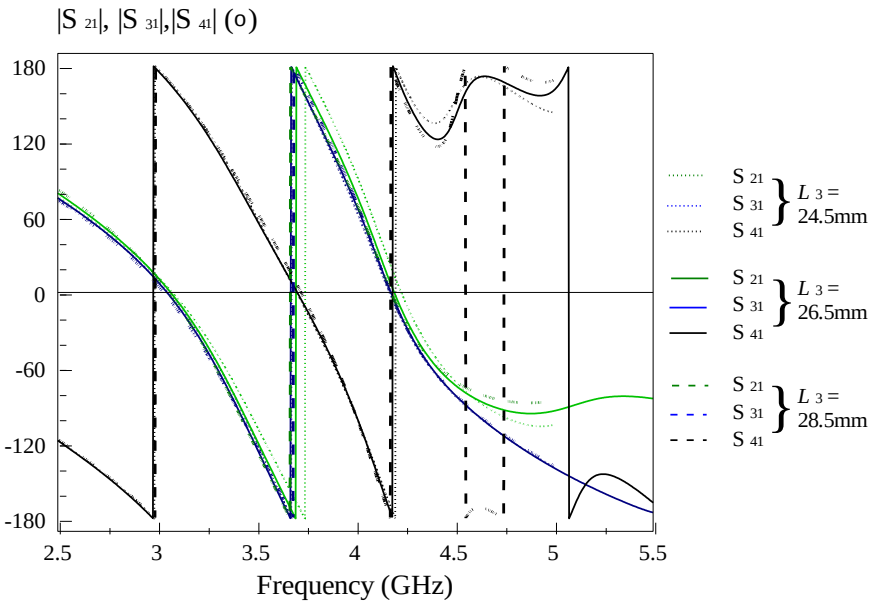


**Figure 4-20: Phase Response due to variation of length L3**

Observation

From figure 4.19, we can observe that L3 apparent determine the insertion loss of the divider. Setting L3 = 24.5mm and L3 = 28.5mm causes unequal power division at the outputs. However, the passband bandwidth is approximately the same. When L3 = 24.5mm, in phase outputs at Port 2 and Port 3 are not possible. However, L3 = 28.5 stills produce in phase output at Port 2 and Port 3.

Case 4: Variation of length L4

$L_4$ = 25mm

$L_4$ = 27mm

$L_4$ = 29mm

Result

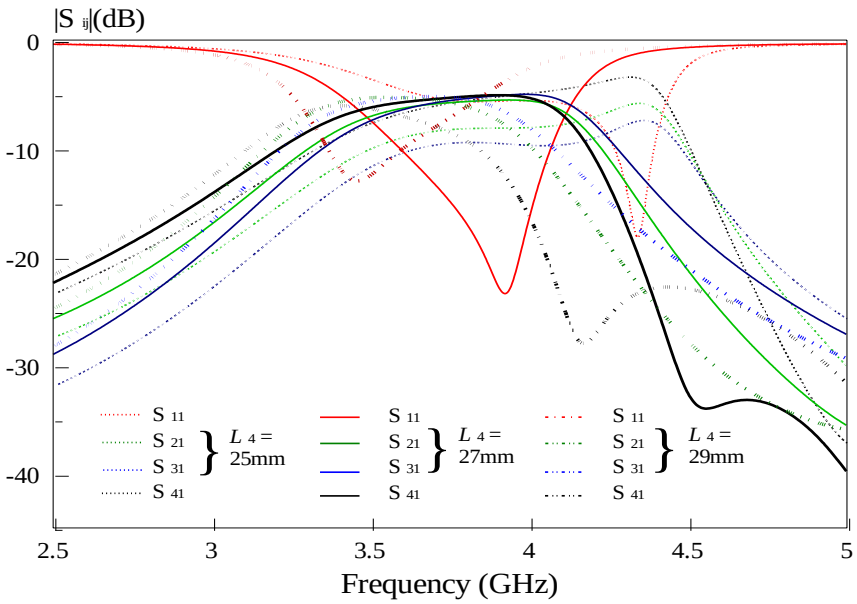


**Figure 4-21: Amplitude Response due to variation of length L4**

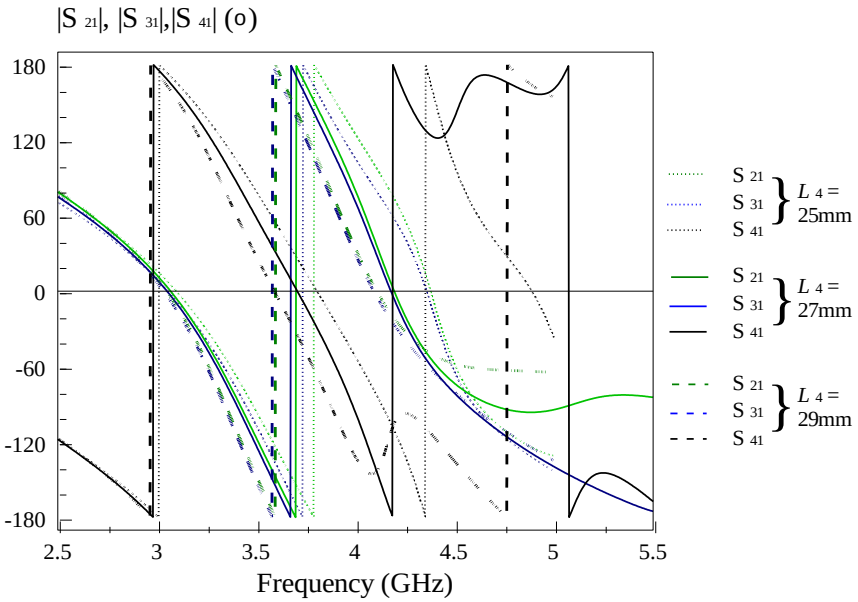


**Figure 4-22: Phase Response due to variation of length L4**

Observation

The reduction in centre patch length causes the pole to shift to the upper frequency spectrum. Increase in centre patch length cause the pole to shift to the lower frequency spectrum. Besides that, the passband bandwidth is hugely affected by the variation. When L4 = 25mm, outputs at Port 2 and Port 3 are not in phase. However, setting L4 = 29mm still produce in phase outputs at Port 2 and Port 3. Therefore, L4 is an important parameter to be considered when designing the multi-way divider.

Case 5: Variation of length L5

$L_5$ = 10mm

$L_5$ = 12mm

$L_5$ = 14mm

Result

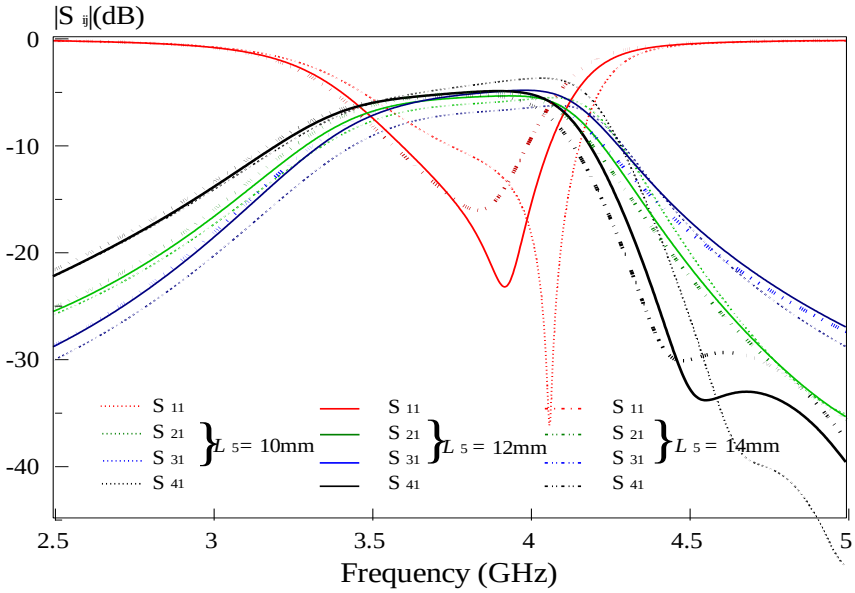


**Figure 4-23: Amplitude Response due to variation of length L5**

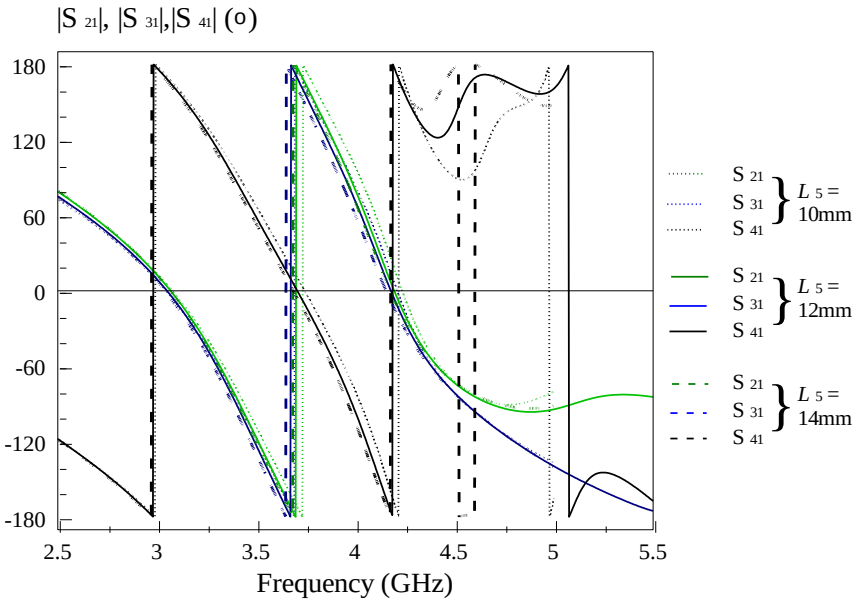


**Figure 4-24: Phase Response due to variation of length L5**

Observation

From the amplitude response shown in figure 4.23, the pole position is determine by the patch length L5. As the patch length gets shorter, the pole moves more to the upper frequency spectrum, thus affecting the operating bandwidth of the divider. There is a slight phase difference between outputs at Port 2 and Port 3.

Case 6: Variation of length L6

$L_6$= 10mm

$L_6$ = 12mm

$L_6$ = 14mm

Result

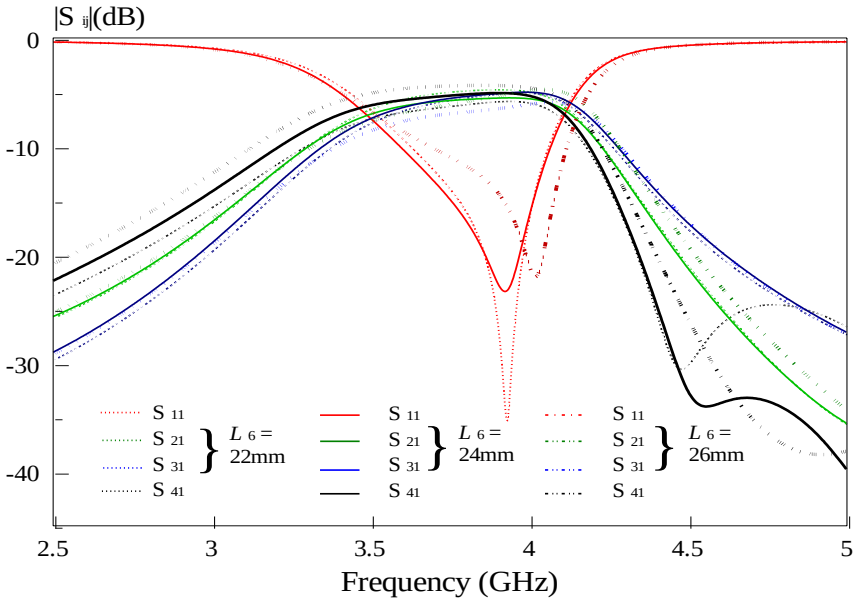


**Figure 4-25: Amplitude Response due to variation of length L6**

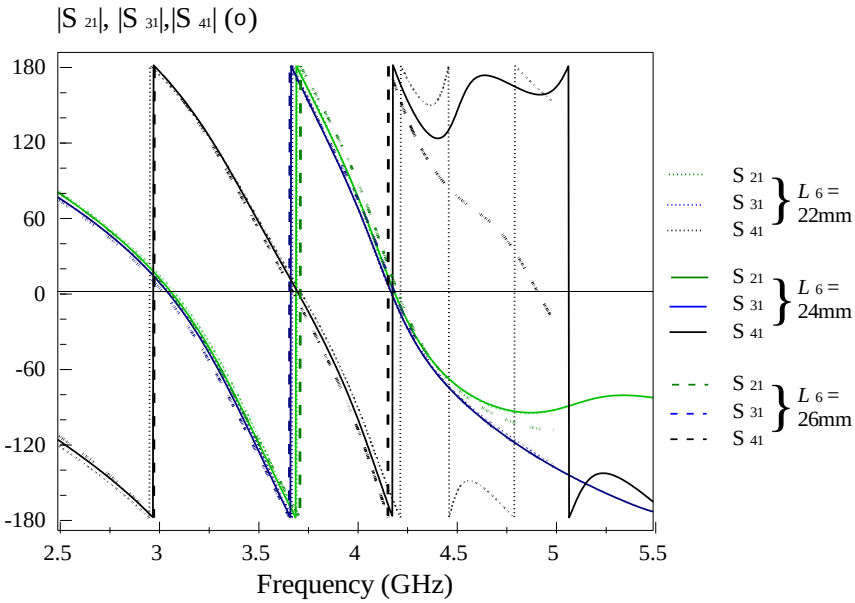


**Figure 4-26: Phase Response due to variation of length L6**

Observation

Here, it can be seen that the major impact of L6 is also the position of the pole and also the return loss of the divider. Longer length moves the pole to the upper frequency spectrum as well as providing lower operating bandwidth. Shorter length improves the return loss of the device. Passband bandwidth is almost similar to the original configuration dimension.

Case 7: Variation of width W1

$W_1$= 10mm

$W_1$= 12mm

$W_1$ = 14mm

Result

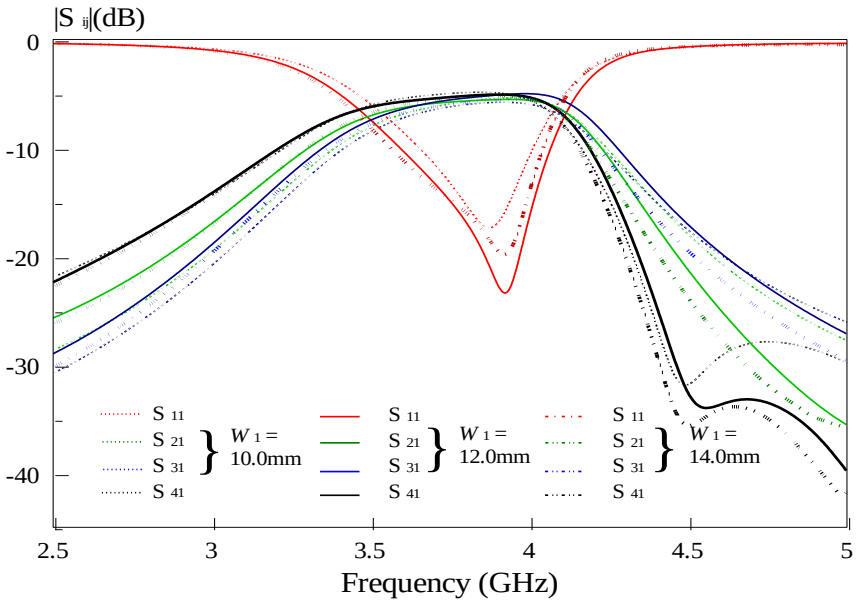


**Figure 4-27: Amplitude Response due to variation of width W1**

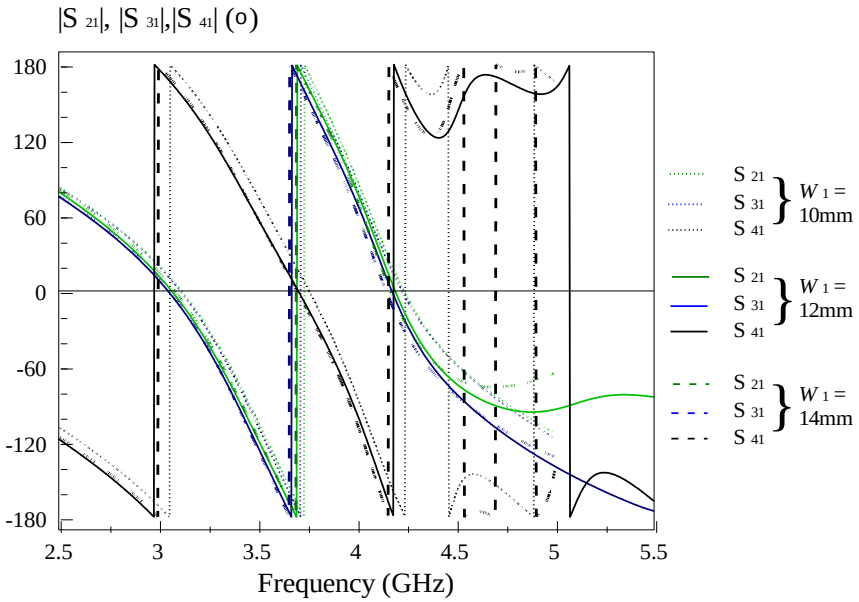


**Figure 4-28: Phase Response due to variation of width W1**

Observation

The parameter W1 does not produce any significant changes to the performance of the divider. Only the return loss of the divider is affected by varying this parameter.

Case 8: Variation of width W2

$W_2$= 10mm

$W_2$ = 12mm

$W_2$ = 14mm

Result

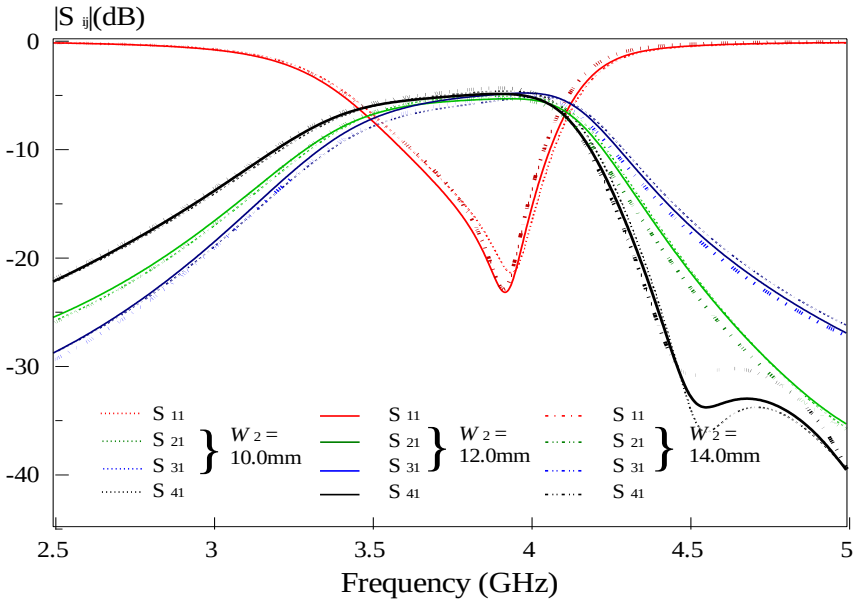


**Figure 4-29: Amplitude Response due to variation of width W2**

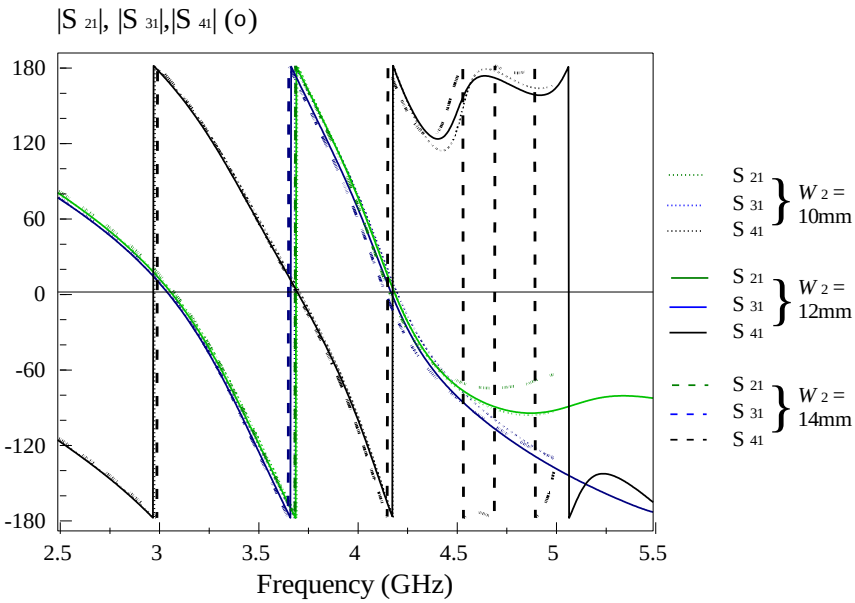


**Figure 4-30: Phase Response due to variation of width W2**

Observation

From figure 4.29, we can observe no change in the amplitude response curve of the multi-way divider. Phase response remains constant as well.

Case 9: Variation of width W3

$W_3$= 10mm

$W_3$ = 12mm

$W_3$ = 14mm

Result

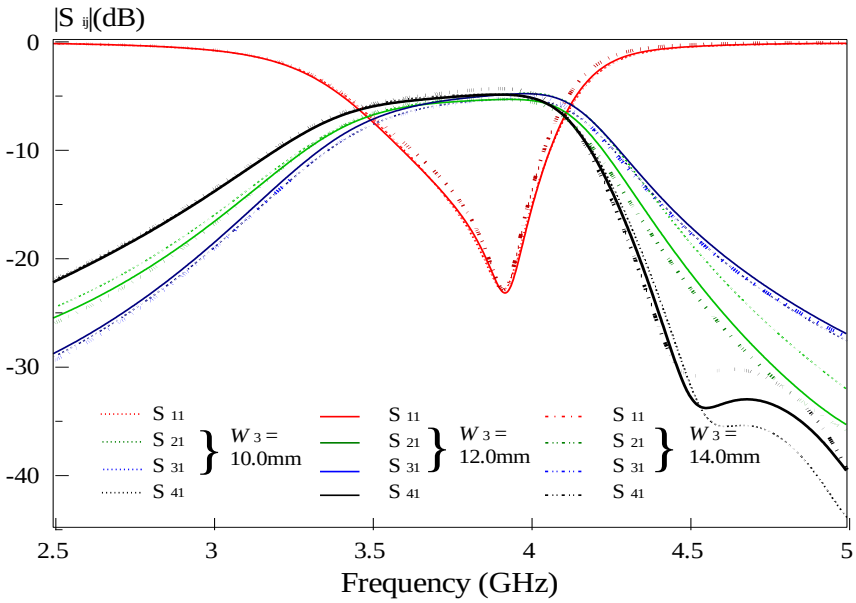


**Figure 4-31: Amplitude Response due to variation of width W3**

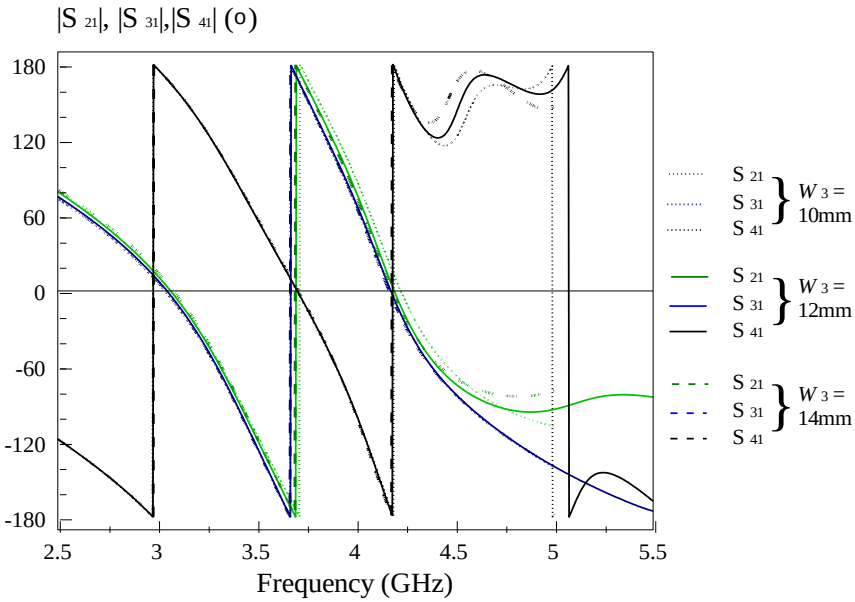


**Figure 4-32: Phase Response due to variation of width W3**

Observation

Since the multi-way divider is almost symmetrical, the effects of W3 are similar to the one shown in case 9.

Case 10: Variation of width W4

$W_4$= 0.5mm

$W_4$ = 1.0mm

$W_4$ = 3.0mm

Result

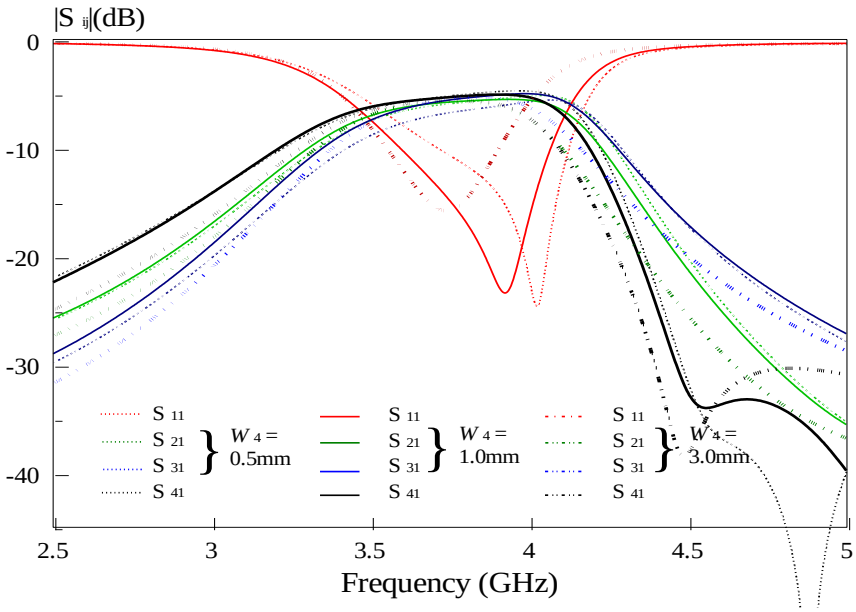


**Figure 4-33: Amplitude Response due to variation of width W4**

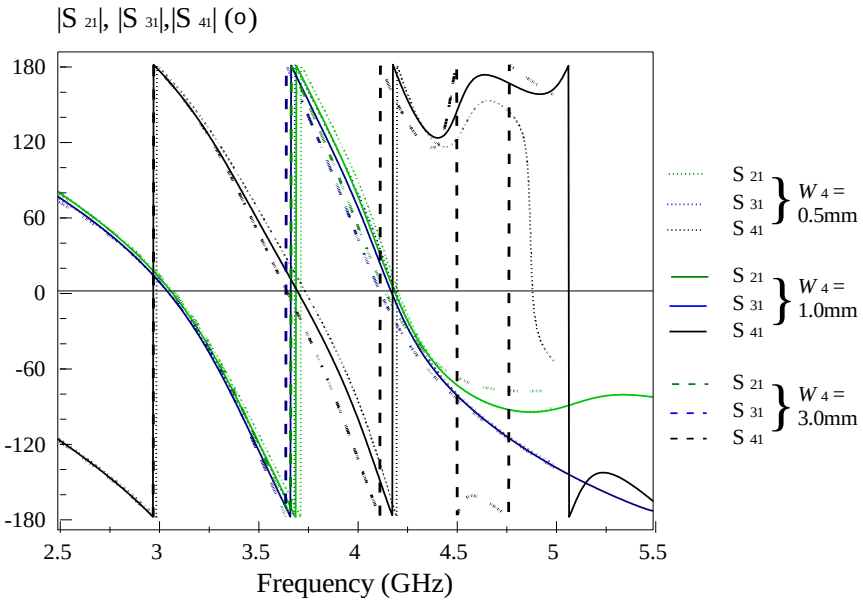


**Figure 4-34: Phase Response due to variation of width W4**

Observation

Figure 4.33 illustrates the amplitude response of the divider for parameter W4. The most significant impact due to W4 is the pole position as well as the passband frequency of the device. Smaller width shifts the passband of the divider to the

higher frequency spectrum while larger width shifts the passband of the device to the lower frequency spectrum.

Case 11: Variation of width W5

$W_5$= 10mm

$W_5$ = 12mm

$W_5$ = 14mm

Result

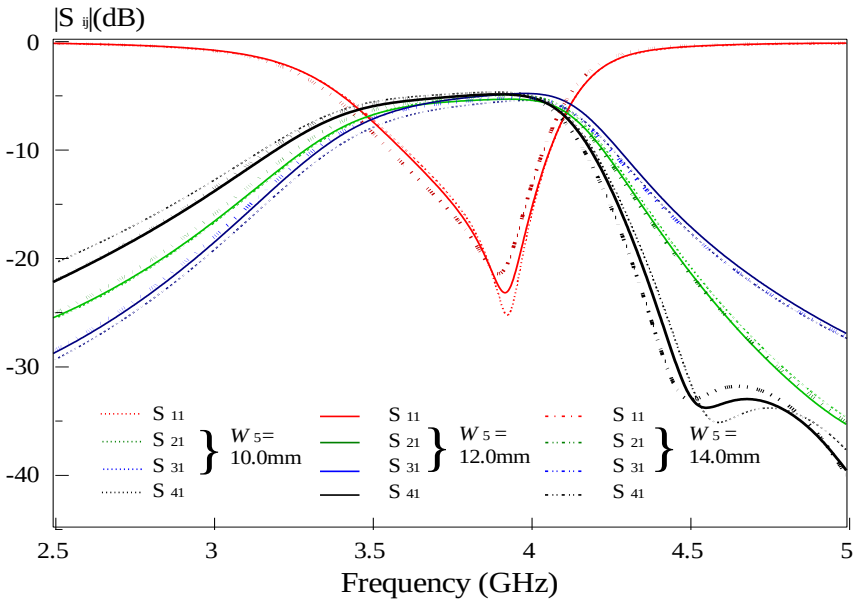


**Figure 4-35: Amplitude Response due to variation of width W5**

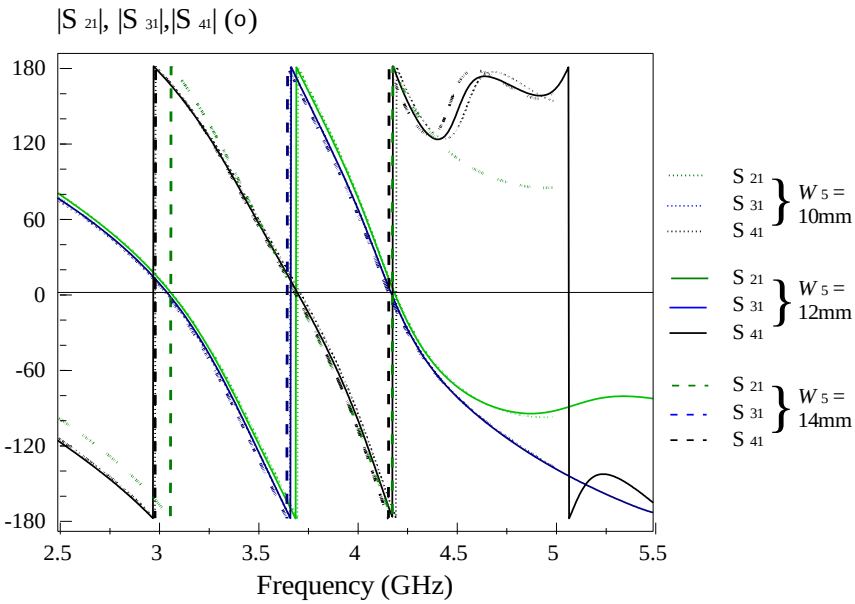


**Figure 4-36: Phase Response due to variation of width W5**

Observation

W5 does not exhibit any significant changes when it is varied. Therefore, it is not an important parameter to determine the performance of the divider.

Case 12: Variation of gap G1

$G_1$= 0.1mm

$G_1$ = 0.3mm

$G_1$ = 0.5mm

Result

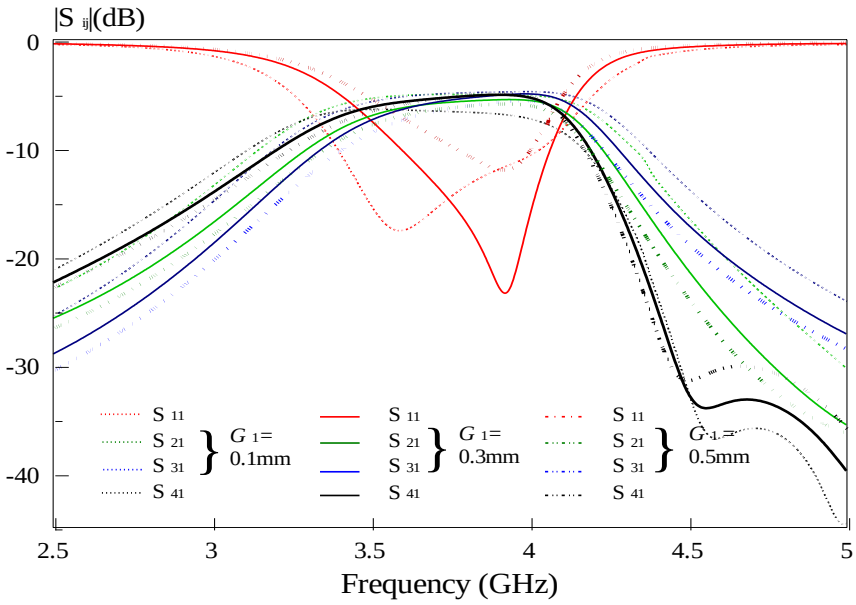


**Figure 4-37: Amplitude Response due to variation of gap G1**

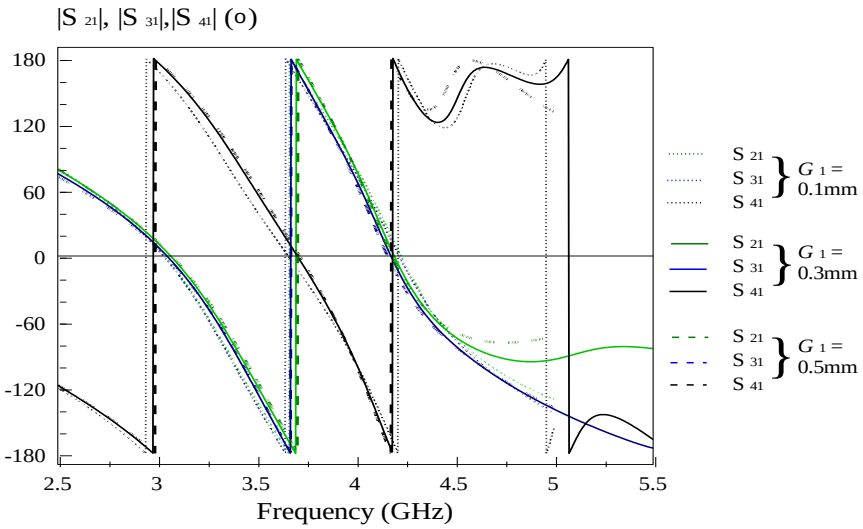


**Figure 4-38: Phase Response due to variation of gap G1**

Observation

The gap G1 determines the passband bandwidth of the divider as well as the passband spectrum. Thinner gap shows poorer return loss at the higher frequency components of the passband. Larger gap displays poorer return loss.

Case 13: Variation of gap G2

$G_2$= 0.5mm

$G_2$ = 0.6mm

$G_2$ = 1.6mm

Result

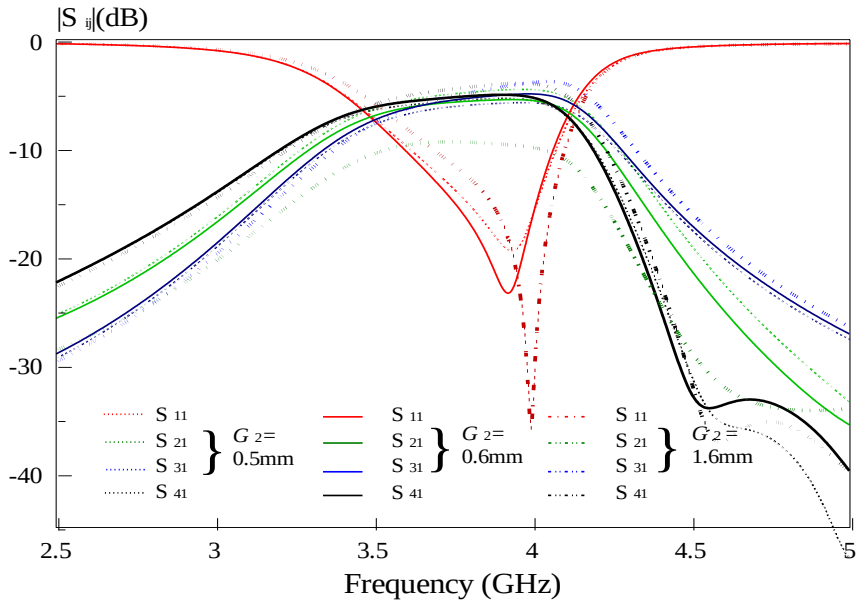


**Figure 4-39: Amplitude Response due to variation of gap G2**

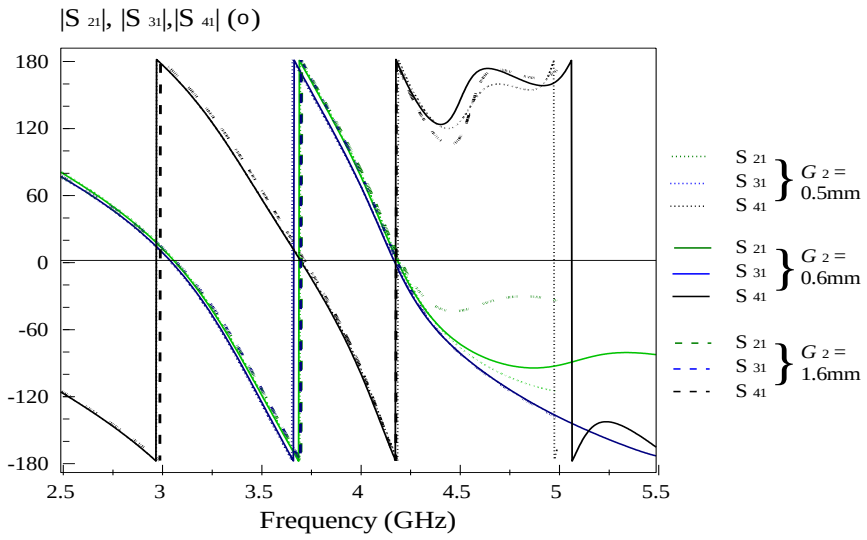


**Figure 4-40: Phase Response due to variation of gap G2**

Observation

By observing the curve shown in figure 4.39, gap G2 determines the return loss and the insertion loss of the divider. Although larger gap shows better return loss, the outputs signals does not contain same power. This means that input power is not equally divided. Smaller gap has lower return loss.

Case 14: Variation of gap G3

$G_3$= 10mm

$G_3$ = 12mm

$G_3$ = 14mm

Result

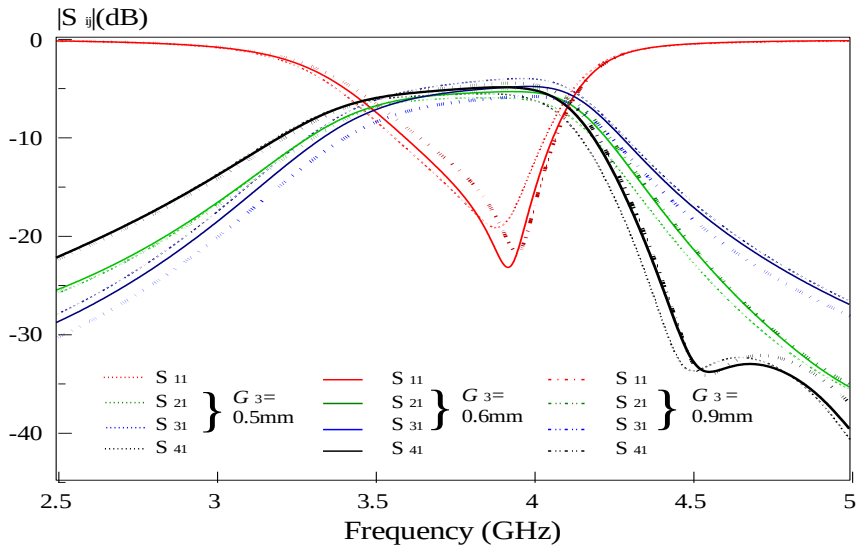


**Figure 4-41: Amplitude Response due to variation of gap G3**

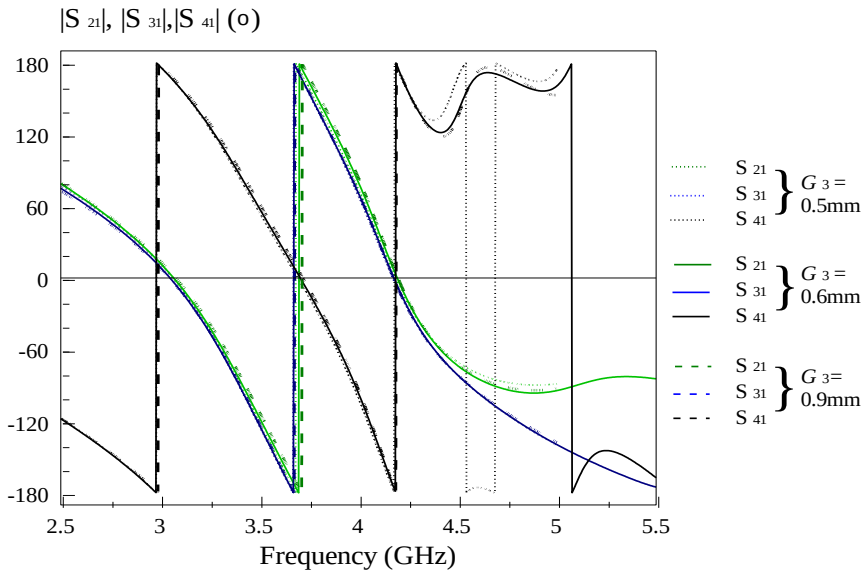


**Figure 4-42: Phase Response due to variation of gap G3**

Observation

The variation of parameter G3 does not affect much on the divider performance. We can observe that G3 = 0.6mm provides the best return loss for the divider. Port 2 and Port 3 has a slight phase difference. However, both Port 2 and Port 3 are still able to produce 180 degree phase difference with the output at Port 4.

Case 15: Variation of gap G6

$G_6$= 0.4mm

$G_6$ = 0.5mm

$G_6$ = 0.9mm

Result

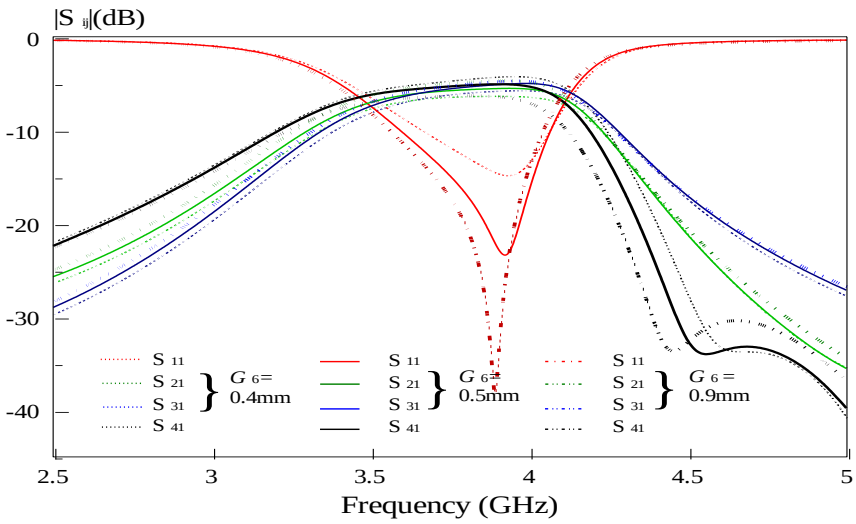


**Figure 4-43: Amplitude Response due to variation of gap G6**

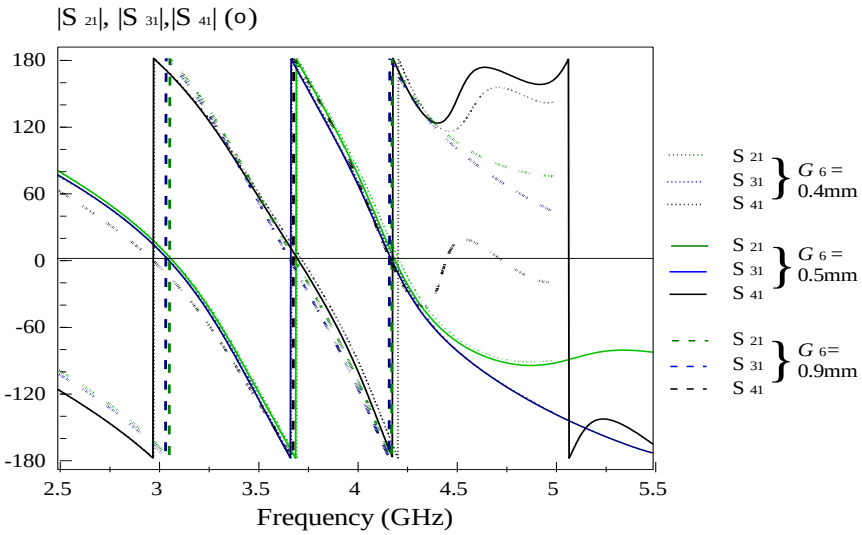


**Figure 4-44: Phase Response due to variation of gap G6**

Observation

From figure 4.43, the parameter G6 mainly affects the return loss of the multi-way divider. From the amplitude response cure, we can observe that smaller G6 will cause the divider to have poorer return loss as well as reducing the operating bandwidth. Meanwhile, wider G6 helps to improve the return loss of the divider while slightly improving the passband bandwidth. Varying the G6 does not affect much on the phase response which can be seen in figure 4.43.

### 4.2.5 Discussion

In the passband region, we can observe that the electric field at all output ports have almost the same intensity, shown in figure 4.45 and figure 4.46. Both frequencies are within the operating bandwidth. This shows that the power divider is able to divide an input signal equally among the output ports in all operating bands because there is good impedance matching between the coupled transmission lines. Therefore, very minor reflection occurs at the input resonator.

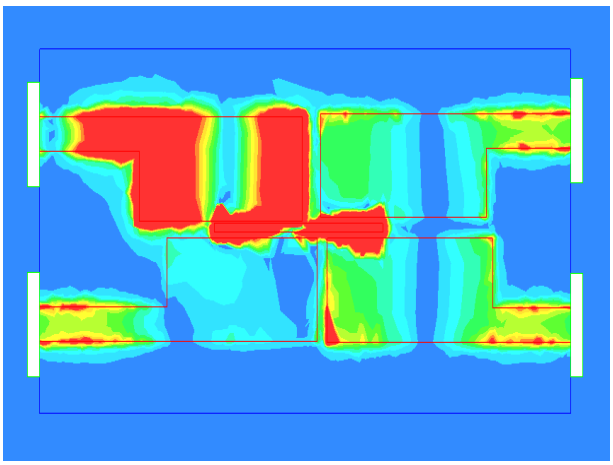

**Figure 4-45: E-field at 3.58GHz**

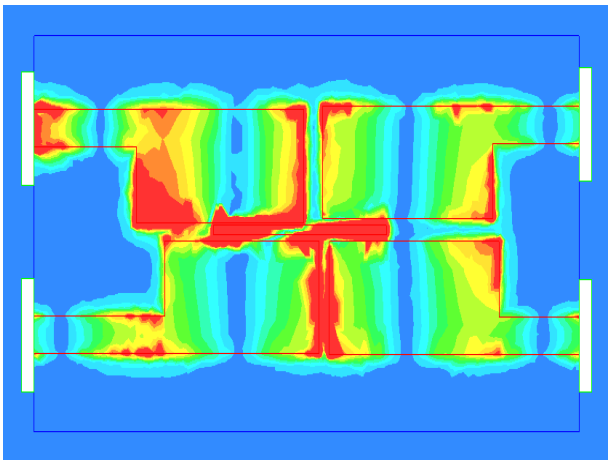

**Figure 4-46: E-field at 4.06GHz**

Besides that, we can observe that the E-field strength at each point is the same at port 2 and port 3 which implies that they are moving in-phase. Unlike the E-field which is seen at port 4, there is a slight delay in propagation, thus producing a phase difference. Beyond the passband bandwidth, we can observe that the E-field intensity at all output ports are almost zero while the E-field level at the input patch is very highly concentrated. This indicates that no signal is almost able to pass through and are all reflected back to the input port. The cause of this is due to impedance mismatch between the transmission lines.

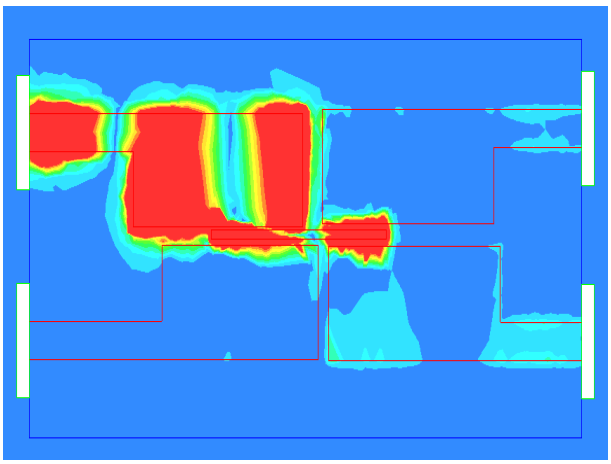

**Figure 4-47: E-field at frequency beyond passband**

# CHAPTER 5

# CONCLUSION AND RECOMMENDATIONS

## 5.1 Achievements

From this project, the author has successfully managed to design an in-phase power divider and an out-of-phase power divider that are both capable to provide equal power division ratio. The in-phase power divider is able to operate at frequency ranging between 3.61GHz to 4.21GHz, thus providing a passband bandwidth of 0.6GHz. Similarly, the out-of-phase divider is able to work at frequency between 3.65GHz to 4.12GHz, which offer passband bandwidth of 0.486GHz. From the two initial design configurations and concepts, the author has managed to modify the two dividers into a three-way power divider by adding an additional rectangular patch resonator. With some amendment to the original configuration dimensions incorporated with the additional rectangular patch, the three-way power divider is also able to produce equal power division ratio to the outputs. Here, two outputs are in-phase while the additional output is 180 degree out-of-phase. The multi-way divider is able to operate at frequencies between 3.59GHz to 4.06GHz. Therefore, the passband bandwidth of the divider is 0.47GHz.

## 5.2 Future Work

Based on the proposed design power dividers, one of the major limitations of the device is the operating bandwidth. Therefore, each of the dividers can be further altered by varying the parameters of the device in order to achieve a larger passband bandwidth. Additional rectangular patches can be incorporated to increase the

number of poles in the amplitude response which can help to improve the operating bandwidth. Besides that, both the in-phase and out-of-phase dividers can be combined into a single microwave circuit so that it can produce both in-phase outputs and out-of-phase outputs by only changing the input port.

## 5.3 Conclusion

The objective of this project is to design power dividers which are capable of providing equal power division ratio in the microwave spectrum. The initial stage in designing the structure of the divider is by performing transmission line modelling using Microwave Office. From the model, we are able to acquire the attributes of the design needed to achieve a certain response characteristic. After that, we are able to investigate the parameters of the design configurations to obtain the optimum performance of the design using any electromagnetic simulation software such as the High Frequency Structure Simulator (HFSS). Lastly, the configuration based on HFSS can be fabricated and measured to test the performance of the proposed design.

In conclusion, rectangular patches can be used to design a 2-way or 3-way power divider with equal power division ratio. All designs can be configured to achieve in-phase or out-of-phase outputs. All simulation, modelling and measurement results displays good agreement during comparision.

## REFERENCES

Annapurna Das, Sisir K. Das, "*Microwave Engineering*", 2000 Tata McGraw Hill, ISBN 0-07-463577-8

V.S. Bagad, "*Microwave Engineering*", 2009 Technical Publications Pune, ISBN 9788184313604

David M.Pozar, "*Microwave Engineering*" 3rd Edition, 2005 John Wiley, ISBN 0-471-44878-8

Tzyy-Sheng Horng, Ching-KuangC.Tzuang, 2011, *Recent Microwave Activities in Taiwan*, Retrieved 7th March 2012http://ieeexplore.ieee.org.libezp.utar.edu.my/stamp/stamp.jsp?tp=&arnumber=6102005&isnumber=6101646

Joseph Z Bih, 2003, *The Microwave Technology*, Retrieved 7th March 2012, http://ieeexplore.ieee.org.libezp.utar.edu.my/stamp/stamp.jsp?tp=&arnumber=1256324&isnumber=27984

Ian C. Hunter, Laurent Billonet, Bernard Jarry, Pierre Guillon, 2002, *Microwave Filters – Applications & Technology*, in IEEE Transactions on Microwave Theory and Techniques, Retrieved 7th March 2012, http://ieeexplore.ieee.org.libezp.utar.edu.my/stamp/stamp.jsp?tp=&arnumber=989963&isnumber=21335

Albert E. Williams, Ali E. Atia, 1982, *Introduction Microwave Filters: A Maturing Art*, Retrieved 7th March 2012, http://ieeexplore.ieee.org.libezp.utar.edu.my/stamp/stamp.jsp?tp=&arnumber=1131251&isnumber=25108

Frederick H. Raab, Peter Asbeck, Steve Cripps, Peter B. Kenington, Zoya B. Popovic, Nick Pothecary, John F. Sevic, Nathan o. Sokal, 2002, *Power Amplifiers and Transmitters for RF and Microwave*, in IEEE Transactions on Microwave Theory and Techniques, Retrieved 8th March 2012, http://home.earthlink.net/~fraab/TP02-1.PDF

Carlos Fuentes, 2008, *Microwave Power Amplifiers Fundamentals*, a Gigatronics Technical White Paper AN-GT-101A, Retrieved 8th March 2012

Y-F. Bai, X.-H. Wang, C-J. Gao, X.-W. Shi, H.-J. Lin,: 'Compact dual-band power divider using non-uniform transmission line',*Electronic Letter*,2011

Yao-Wen, H., and Kuster, E.F:'Direct synthesis of passband impedance matching with non-uniform transmission lines', *IEEE Trans. Microw. Theory Tech.*, 2010

A. C. Papanastasiou, G.E Georghiou, G. V. Eleftheriades,: "A quad-band Wilkinson Power Divider using Generalized NRI Transmission Lines,' *IEEE Trans. Microw. Theory Tech.*, 2008

G. V. Eleftheriades, A. K. Iyer, and P. C. Kremer, "Planar negative refractive index media using periodically L-C loaded transmission lines", *IEEE Trans. Microw. Theory Tech.*, 2002

C. Caloz and T.Itoh, "Novel microwave devices and structures based on the transmission-line approach of meta-materials,"*IEEE MTT-S Int. Dig*., 2003

M. Studniberg and G. V. Eleftheriades, "Physical Implementation of a generalized NRI-TL medium for quad-band applications," *Proc. Eur. Microw. Conf*, 2007

Kaijun Song, "Novel Ultra-Wideband Multilayer Slot line Power Divider With Bandpass Response*", IEEE Microwave and Wireless Components Letters*, 2010

E. J. Wilkinson, “An N-way power divider,” *IEEE Trans. Microw. Theory Tech.*, vol. MTT-8, pp. 116–118, Jan. 1960, Retrieved 7th April 2012 http://ieeexplore.ieee.org.libezp.utar.edu.my/stamp/stamp.jsp?tp=&arnumber=1124668&isnumber=24846

Jui-Chieh Chiu; Jhi-Ming Lin; Yeong-Her Wang; , "A Novel Planar Three-Way Power Divider," *Microwave and Wireless Components Letters, IEEE* , vol.16, no.8, pp.449-451, Aug. 2006, Retrieved 7th April 2012 http://ieeexplore.ieee.org.libezp.utar.edu.my/stamp/stamp.jsp?tp=&arnumber=1661640&isnumber=34768

Y. Wu, Y. Liu, X. Liu “Dual-frequency power divider with isolation stubs”, *Electronic Letters*, 2008

Wai-Kai Chen, “*The Electrical Engineering Handbook*”, 2005, Elsevier Academic Press, ISBN: 0-12-170960-4

J.-X. Chen, Z.-H. Bao, Q.Xue, “Analysis and design of out-of-phase power divider with arbitrary division ratio,”*IET Microwaves Antennas &Propogation*, 2009, Retrieved 11th April 2012